Particle Settling Through Emulsions: System Stability and Prediction of Settling Velocity

by

Aref Fozooni Kangarshahi

A thesis submitted in partial fulfillment of the requirements for the degree of

Master of Science

in

Chemical Engineering

Department of Chemical and Materials Engineering
University of Alberta

© Aref Fozooni Kangarshahi, 2021

Abstract

Particle settling in emulsions is encountered in a number of industrial processes. For instance, multiphase separators are used to separate oil from mixtures that also contain water, gas, and particles. In such separators, an "emulsion layer" forms through which the solid particles must settle. To design these separators, the prediction of the particle settling rate is required. If the particle settling velocity prediction through any medium (including the emulsion layer) is incorrect, the settler may not operate effectively.

Past experimental works on particle settling in emulsions have shown that these systems can become unstable when the droplet and particle sizes are similar, which leads to the formation of finger-shaped streams. These "fingering streams" include both downward-flowing liquid streams transporting solids and upward-flowing streams transporting emulsion droplets. When the fingering phenomenon occurs, the actual particle settling velocity is significantly higher than predicted values from correlations appropriate for batch sedimentation.

In other settling systems comprised of suspensions of light and heavy particles, a similar phenomenon takes place. Studies on these heavy-light particle systems show that the size, concentration, and density of both heavy and light particles determine the system stability. According to the similarities between the two settling systems, the same properties of the settling particles and emulsion droplets have been considered as controlled variables for studying emulsion-particle settling systems stability in the current project. In other words, the emulsion droplets and solid particles have been considered as light and heavy particles, respectively.

Two main objectives of this project are: 1- To develop a tool for defining the stability status of emulsion-particle settling systems under a variety of conditions; 2- To study the velocity

enhancements caused by the fingering phenomenon and improve the understanding of unstable emulsion-particle settling systems.

A series of experimental studies have been conducted in this project. The settling of glass beads with different sizes in oil-in-water emulsions was observed through the transparent wall of a Plexiglas settler. The results include a set of 'stability maps,' which show the stability status of the emulsion-particle settling systems under different conditions, including oil droplet density, size and concentration, and particle size and concentration. Since standard settling velocity correlations cannot be used for unstable settling, the stability maps prepared in this project could be used to predict the stability status of the emulsion-particle settling systems.

In addition to the stability observations, particle settling velocities were measured for each settling test. Settling velocities predicted using the Richardson-Zaki equation for both stable and unstable tests were compared to the measured values. In all of the velocity predictions, the emulsion is considered to be a "continuous phase." The analysis of the results shows that the Richardson-Zaki equation can only predict the settling velocities of the stable systems. In other words, the emulsion cannot be considered as a continuous phase when a system is unstable.

The final task in this project was developing a model for fingering conditions by considering the emulsion as a non-continuous phase and assuming that fluid movements inside the fingers carry particles and emulsion droplets. The model predicts the behavior of the system with high accuracy. One key conclusion from this study is that emulsion droplets act like rising particles moving through water during the fingering phenomenon. Another significant conclusion is that fluid movement inside the fingers is the main reason for settling velocity enhancements. This

achievement expands the understanding of unstable emulsion-particle settling systems and broadens the knowledge in this area of research.

At the end, two recommendations are provided for the future work in this area: 1- Conducting emulsion-particle settling experiments using advanced methods like particle image velocimetry (PIV) to more accurately measure phase velocities during unstable settling; and 2- Conducting stability tests for particle settling through water-in-oil emulsions (since oil-in-water emulsions were tested here).

Dedicated to my parents, who are the pillars of my life.

Acknowledgments

Contents

List of Figures

List of Tables

Nomenclature

Symbol	Description	Unit
A	Cross-sectional area	m^2
C_D	Drag coefficient	-
d	Diameter	m
F	Force	N
g	9.81 m/s^2 (Gravitational acceleration)	m/s^2
Ga	Galileo number (Eq. 2.10)	-
M_p	Mass of particles	kg
n	Richardson-Zaki index	-
Q	Flow rate	m^3/s
$Re_{p\infty}$	Particle Reynolds number	-
t	Time	s
v	Velocity	m/s
$\forall$	Volume	m^3
β	Volume fraction in emulsion	-

γ	Oil to particle (or heavy to light particle) reduced density ratio (Eq. 2.21)	-
λ	Droplet to particle (or heavy to light particle) size ratio (Eq. 2.20)	-
μ	Dynamic viscosity	$Pa.s$
π	3.14	-
ρ	Density	kg/m^3
φ	Volume fraction in the whole mixture	-

Subscript	Description
b	*buoyancy*
d	for **F**: *drag* for **d** and **v**: *emulsion droplet*
D	*Disengagement point*
$d - fing$	for **A**: *area occupied by emulsion fingers* for **v**: *oil droplet velocity in fingering region*
$d\infty$	*droplet terminal velocity*
dis	*disengaged*
e	*emulsion*
eng	*engaged*
f	*fluid*
$fing$	*fingering region*
g	*gravity*

m	*maximum attainable concentration*
o	*oil*
p	*particle*
$p-fing$	for $\boldsymbol{A}$: *area occupied by suspension fingers* for $\boldsymbol{v}$: *particle velocity in fingering region*
$p\infty$	*particle terminal velocity*
r	*relative to water viscosity*
rel	*relative to the water velocity*
$total$	*settler (area)*
$w\uparrow$	*upward moving water in emulsion fingers*
$w\downarrow$	*downward moving water in suspension fingers*

Chapter 1
Introduction

1.1. Background and context

Sedimentation is the process through which particles settle in a fluid. It is encountered in different branches of science and industry [1]–[4]. The study of sedimentation can provide valuable information about particle-particle interactions, particle-fluid interactions, and settling characteristics of particles under specific conditions. Ultimately, this information is needed in the study of natural phenomena such as coastal erosion or designing industrial equipment such as gravity settlers [5].

In the oil sands industry, gravity settling plays a significant role in various parts of the bitumen recovery process, such as settling vessels for primary bitumen separation [6], [7], inclined settlers for froth treatment [8] and tailing ponds for tailings management [9]. In most bitumen recovery processes (except for the hydrotransport and tailings pipelines [10]), it is desirable for the particles to settle as fast as possible.

Figure 1.1 shows a settling unit for oil sands recovery that is designed to separate solid particles, water, and asphaltenes from solvent-diluted bitumen [11]. The key parameter in designing such equipment and any other type of settler is the settling velocity of each of the different species that is going to be separated through the process. Slow sedimentation requires more time and a larger settler, while for faster settling rates, smaller equipment can work well.

Settling rate is affected by the particle characteristics such as their size, shape and density and the features of the medium that through which the particles must settle. The settling medium could be a simple liquid such as water or a more complex one like an emulsion. An emulsion is a mixture of two or more liquids that are immiscible [12]. An emulsion-particle settling system is one in which particle sedimentation occurs through an emulsion. Particle settling in emulsions is encountered in many industrial processes such as metal cuttings recovery from emulsions [13], and crude oil production [14].
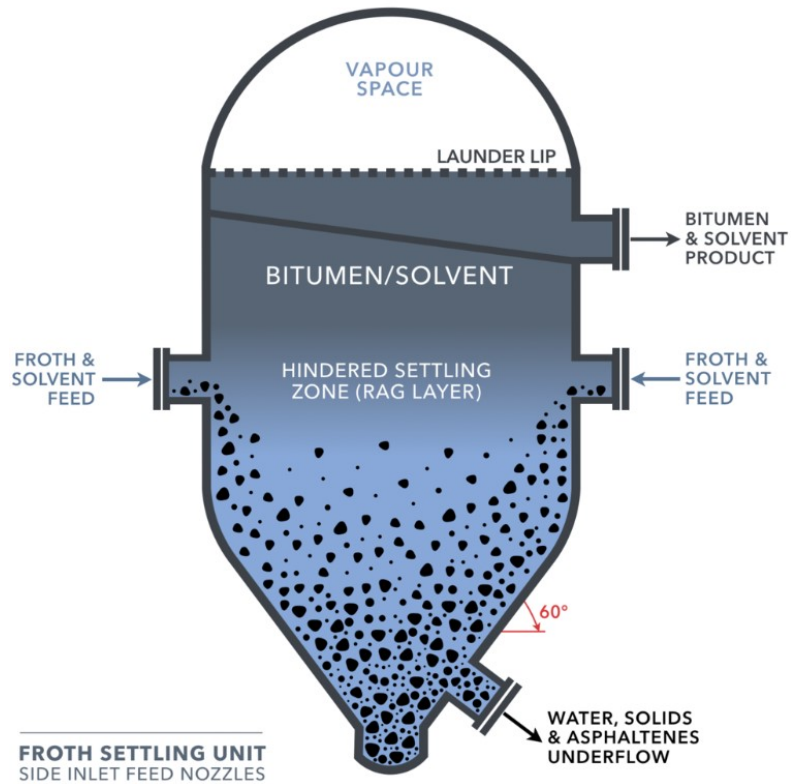
Figure 1.1- Schematic view of a froth settling unit (Reproduced from Oil Sands Magazine [11]**)**

In the oil production industry, separation of oil from a mixture that also contains water, gas, and sand requires multiphase separators [14]. A schematic view of this type of separator is shown in Figure 1.2. As can be seen in Figure 1.2, in such separators, an emulsion layer is formed through which the solid particles must settle. The design of these separators (residence time and equipment size) is based on the calculated rise/settling velocity of each species, including the particles. Therefore, the separator may not operate as designed if the particle settling velocity prediction is incorrect.
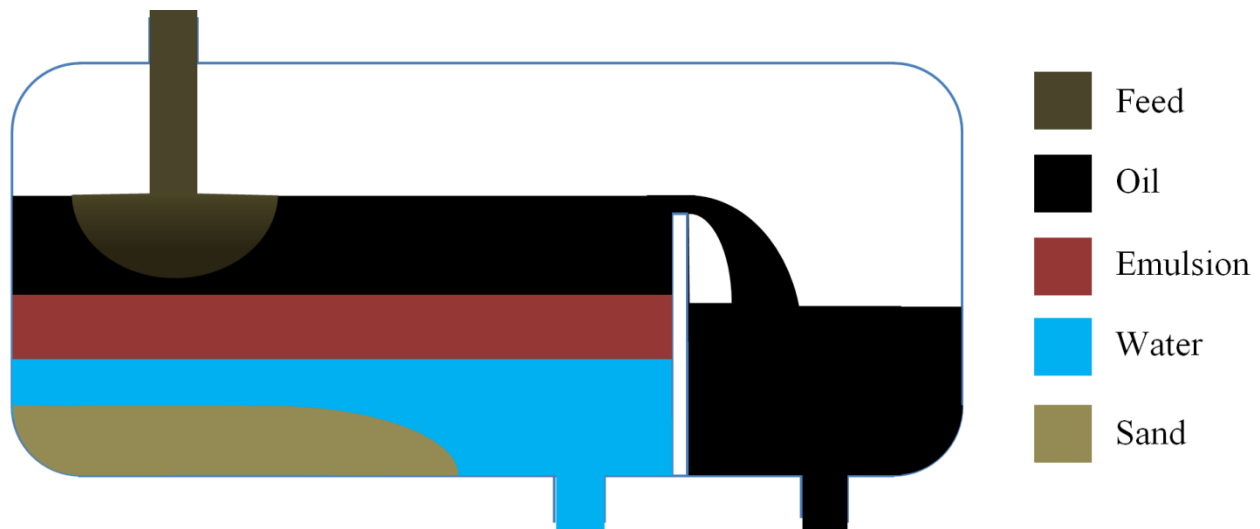
Figure 1.2- Schematic view of a multiphase separator used in oil production

The question is if conventional settling velocity correlations always provide accurate predictions for emulsion-particle settling systems? One of the early studies performed to answer this question was conducted by Tipman and Hodgson [15]. In their experiments (see Chapter 2 for more details), they measured the terminal settling velocity of particles with different sizes in an emulsion. Their measured values at $Re_{p\infty}(particle\ Raynolds\ number) < 1$ were consistent with the predicted velocities from Stokes' law. Since Stokes' law is defined for very low particle Reynolds numbers, it could be concluded that the conventional velocity prediction methods work well for the conditions under which Tipman and Hodgson [15] performed their experiments. However, their study was performed under limited conditions. One limitation of their work is that they only tested the accuracy of available equations for the settling of single particles in emulsions. They also did not measure the emulsion droplet size to see how it can affect the system. Hence, it is necessary to study emulsion-particle settling systems over a broader range of conditions to test the accuracy of conventional settling velocity correlations for these systems.

After the Tipman and Hodgson [15] work, the following questions about emulsion-particle settling systems remain:

- They measured the settling velocity of single particles. Are the conventional velocity prediction methods still accurate at higher particle concentrations?
- In their velocity calculations, they considered the emulsion as a continuous phase. Is this assumption always correct?
- They did not measure the emulsion droplet sizes in their study. Can this parameter affect the particle settling velocity in an emulsion?

To answer these questions, more experiments conducted over a broader range of conditions must be performed.

1.2. Problem statement

Yan and Masliyah [16] studied emulsion-particle settling systems under a wider range of conditions. They used three different sizes of particles to study their hindered settling velocity in emulsions. They performed multiple settling tests with different particle and emulsion concentrations. Emulsion droplet sizes were also measured in their study.

For large particles, settling velocities were successfully predicted by conventional correlations. This was not the case for smaller particles whose sizes were closer to those of the emulsion droplets. Measured settling velocities by Yan and Masliyah [16] significantly exceeded the predicted values when the particle size approaches the emulsion droplet size. In all of their tests with enhanced settling rate, they reported an unusual phenomenon called "fingering." They realized that in all the tests with increased settling velocity, the particles start forming segregated finger-shaped streams shortly after the sedimentation process starts. When the fingering phenomenon happens, the settling system is called "unstable."

As mentioned earlier in this Chapter, it is important to know if the sedimentation rates can be predicted accurately before designing any settling equipment. Therefore, since the settling rate enhancement occurs in unstable emulsion-particle settling systems, it is crucial to know about the stability of the settling process if it involves particle sedimentation through an emulsion. However, such tool for predicting the stability status of emulsion-particle settling systems is

currently unavailable. Also there is little knowledge about what happens in "unstable" emulsion-particle settling systems that causes the particle settling rates to enhance over that which would be predicted using standard settling velocity correlations. Hence, there is a need to develop a model to describe the "unstable" emulsion-particle settling systems.

1.3. Project objectives

Further to the discussions of Section 1.2, the following project objectives have been identified:

- **To define the stability status of emulsion-particle settling systems under a variety of conditions:** The first goal is to study the parameters contributing to system instability. The results are stability maps that define the stability status of the emulsion-particle settling systems under various conditions.

- **To study the settling velocities and develop a model for unstable emulsion-particle settling systems:** The other objective of the project is to investigate the settling velocities in both stable and unstable systems. The goal is to improve the understanding of the fingering phenomenon about how it accelerates particle settling.

1.4. Thesis outline

This thesis contains six chapters, including the current one. Chapter 2 provides a literature review on the subject. Section 2.1 explains the fundamentals of the settling process, including the terminal settling velocity of a single particle, and the introduction of the Richardson-Zaki equation for predicting the sedimentation rate in batch settling systems. Section 2.2 focuses on previous studies on emulsion-particles settling systems, in which the differences between stable and unstable emulsion-particle settling systems are explained and the concept of fingering phenomenon as the source of settling velocity enhancement is introduced. Section 2.3 introduces another type of bi-dispersed settling system, a light-heavy particle suspension that experiences instability. An explanation of how understanding of these particulate systems could help study of emulsion-particle settling systems is also provided. The concept of a "stability map" and parameters contributing to the instability of bi-dispersed settling systems is introduced. Section 2.4 concludes the literature review by summarizing the key findings about emulsion-particle settling systems and discussing the major questions and knowledge gaps. Section 2.5 explains

how this study will address those gaps and broaden the knowledge of emulsion-particle settling systems.

Chapter 3 describes the experimental method. Section 3.1 introduces the materials used in the experiments. Section 3.2 introduces all the equipment utilized in this project. Section 3.3 covers the experimental procedures followed for this project, including emulsion preparation, droplet size measurement, settling tests, and velocity measurements. Section 3.4 introduces the velocity calculation procedure employed to predict the particle settling velocities. Section 3.5 describes the project experimental design and explains how the test points were chosen to fulfill the project objectives. It also illustrates how unnecessary tests have been eliminated to save time by reducing the size of the experimental matrix.

Chapter 4 provides the results of the stability tests. Section 4.1 explains how the controlled variables were chosen to improve the probability of finding the stability boundary for the emulsion-particle settling systems. Section 4.2 provides photographs taken from the settling experiments, which illustrates the differences between stable and unstable tests. Section 4.3 shows the results of the tests carried out for the first two key maps. Based on the experimental design of the project, the results of these two maps are necessary for deciding how develop the remaining maps. Section 4.4 illustrates the results of tests for the remaining maps. Section 4.5 provides the full set of the 12 stability maps produced from this project. It also explains how these maps can be used as a valuable tool by researchers and engineers working on emulsion-particle settling systems.

Chapter 5 presents and discusses the results of the velocity measurements and describes a model for unstable tests. Section 5.1 provides an introduction to the Chapter. Section 5.2 compares measured settling velocities of the stable tests to the predicted values obtained using the Richardson-Zaki equation. Section 5.3 compares measured particle settling velocities in the unstable tests to the predicted values by the Richardson-Zaki equation. It includes two sets of velocity calculations for the particles before and after they disengage from the emulsion. Section 5.4 develops a model for the unstable emulsion-particle settling systems. The model is designed to give a deeper insight and improve knowledge about what happens in an unstable emulsion-particle settling system. The accuracy of the model is verified by comparing the measured rising velocity of the oil droplets in the unstable tests with the predicted velocities from the model.

Chapter 6 provides conclusions and recommendations, including a summary of the work and the conclusions made from the research. Section 6.2 provides recommendations for future works in this area of research. Section 6.3 contains a suggestion for potential industrial applications of the project results.

1.5. Authors' contribution

In this study, the author has designed the experimental plan of the entire project, including picking suitable materials for the tests, selecting controlled variables, and defining settling tests conditions and stability maps oil/particle concentrations.

Prof. Sean Sanders and Dr. David Breakey had an essential contribution to the conceptualization and scoping of the project. Also, they provided guidance, advice, and recommendations at each step of the project.

The author has performed all the stability experiments, settling velocity measurements, and analyses related to this thesis. The batch settling tests performed by the author are similar to the experimental procedure employed by Yan and Masliyah [16].

The interpretation of the stability test observations, which led to drawing the stability maps for emulsion-particle settling systems, has been thoroughly accomplished by the author.

The author has performed settling velocity predictions using the Richardson-Zaki equation for all the stable and unstable tests conducted in this project.

Also, the author developed a method for measuring the "disengagement concentration" in unstable settling tests.

The author has developed a physical model for unstable emulsion-particle settling systems. The model is presented in Chapter 5 of this thesis.

The equipment and the materials for the settling experiments performed in this project were provided by the Pipeline Transport Processes Research Group. The homogenizer used to prepare emulsions was provided by Dr. Hongbo Zeng's research group. The microscope with which the emulsion droplets were observed was provided by the NanoFab center at the University of Alberta.

The procedures for emulsion preparation and droplet microscopy was introduced and initially performed by Bach Vo and Carlos Sanchez. All the emulsion preparation and droplet size measurements presented in this thesis have been performed by the author.

A MATLAB script for processing the microscope images to obtain the oil droplet size distributions was written by and Bach Vo and Dr. David Breakey.

The Safe Work Procedures for settling experiments, emulsion microscopy, and homogenizer cleaning are developed by the author. The Safe Work Procedure for emulsion preparation was first written by Bach Vo and Carlos Sanchez. That part of the SWP was later revised and rewritten by the author.

Chapter 2
Literature review

2.1. Fundamentals of batch settling systems

It is important to understand the physics of a batch settling system. This will support the explanation of the emulsion-particle settling systems and the phenomenon studied in this research project. This Section provides a detailed derivation of the Richardson-Zaki equation since it is used for velocity prediction in this study. Parameters introduced here will be used in the velocity calculation method of the project introduced in Chapter 3.

A single particle falling through quiescent surrounding fluid is shown in Figure 2.1. Also shown in the figure forces acting on the particle surface at its terminal settling terminal velocity, $v_{p\infty}$.
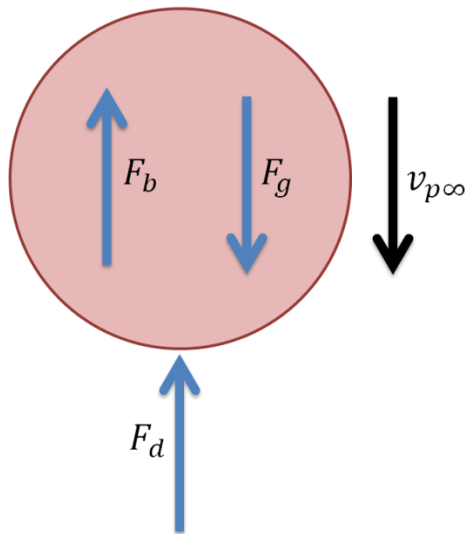
Figure 2.1- Three forces (F_g: gravity, F_b: buoyancy, and F_d: drag) acting on a single particle falling in a fluid at its terminal velocity ($v_{p\infty}$)

The mathematical definition of the forces shown in Figure 2.1 are [17]:

- Gravity:

$$F_g = \frac{\pi}{6}\rho_p d_p^3 g \qquad\qquad 2.1$$

- Buoyancy:

$$F_b = \frac{\pi}{6}\rho_f d_p^3 g \qquad\qquad 2.2$$

- Drag:

$$F_d = \frac{\pi}{8} C_D \rho_f |v_{p\infty}| v_{p\infty} d_p^2 \qquad\qquad 2.3$$

where $v_{p\infty}$ is the particle terminal settling velocity which is defined as the ultimate settling velocity of a single particle in an infinite expanse of a surrounding fluid; d_p and ρ_p are the particle diameter and density respectively; g is the gravitational acceleration; ρ_f is the fluid density, and C_D is the drag coefficient.

A balance between the forces mentioned above gives [17]:

$$|v_{p\infty}| v_{p\infty} = \frac{4 d_p g (\rho_p - \rho_f)}{3 \rho_f C_D} \qquad\qquad 2.4$$

Equation 2.4 shows that the drag coefficient is required to calculate the terminal velocity. The drag coefficient is a function of particle Reynolds number which has the following definition:

$$Re_{p\infty} = \frac{\rho_f v_{p\infty} d_p}{\mu_f} \qquad\qquad 2.5$$

where μ_f is the fluid dynamic viscosity.

Figure 2.2 shows how the drag coefficient varies with the particle Reynolds number. This graph is often divided into different zones based on Reynolds number: Stokes regime ($Re_{p\infty} \to 0$), Schiller-Naumann [18] regime ($Re_{p\infty} < 10^3$), and Newtonian regime ($10^3 \leq Re_{p\infty} \leq 2 \times 10^5$). For each regime [17], the drag coefficient can be defined by the following equations:

- Stokes regime:

$$C_D = \frac{24}{Re_{p\infty}}$$

2.6

- Schiller-Naumann regime:

$$C_D = \frac{24[1 + 0.15 Re_{p\infty}^{0.687}]}{Re_{p\infty}}$$

2.7

- Newtonian regime:

$$C_D \sim 0.44$$

2.8

Figure 2.2, along with Equation 2.4, shows that the particle terminal velocity is related to the particle Reynolds number. To calculate the terminal velocity for each regime, one of the Equations 2.6, 2.7, or 2.8 should be substituted into Equation 2.4. For example, for Stokes' regime, terminal velocity [19] is given by the following equation:

$$v_{p\infty} = \frac{g d_p^2 (\rho_p - \rho_f)}{18 \mu_f}$$

2.9
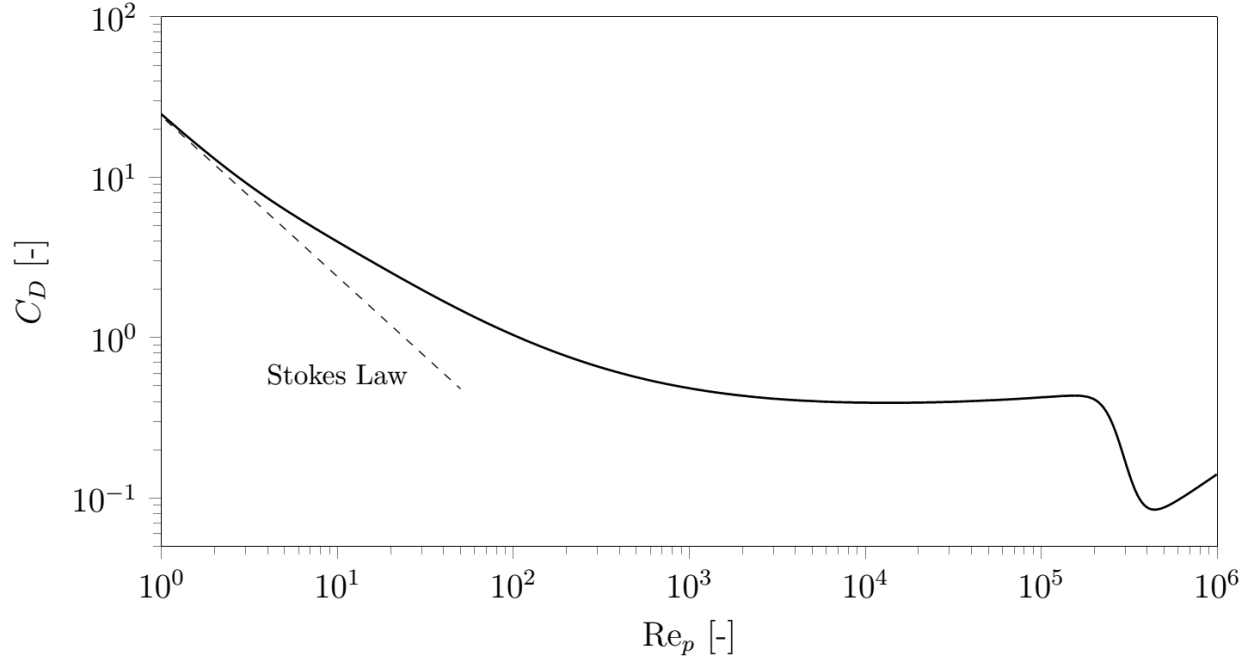
Figure 2.2- Variation of drag coefficient of a particle with the particle Reynolds number (Reproduced from Acher[20])

Equation 2.9 only applies if the particle Reynolds number is very low (i.e. $Re_{p\infty} \to 0$) [19]. Since $Re_{p\infty}$ is a function of $v_{p\infty}$, but $v_{p\infty}$ is a function of $Re_{p\infty}$ (through C_D), it is useful to define a parameter by which the Reynolds number could be calculated independently, e.g. using the Galileo number [17]:

$$Ga = \frac{g\, d_p^3 \rho_f \left|(\rho_p - \rho_f)\right|}{\mu_f^2} \qquad 2.10$$

Numerous equations are available to calculate the Reynolds number using the Galileo number [21], [22]. A useful equation of this type is given by Turton and Clark [22]:

$$Re_{p\infty} = Ga^{\frac{1}{3}}\left(\left(\frac{18}{Ga^{\frac{2}{3}}}\right)^{0.824} + \left(\frac{0.321}{Ga^{\frac{1}{3}}}\right)^{0.412}\right)^{-1.214} \qquad 2.11$$

14

Equation 2.11 applies for a wide range of Reynolds numbers ($Re_{p\infty} < 2.6 \times 10^5$). The advantage of using Equation 2.11 is its estimation of terminal velocity directly.

In a suspension, the presence of the other particles affects the movement of each particle. For particles settling in a suspension, a general relation between particle velocity and the fluid is given by Wallis [23]:

$$v_p - v_f = v_{p\infty}\varphi_f F(\varphi_f, Re_{p\infty})$$

2.12

where v_p and v_f are particle and fluid velocity respectively and φ_f is the fluid volume fraction. The function $F(\varphi_f, Re_{p\infty})$ in Equation 2.12 is the hindered settling function. This function has been defined by many researchers [24], [25]. One of the best known and most practical expressions for the hindered settling function is proposed by Richardson and Zaki [24]:

$$F(\varphi_f, Re_{p\infty}) = \varphi_f^{n-2}$$

2.13

where n is called the Richardson-Zaki index.

The Richardson-Zaki index (or R-Z index) itself varies with particle Raynolds number:

$$n = F(Re_{p\infty})$$

2.14

Numerous correlations that relate the R-Z index to particle Reynolds number are available [23], [26], [27], including one proposed by Rowe [26] that is commonly used:

$$n = 2.35 \frac{2 + 0.175\,Re_{p\infty}^{3/4}}{1 + 0.175\,Re_{p\infty}^{3/4}}$$

2.15

15

Equation 2.15 is applicable for $Re_{p\infty} < 10^5$. Substituting Equation 2.13 in Equation 2.12 gives:

$$v_p - v_f = v_{p\infty}\varphi_f^{n-1} \qquad\qquad 2.16$$

In a batch settling system, since the particles are moving downward and deposit at the bottom of the settler, the fluid necessarily moves upward. The downward volumetric flow rate of the particles should be equal to the upward flow rate of the fluid [17]:

$$A\varphi_p v_p + A\varphi_f v_f = 0 \qquad\qquad 2.17$$

where A is the cross-sectional area of the settler.

The phase volume fractions necessarily sum to 1, i.e.

$$\varphi_f + \varphi_p = 1 \qquad\qquad 2.18$$

By merging Equations 2.16, 2.17, and 2.18 for a batch settling system, the Richardson-Zaki equation becomes:

$$v_p = v_{p\infty}(1 - \varphi_p)^n \qquad\qquad 2.19$$

To measure the settling velocity of the particles in a batch settling column, typically a test similar to that shown in Figure 2.3 would be conducted. In such tests, particle settling velocity is measured by dividing the displacement of the upper interface by the time it takes for that displacement. In Figure 2.3, φ_{max} is the concentration of the packed bed of particles that have settled at the bottom of the settling column.
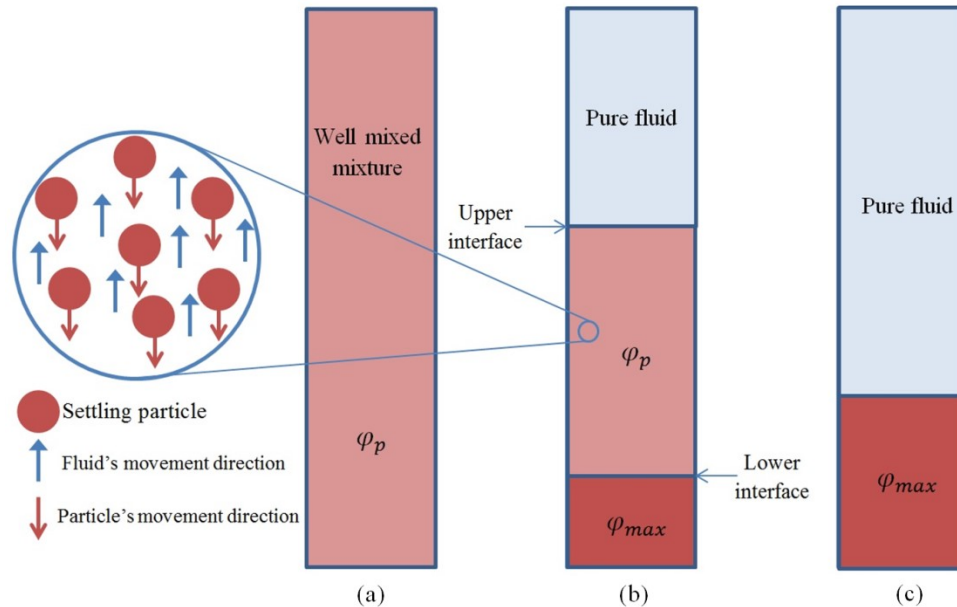
Figure 2.3- Schematic view of the time evolution of a batch settling system process: a) Initially well mixed mixture at the beginning, b) particles settling through the fluid, and c) settling completed

2.2. Emulsion-Particle Settling Systems

Particle settling in emulsions has been investigated by a number of researchers [13], [15], [16], [28],. To calculate the hindered particle settling velocity in an emulsion, one could assume the emulsion behaves as a continuum. With this assumption, the density and viscosity of the emulsion can be used in place of fluid density and viscosity in the velocity calculations presented in Section 2.1. This assumption should be valid under negligible hydrodynamic interactions between the emulsion droplets and their surroundings. In fact, when the particle and droplet sizes are comparable, the droplets may take the role of the second dispersed phase in the system i.e. they cannot be considered to be part of the fluid continuum.

In one of the first studies in this area, Tipman and Hodgson [15] tried to predict the terminal settling velocity of particles in water-in-oil emulsions using commercial steel ball bearings of different sizes (from 1.5 to 9.5 mm).

They considered the emulsion as the continuous fluid phase and used Stokes' law to predict the terminal settling velocity. Figure 2.4 shows the results of their study, with the vertical axis given as the ratio of the predicted velocity, from the Stokes' law, to the measured value.
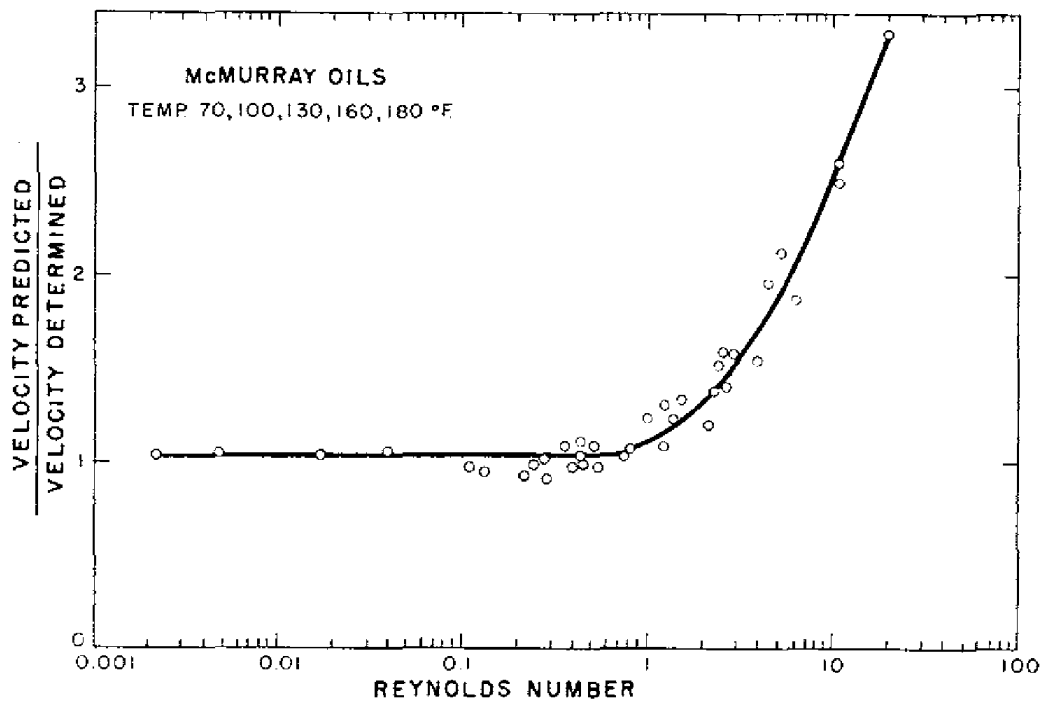
Figure 2.4- Comparison of the predicted and measured particle terminal velocities settling through water-in-oil emulsions. The particles had various sizes from 1.5 to 9.5 mm (Reproduced from Tipman and Hodgson[15])

Figure 2.4 shows that the predictions agree well with the measured velocities at low Reynolds numbers ($Re_{p\infty} < 1$) indicating that considering the emulsion as a continuum was reasonable.

In a subsequent and far more detailed study, Yan and Masliyah [16] used three different sizes of glass beads (29 μm, 57 μm, and 157 μm) with different concentrations settling in oil-in-water

emulsions. To study the effect of the oil concentration, they prepared emulsions with the oil concentrations up to 40%. The measured droplet size for all emulsions was around 10 μm in their study.

The results of the Yan and Masliyah study [16] show that conventional correlations could predict settling velocities for the large particles (157 μm). Therefore, assuming the emulsion as a continuous phase is valid under those conditions. However, the continuum assumption was not valid for the 29 μm particles. Their measurements showed that the settling velocity of the 29 μm particles was higher than the values calculated from when the emulsion was treated as a fluid continuum.

The viscosity of the emulsion is greater than that of water; therefore, one would expect lower settling velocity of particles in emulsions than in water under the assumption of a continuous-phase emulsion. The Yan and Masliyah [16] study showed that with the 29 μm particles, the particle settling is higher than their settling velocity in water.

Yan and Masliyah [16] observed the occurrence of a "fingering phenomenon" for all experiments with enhanced settling velocity. The fingering phenomenon is defined as the gathering of settling particles into segregated vertical finger-shaped streams. When the fingering phenomenon occurs, the settling system is called "unstable." They reported that the fingering streams appear a short time after the settling process begins. The streams weaken and disappear right before the settling particles disengage from the rising emulsion. After the disengagement, solid particles settle in the water while the emulsion creams at the top. Eventually, high concentrations of oil droplets at the top and solid particles at the bottom of the container were found. Figure 2.5 [16] shows how settling particles form segregated finger-shaped streams (which disappear when disengagement happens) in an unstable emulsion-particle settling system.

Based on their description of the unstable emulsion-particle settling, the fingering phenomenon could be interpreted as consisting of consecutive stages depicted in Figure 2.6.
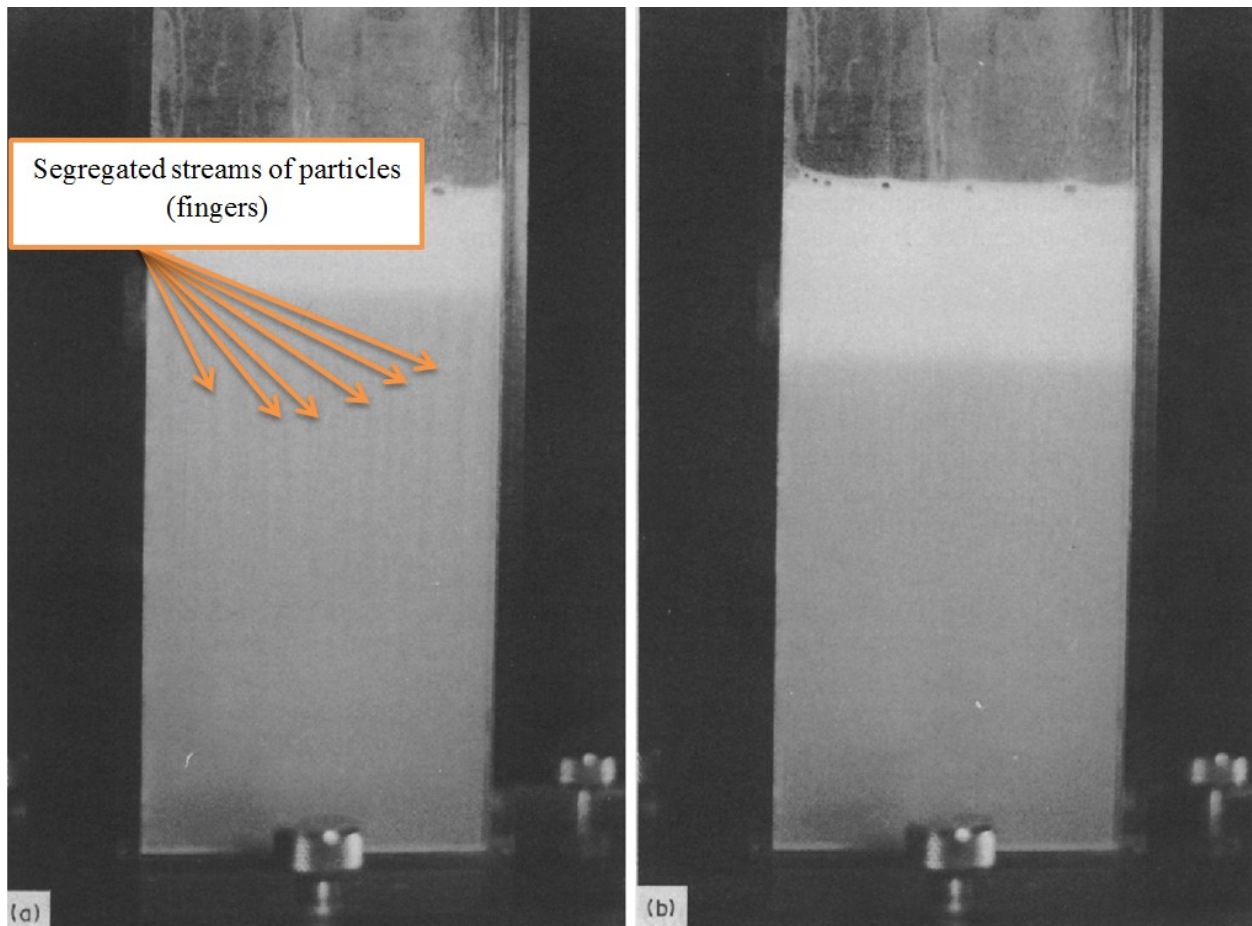
Figure 2.5- Settling of 29 μm particles with $\varphi_p = 0.3$ in a 20% emulsion: a) 180s after the settling begins (strong fingering streams); b) 283s after the settling begins (weak fingering shortly before disengagement). (Reproduced from Yan and Masliyah [16]**)**

In Figure 2.6 (a) a homogenous mixture of water, solid particles, and oil droplets found at the start of the settling process is shown. After a short period, segregated downward streams of particles (fingers) form alongside rising streams of oil droplets (Figure 2.6 b). During this stage, the settling area is divided into five zones from top to bottom: 1- packed bed of oil droplets in water, 2- oil droplets rising (creaming) in water, 3- the region where the fingering phenomenon occurs, 4- particles settling in water, and 5- packed bed of particles in water. The process of rising droplets and settling particles continues until the dispersed phases entirely disengage from each other at time t_D (Figure 2.6 c). After disengagement, particles and droplets settle/rise in

water independently (Figure 2.6 d) until packed beds of particles and oil droplets form at the top and bottom of the settler with a clear water zone separating them.
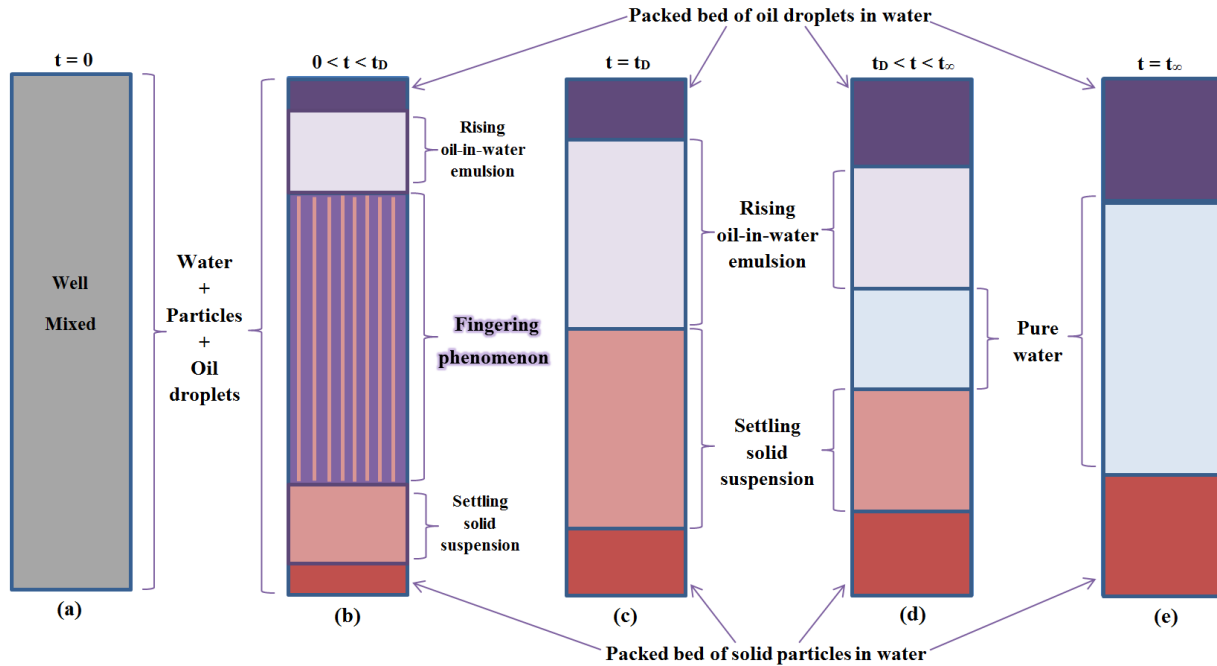
Figure 2.6-Consecutive stages of an unstable particles settling in emulsion; (a) well-mixed, (b) fingering phenomenon period, (c) disengagement of the settling particles from rising emulsion (fingers disappear at this stage), (d) independently settling of solids and rising of oil droplets, (e) packed beds of droplets at top and particles at bottom with a water zone in between.

The results from Yan and Masliyah [16] show that the likelihood of fingering phenomenon occurring increases as the particle size approaches that of the emulsion droplets (i.e. $d_p/d_d \rightarrow 1$).

However, their observations for the settling of the 57 μm particles demonstrate that there are other parameters controlling the occurrence of the fingering phenomenon apart from d_p/d_d. Their observations show that the fingering phenomenon does not occur for 57 μm particles when the oil volume concentration in the emulsion is less than 20%. At higher oil concentrations, the fingering phenomenon occurs, indicating that d_p/d_d and the emulsion properties affect the occurrence of the fingering phenomenon.

There was no additional research in this area after the study of Yan and Masliyah [16] until Beydoun et al. [13] made hindered settling measurements for chrome steel particles in oil-in-

water emulsions. The smallest value of d_p/d_d in their work was 20. Assuming the emulsions to be a continuous phase, their measured settling velocities of the particles agreed with the predicted values from correlations. However, they stated that the assumption of emulsion behaving as a continuum might no longer be valid if the particle size was close to the droplet size. To support their claim, they referred to the Yan and Masliyah study [16].

2.3. Heavy-Light Particle Systems and Stability Theory

Despite the limited research published on emulsion-particle settling systems and their instability, a similar instability occurs in bi-dispersed particulate settling systems. These bi-dispersed settling systems consist of suspensions of light and heavy particles in a liquid. They usually have heavy and light particles of higher and lower density than the fluid, respectively. This thesis will subsequently refer to the aforementioned bi-dispersed mixtures as heavy-light particle systems. These settling systems are similar to emulsion-particle systems. Both include settling and rising species.

In one of the earliest studies in this area, Whitmore [29] investigated the settling rate of methyl-methacrylate particles in an aqueous solution of lead nitrate. To inhibit possible flocculation of the particles, he added 0.1% dispersant to the system. In the two-component system (fluid and one species of particles), measured settling velocities showed good agreement with the theory. However, the addition of polystyrene particles (with a density close to that of fluid) as a third component to the system increased the settling velocity of the methyl-methacrylate particles [29].

After Whitmore discovery [29], Weiland and his coworkers [30]–[34] conducted further investigations on instabilities in heavy-light particle systems. In a study by Weiland and McPherson [30], in which density difference between the light particles and the fluid was greater than that of the Whitmore study [29], measurements showed significant enhancement in the settling rate of the heavy particles. Fessas and Weiland [33] attributed the settling velocity enhancement of the heavy particles to the density difference between the settling and rising streams. They proposed that this density difference can produce a convective force that increases the settling rate of the particles.

Another similarity between the two systems (emulsion-particle and heavy-light particle settling systems) is the successive stages of their settling process. Weiland and coworkers [30]–[34] reported the formation of fingering streams of particles a short time after the settling process starts. The fingers disappeared shortly before the disengagement between the heavy and light particle streams. Figure 2.7 [34] shows a heavy-light particle settling system experiencing unstable settling. In the test shown in Figure 2.7, the colors of the two particle species involved in the settling process were not distinguishable. To observe the instabilities, Weiland et al. [34] coated the heavy particles with a fluorescent dye. To visualize the unstable streams, they took photographs under ultraviolet illumination in a dark room [34]. At the early stages of the settling process (starting from the top left picture in Figure 2.7), heavy particles settle through segregated vertical finger-shaped streams. The fingering phenomenon proceeds until the disengagement settling heavy and rising light particles occurs (bottom right picture in Figure 2.7).

Batchelor and his coworkers [35]–[37] studied the bi-disperse sedimentation of heavy-light particle systems from a different point of view. Their goal was to determine the conditions controlling the formation of fingering streams. They defined the following parameters [37]:

$$\lambda = \frac{d_2}{d_1} \qquad\qquad 2.20$$

$$\gamma = \frac{\rho_2 - \rho_f}{\rho_1 - \rho_f} \qquad\qquad 2.21$$

where subscripts 1, 2, and f refer to heavier particles, lighter particles, and the fluid, respectively.

They presented their results in as a stability map as illustrated in Figure 2.8 [37]. Figure 2.8, indicates settling system stability status in terms of λ and γ. The experimental points in Figure 2.8 were obtained at $\varphi_1 = \varphi_2 = 0.15$ (φ is the volume fraction).
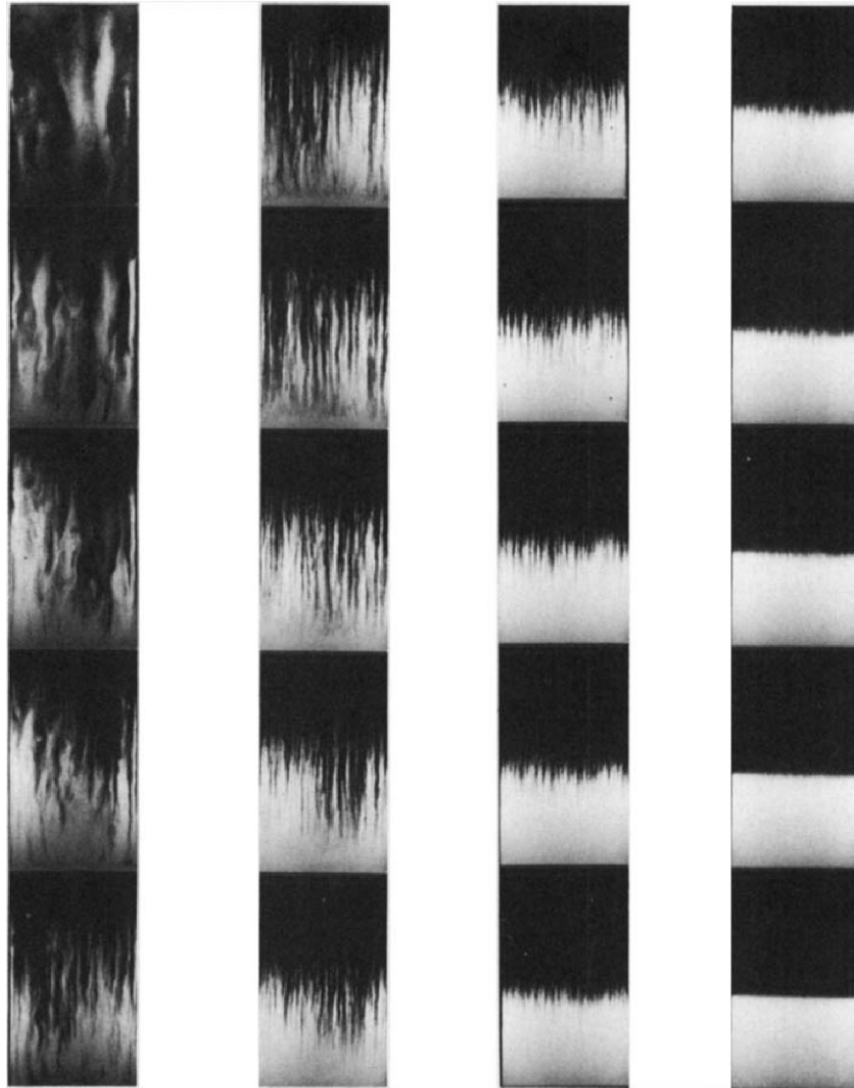
Figure 2.7- Different stages of an unstable heavy-light particle settling process from the beginning (top left) to the disengagement of the settling heavy particles from rising light particles (bottom right) (Reproduced from Weiland et al.[34])

The stability map shown in Figure 2.8 is divided into three zones: stable, marginal, and unstable. The region surrounded by the hatched area (marginal zone) is called the unstable region. Instability occurs in all experiments carried out with (γ, λ) values within the unstable region. The region outside the marginal zone is called the stable region where particles settle uniformly without the formation of any segregated streams. The marginal zone of the map is also called the "stability boundary." Batchelor and Van Rensburg [37] stated that some segregated structures could appear for a short time in this marginal zone despite particles generally settling uniformly. Therefore, they could not categorize this as either stable or unstable settling.
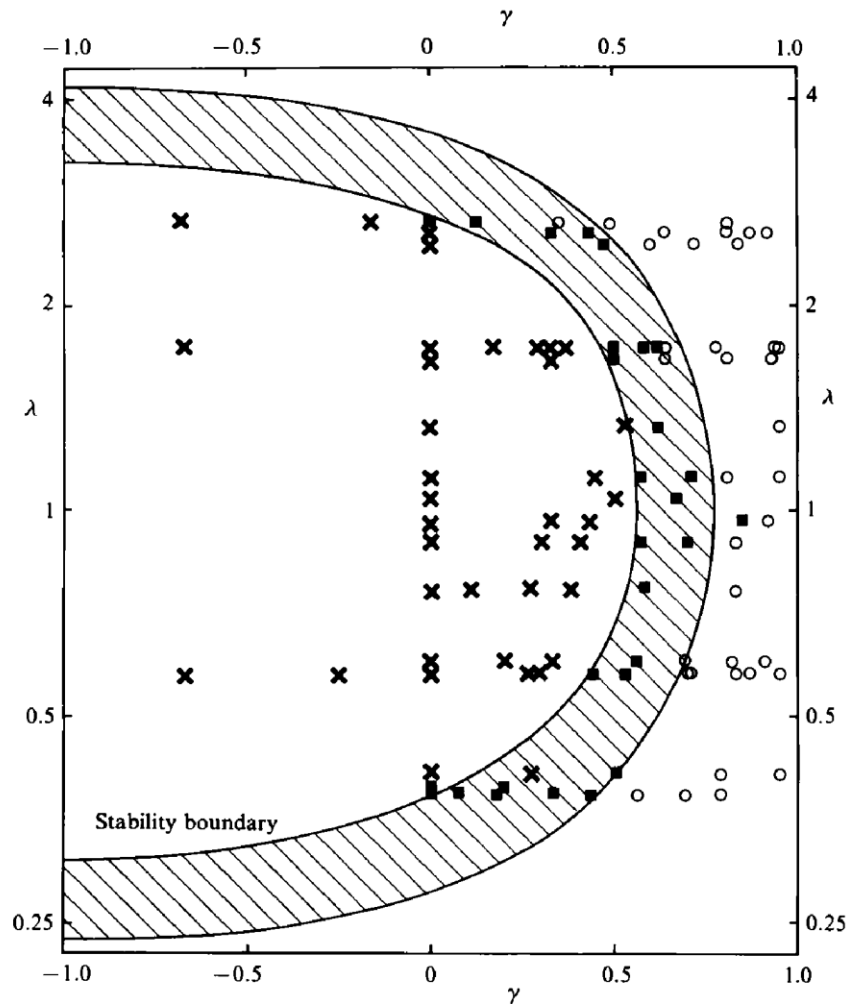
Figure 2.8- Stability map for heavy-light particle settling systems. The symbols ×, ■, ○ represent unstable, marginal, and stable settling, respectively. (Reproduced from Batchelor and Van Rensburg[37])

The formation of fingering streams results from the accumulation of particles in different locations of the mixture such that the particles are no longer in a fully dispersed state. Batchelor and Van Rensburg [37] noted that random local perturbations in the concentration of the particles could trigger this deviation from the homogeneous dispersed state in heavy-light particle systems.

Batchelor and Van Rensburg [37] modeled the response of heavy-light particle systems to the concentration perturbations using the following equation:

25

$$\frac{\partial \varphi_i}{\partial t} = -\sum_{j=1}^{2} \left(\frac{\partial \varphi_i v_i}{\partial \varphi_j}\right)^{(0)} . \nabla \varphi_j , \qquad i = 1, 2 \qquad\qquad 2.22$$

where v_i is the velocity of particle type i relative to the zero-volume-flux axes, and t represents the time. The superscript (0) indicates the values of the parameters in the undisturbed dispersion. Each v_i is a function of λ, γ and both φ_1 and φ_2.

To investigate the evolution of the small concentration disturbances into the regions with accumulated number of particles of one species (i.e., fingers), φ_i should be defined as a function of location/distance from an stationary origin of coordinates (x) and time (t) [37]:

$$\varphi_i = \varphi_i^{(0)} + A_i \exp[\sigma t + \mathrm{i}k.(x - ct)] , \qquad i = 1, 2 \qquad\qquad 2.23$$

where i is imaginary and A_i, σ, k, and c are the wave amplitude, phase shift, wavenumber vector, and angular frequency, respectively.

By substituting Equation 2.23 into 2.22 and solving the resulting equation, eventually, it can be shown that to have an exponentially growing concentration disturbance, the following condition should be satisfied:

$$I = \left(\frac{\partial \varphi_1 v_1}{\partial \varphi_1} - \frac{\partial \varphi_2 v_2}{\partial \varphi_2}\right)^2 + 4\frac{\partial \varphi_1 v_1}{\partial \varphi_2}\frac{\partial \varphi_2 v_2}{\partial \varphi_1} < 0 \qquad\qquad 2.24$$

If concentration disturbances grow through time, they finally form fingers. In other words, Equation 2.24 is the required condition for the formation of the fingering streams.

Unfortunately, there is little information available about the dependence of v_i on the parameters φ_i, γ, and λ; therefore, the only way to define the boundary, as Batchelor and Rensburg [37] have done in their study, is to do experiments. Rewriting Equation 2.24 for the emulsion-particle systems, the condition for the formation of the fingering streams is:

$$I = \left(\frac{\partial \varphi_p v_p}{\partial \varphi_p} - \frac{\partial \varphi_d v_d}{\partial \varphi_d} \right)^2 + 4 \frac{\partial \varphi_p v_p}{\partial \varphi_d} \frac{\partial \varphi_d v_d}{\partial \varphi_p} < 0 \qquad 2.25$$

where subscripts p and d represent the particles and droplets, respectively.

Although Equation 2.25 cannot be used to define the stability boundary, it can be helpful to justify some behaviors of the emulsion-particle settling systems. As a limiting case, Batchelor and Van Rensburg [37] used Equation 2.24 to check the stability status of the heavy-light particle settling systems when $\lambda \ll 1$. It is possible to apply the same approach used by Batchelor and Van Rensburg [37] to check for similar conditions in emulsion-particle settling systems (i.e., a condition where the particles are significantly larger than emulsion droplets). In that condition, the emulsion behaves as a continuum with the density of:

$$\rho_e = \rho_w + \beta (\rho_d - \rho_w) \qquad 2.26$$

where $\beta = \frac{\varphi_d}{1 - \varphi_p}$ is the volume fraction of the droplets in the emulsion. The viscosity of the emulsion can be defined as a function of β (i.e. $\mu_e = \mu_w f(\beta)$). In such conditions, it can be stated that:

$$v_p = v_{p\infty} B(\varphi_p) \frac{1 - \gamma \beta}{f(\beta)} = v_{p\infty} B(\varphi_p) C(\beta) \qquad 2.27$$

where $v_{p\infty}$ is the terminal settling velocity of the particle in pure water, and $B(\varphi_p)$ is the mobility function (in R-Z equation: $B(\varphi_p) = (1 - \varphi_p)^n$). The velocity of the oil droplets is:

$$v_d = v_{d\infty} B(\beta) - \frac{\varphi_p v_p}{1 - \varphi_p} \qquad 2.28$$

27

where $v_{d\infty}$ and $B(\beta)$ have the same definitions for the droplets that $v_{p\infty}$ and $B(\varphi_p)$ had for the particles. It should be noted that $v_{d\infty} = \gamma\lambda^2 v_{p\infty}$. Substituting Equations 2.27 and 2.28 into Equation 2.25 gives:

$$I = v_{P\infty}^2 \left[C(\beta) \times \left(\frac{B(\varphi_p)}{1 - \varphi_p} + \varphi_p B'(\varphi_p) \right) - \gamma\lambda^2 (B(\beta) + \beta B'(\beta)) \right]^2 - 4\gamma\lambda^2 v_{P\infty}^2 \frac{\varphi_p \beta}{1 - \varphi_p} B(\varphi_p) B(\beta) C'(\beta) \qquad 2.29$$

In Equation 2.29, when $\lambda \to 0$, the terms with λ^2 become negligible. After eliminating the terms including λ^2, only a squared term survives. In the other words, when $\lambda \to 0$, the right hand side of the Equation 2.29 is always positive (i.e. $I > 0$). This result shows that the system remains in a homogenously dispersed state (stable state) with no fingering phenomenon occurring provided the size of the particles is considerably larger than the size of the droplets, regardless of the values of φ_p, φ_d, and γ.

The fact remains that, as Equation 2.25 shows, the stability boundary can vary with λ, γ, φ_p, and φ_d. Therefore, these parameters should be control variables in the proposed experiments to study the stability status of the emulsion-particle settling systems.

2.4. Conclusions

Except for Yan and Masliyah paper [16], the literature review for this project shows little information about emulsion-particle settling systems. The key points from the Yan and Masliyah study [16] are:

- When the particle size approaches that of the oil droplets, a phenomenon called fingering happens, which is defined as the settling of particles in segregated finger-shaped streams.
- At high oil concentrations, there is a greater possibility for the fingering phenomenon to occur.
- The fingering phenomenon enhances particle settling velocity.

- The emulsion cannot be considered as a continuous phase once the fingering phenomenon occurs.

Below are some limitations of the Yan and Masliyah [16] research:

- They revealed that the conditions $\frac{d_d}{d_p} \rightarrow 1$ and higher oil concentration (dispersed phase) in emulsion increases the likelihood of instability and formation of fingers. As discussed in the preceding Section other parameters also affect system stability, and these must be investigated

- System stability is a critical issue: when the fingering phenomenon occurs, conventional correlations for settling rate predictions are not valid. If one does not know the conditions under which the system becomes unstable, it would be impossible to know if equations like Richardson-Zaki are applicable.

- They gave no additional information on the behaviour of the unstable emulsion-particle settling system during the fingering phenomenon except that settling velocity increases. The following questions thus require answers:
    - Are concentrations of particles and droplets inside the fingers different from their initial values in the homogenous mixture? If so, are they higher or lower than the initial concentrations?
    - What is the role of fluid movement inside the fingers? How does it contribute to the particle velocity enhancement?

The review of the studies related to heavy-light particle settling systems shows that they are similar to emulsion-particle settling systems. Batchelor and Van Rensburg [37] produced a stability map of $\lambda = \frac{d_{light}}{d_{heavy}}$ vs. $\gamma = \frac{\rho_{light} - \rho_f}{\rho_{heavy} - \rho_f}$ (in a constant value of $\varphi_{heavy} = \varphi_{light} = 0.15$) for heavy-light particle settling systems. The map defines the stability status of the systems for different (γ, λ) values.

Equation 2.24 shows that concentrations of both heavy and light particles affect the stability of settling systems, in addition to the λ and γ parameters from the Batchelor and Van Rensburg [37] stability map (Figure 2.8).

However, there is no stability map for emulsion-particle settling systems. Stability maps would be an important tool to determine if an emulsion-particle system with certain given properties is stable or not.

2.5. Research Objectives

Regarding the conclusions from the literature review, provided above, the main objectives of the current research project can be written:

- To produce stability maps for emulsion-particle settling systems by designing and conducting stability tests using λ, γ, φ_p, and oil concentration in the emulsion as controlled variables.
- To develop a model that describes the movement of particles, droplets, and the fluid inside the fingers. The goal is to extend the knowledge about the fingering phenomenon and explain how fluid flow inside the fingers accelerates particle settling.

Chapter 3
Experimental and Calculation Methods

3.1. Materials

3.1.1. Particles

In the preliminary settling tests on sand particles available in the lab, it turned out that one important challenge was distinguishing the particles in emulsion-particle systems. The particle color should be distinguishable from the white emulsion to enable the upper interface of the settling particles and the fingering streams to be visible through the emulsion. The other important feature of the particles is their density. Particle density should be higher than that of water so that they settle down. The ratio λ, which is defined as $\frac{droplet\ diameter}{particle\ diameter}$, is one of the key parameters in this project. Since it is difficult to produce a range of droplet diameters during the emulsion preparation procedure, it was more convenient to purchase particles with different sizes.

According to the points mentioned above, the particles of choice for the experiments were silver-coated glass beads, which their credibility was confirmed through a set of preliminary tests (see Appendix A). Four packages of silver-coated glass beads (model numbers: TP12S16, TP25S12, TP50S06, TP100S02) with different sizing (Sauter mean diameters: 13 µm, 26 µm, 51 µm, and 101 µm) were purchased from Potters Industries co. The particles density was 2500 kg/m³.

3.1.2. Oils

Density is the key consideration in choosing the oils for the experiments. On the one hand, the oil should be lighter than water so that the oil droplets can rise through water and produce a counter-current movement to that of the particles (which is needed for the formation of the fingering streams). On the other hand, $\gamma = \frac{\rho_o - \rho_w}{\rho_p - \rho_w}$ is one of the main parameters of this project to define the stability boundary. Since ρ_p and ρ_w are constant, the only way to obtain different values of γ is to use oils with different densities. Therefore, three types of oils were used to prepare emulsions: Isopar M (Kane Instrumentation, Model #: F102), Light Mineral Oil (Sigma-

Aldrich, Model #: MKCC7165), and Silicone Oil (Sigma-Aldrich, Model #: MFCD00132673) with the densities of 789, 838, and 913 kg/m^3 respectively.

Of the oils mentioned above, Silicone Oil was provided in different viscosities by the supplier. It is easier for the homogenizer to disperse the oil droplets with a lower viscosity through the water. Therefore, Silicone Oil with the lowest available viscosity (5cSt) was selected and purchased for this project.

3.1.3. Surfactant

An emulsion is a mixture of two or more immiscible liquids. From the dispersed/continuous phase point of view, there are two types of oil-water emulsion: oil-in-water (oil is the dispersed phase) and water-in-oil (water is the dispersed phase) [38]. All emulsions made and used in this project are oil-in-water. Emulsions are naturally unstable, meaning that the droplets of the dispersed phase start to coalesce and eventually form two separate phases shortly after its dispersal in the continuous phase. Stabilizing the dispersed droplets and preventing their coalescence requires the addition of "surfactants" to the emulsion. This is because surfactants are organic molecules with a hydrophilic head and a hydrophobic tail, making them suitable as emulsion stabilizing agents [39]. The surfactants do this action by dissolving their head into the water phase and their tail into the oil phase. As shown in Figure 3.1, they form a barrier around dispersed droplets to prevent their coalescence.

Triton X-100 is the surfactant used to prepare the emulsions for this project. Hydrophilic-lipophilic balance (HLB) [39] is an empirical scale for choosing a surfactant to prepare an oil-in-water or a water-in-oil emulsion. It should be between 8 and 18 for preparing an oil-in-water emulsion. Triton X-100 HLB value of 13.5 [40] makes it an appropriate surfactant for producing oil-in-water emulsions.
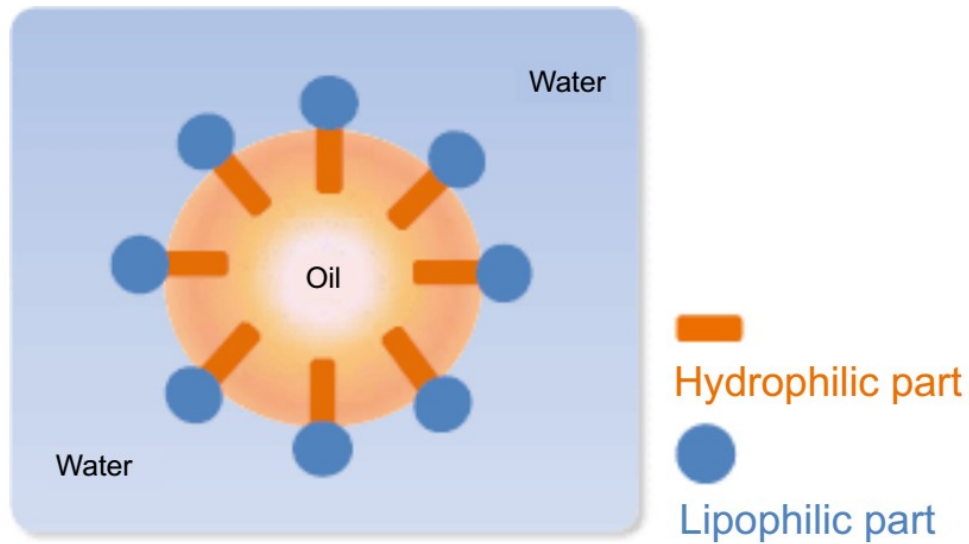
Figure 3.1- Surfactant molecules covering the oil droplet surface and stabilizing the emulsion. (Reproduced from Menaa [41]**)**

3.1.4. Deionized Water (DI water)

To ensure the absence of ions in the systems and accuracy of the experimental results, all emulsions in this study were prepared using deionized water produced by the water purification equipment at PTP lab (For more information about the equipment see Section 3.2.5)

3.2. Equipment

3.2.1. Settling Column

All settling tests in this project were done in the Plexiglas settling column shown in Figure 3.2. For the purpose of settling velocity measurements, the right side of the column was graduated in millimeters. Internal dimensions of the settler are 2.3×7.7 cm.
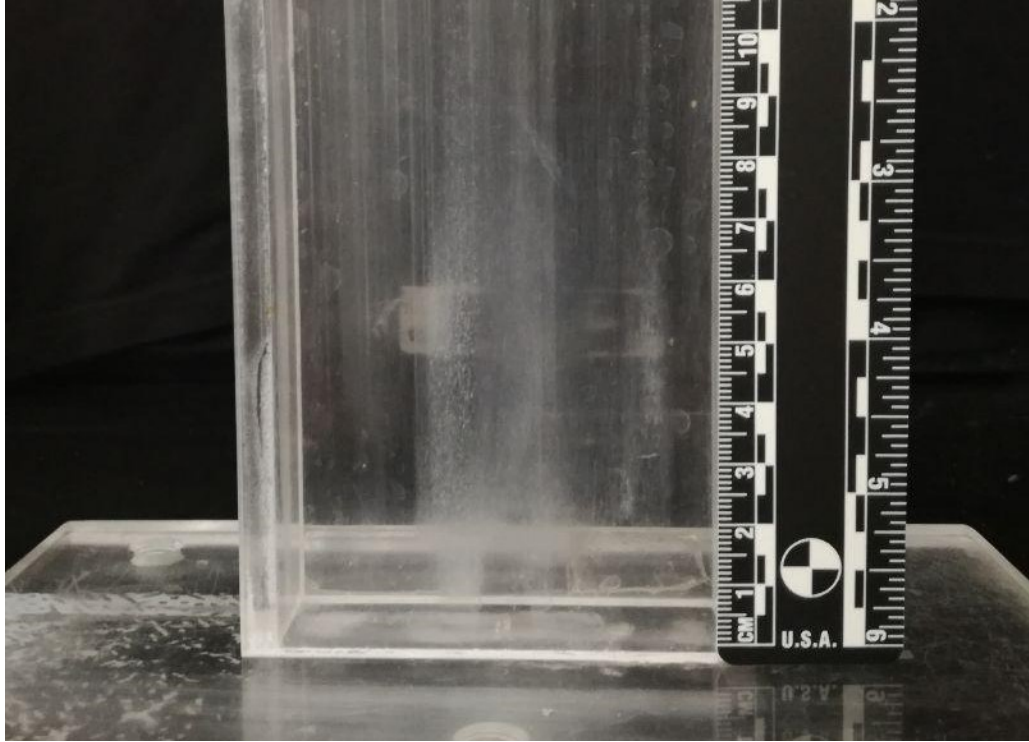
Figure 3.2- The settling column in which all the settling tests of the project were performed

3.2.2. Homogenizer and Probe

A VWR 250 homogenizer with high revolutionary speed was used to properly disperse oil droplets into water during emulsion preparation. This homogenizer revolutionary speed was set to 10000 rpm for each emulsion prepared.

A suitable VWR Saw-Tooth probe (dimensions of 11.5*1 cm) for emulsion preparation in small and medium-sized beakers was installed on the homogenizer generator.

3.2.3. Microscope

A ZEISS AxioLab.A1 microscope was used to observe and take photographs of the emulsion droplets (using a camera mounted on the microscope). The photographs were used for droplet size analysis.

3.2.4. Photography Equipment

A Canon EOS Rebel T3i DSLR camera was used to record the settling tests. It can simultaneously take photographs and record video. This feature enables accurate measurements and observations of the settling tests.

The lens mounted on the camera was a Canon EF-S 10-18mm with autofocus capability that made it a suitable lens to take clear pictures and videos of the settling tests.

Two sets of work lights covered with tissue papers as light diffusers were used to adjust the illumination of the settling column. A piece of black cloth was used as background.

3.2.5. Other Equipment

Other equipments used in this project experiments include:

- Water Deionizer: An Elix Advantage 5 Water Purification System was used to produce DI water for preparing the emulsion. It can produce 5 liters of DI water per hour.
- Pipette: 3 ml Cole-Parmer plastic transfer pipettes were used to gradually add the oil to the stirring mixture during emulsion preparation.
- Mass scale: A&D FX-3000 Electronic Balance (accuracy of 0.01 grams) was used to measure the mass of particles required for conducting each batch settling test.
- T-shape stirrer: A wooden T-shape stirrer (head width: 7 cm, length: 30 cm) was used to mix the particles and emulsion at the beginning of each settling test.
- Graduated cylinders: 50 ml and 20 ml graduated cylinders were used to measure and transfer assigned volumes of water and oil during emulsion preparation.
- Syringes: 5 ml syringes were used to measure and transfer the assigned amounts of Triton X-100 surfactant during emulsion preparation.
- Beakers: 400 ml and 300 ml beakers were used to prepare and carry emulsions.
- Glass rods: Glass rods were used to stir the 1% surfactant solution needed for emulsion preparation. They also were used to stir the emulsion before pouring it into the settling column.

- Micropipette: A micropipette was used to place a very small sample of emulsion on the microscope slide.
- Microscope slides and coverslips: Fisherbrand microscope slides (25mm×75mm×1mm) and coverslips (24mm×50mm×0.13mm) were used to hold the emulsion samples under the microscope.
- Parafilm: It was used to cover the beakers containing oil, surfactant solution, or emulsion.

3.3. Experimental Procedure

3.3.1. Emulsion Preparation

The following steps illustrate the emulsion preparation procedure in this project (Note: safety measures for the whole procedure are available in greater detail in the Safe Work Procedure in Appendix F):

1- Take two beakers, graduated cylinders, a syringe, and a funnel alongside the oil and surfactant. One of the beakers should be either a 400 or a 300 ml beaker (depending on the desired emulsion volume)
2- Use the following equations to calculate the volume of DI water and surfactant required to prepare the 1% surfactant aqueous solution:

$$Volume\ of\ 1\%\ surfactant\ solution$$
$$= Volume\ of\ emulsion\ to\ be\ prepared \times \frac{100 - Emulsion\ oil\%}{100} \qquad 3.1$$

$$Volume\ of\ water = 0.99 \times Volume\ of\ 1\%\ surfactant\ solution \qquad 3.2$$

$$Volume\ of\ Triton\ X\_100\ (surfactant) = 0.01 \times Volume\ of\ 1\%\ surfactant\ solution \qquad 3.3$$

3- Use a graduated cylinder to measure the volume of water calculated in Step 2 and pour this volume into the beaker that is to be used for the emulsion preparation.

4- Use the 5 ml syringe to take the volume of Triton X-100 calculated in Step 2 and add it to the water.

5- Gently stir the surfactant solution with a glass rod for around half an hour until the surfactant is completely dissolved into water.

6- Cover the beaker containing the surfactant solution with a Parafilm.

7- Use the following equation to calculate the volume of the oil needed for preparing the emulsion with desired oil volume%:

$$Oil\ volume\ =\ Volume\ of\ emulsion\ to\ be\ prepared \times \frac{Emulsion\ oil\%}{100} \qquad 3.4$$

8- Use a graduated cylinder and a funnel to measure the amount of oil calculated in Step 7, and then pour this volume into the other beaker.

9- Put the beakers of prepared surfactant solution and the oil alongside a pipette on a cart and bring them to the homogenizer, which is in a different lab. (Also put mopping pads and two wash bottles on the cart. One of the wash bottles should contain DI water and the other toluene to clean the homogenizer after using it.)

10- Plug in the homogenizer and set its revolutionary speed on 10000 rpm.

11- Put the 1% surfactant solution under the homogenizer so that the probe tip is completely inside the solution.

12- Turn on the homogenizer.

13- Gradually add the oil to the surfactant solution (with the approximate rate of 1 ml per second) using the plastic transfer pipette. During this action, the clear solution gradually becomes opaque and white. This color change is shown in Figure 3.3, which indicates that the oil droplets are being dispersed through water.

14- Turn off and unplug the homogenizer after the shearing period is completed. Carefully remove the beaker containing the prepared emulsion from under the homogenizer.

15- Cover the beaker with Parafilm and store the emulsion in a safe place for subsequent use in the settling tests.

16- Carefully rinse the homogenizer probe with toluene then clean it with DI water and and allow it to dry for the next use. Pour the waste water and toluene into the organic waste bottle.
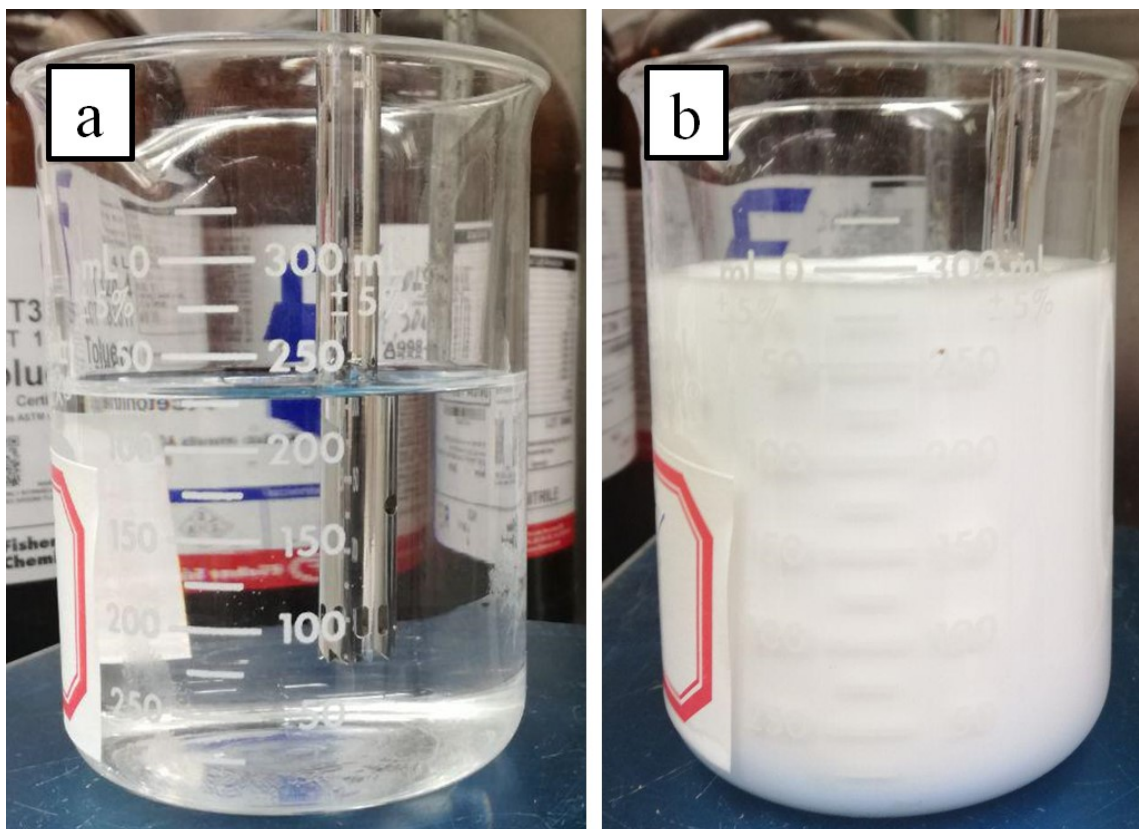
Figure 3.3- Initial transparent surfactant aqueous solution (a) gradually becomes an opaque and white emulsion (b) as the oil droplets form during the emulsion preparation process

During a set of preliminary tests, different emulsion preparation procedures with different beaker sizes and different shearing times were performed. The goal was to find the best emulsion preparation conditions for each oil so that the smallest oil droplet size with the largest possible

emulsion volume could be achieved. Table 3.1 shows the final results. The volumes and shearing times shown in Table 3.1 were the values used in preparing all emulsions in this project.

Table 3.1- Maximum attainable emulsion volume to reach the desired droplet size for the oil-in-water emulsions made using different oils

Oil Type	Beaker Size (ml)	Shearing Time (min)	Prepared Emulsion Volume (ml)
Isopar M	400	10	300
Light Mineral Oil	300	20	200
Silicone Oil	400	20	300

3.3.2. Droplet Size Measurement

Droplet size measurements were made through the following steps (Note: safety measures for the whole procedure are available in greater detail in the Safe Work Procedure in Appendix F):

1- Take a small drop of the emulsion using the micropipette and put it on the microscope slide.

2- Carefully put the coverslip on the emulsion drop and let it completely expand in the gap between the slide and coverslip.

3- Put the prepared slide under the microscope lens.

4- Turn on the microscope light and set it on the dark field (DF) setting.

5- Adjust the clarity of the picture using the focusing drive screws of the microscope. Do this task until a clear view of the oil droplets is obtained.

6- Take a snapshot and save the file for further processing.

7- Use the scale on the microscope snapshot to calculate the ratio of the $\frac{real\ length\ in\ \mu m}{length\ in\ the\ image\ in\ pixels}$. This can be done using ImageJ software.

8- A Matlab script was written to process the images taken with the microscope camera and produce the droplet size distribution. As can be seen in Figure 3.4, this Matlab

script can detect the oil droplets. Insert the ratio calculated from Step 7 in the Matlab script to measure the diameter and size distribution of the oil droplets.
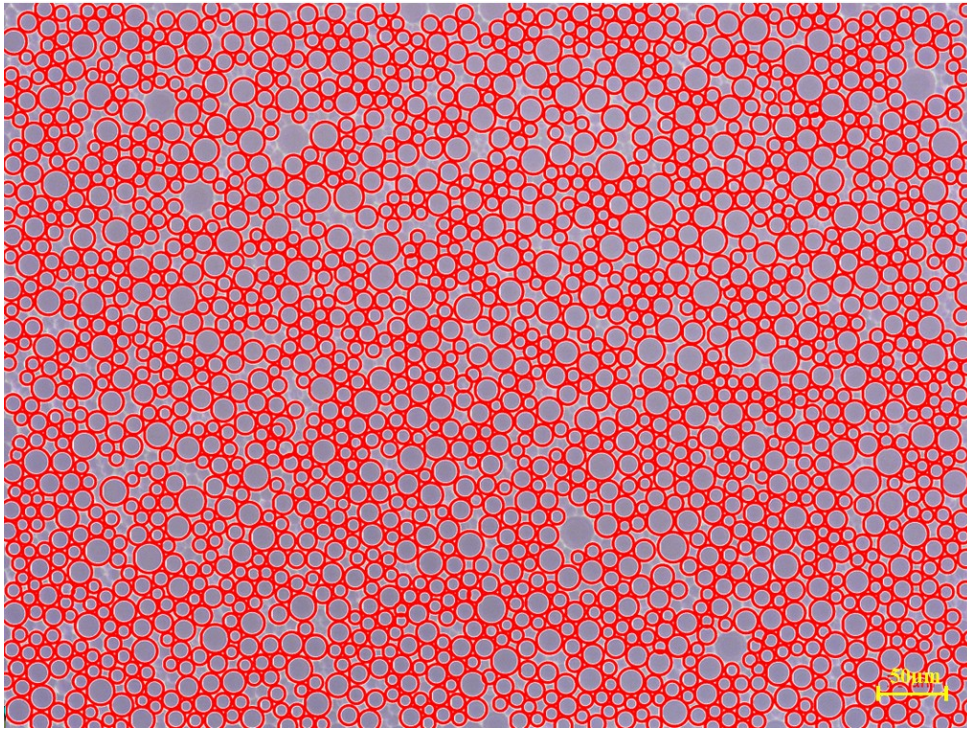
Figure 3.4- Oil droplets detected by the MATLAB script for a 20% Silicone Oil emulsion sample of the project

3.3.3. Batch Settling Tests and Velocity Measurements

The settling tests in this project were done using the following procedure (Note: safety measures for the whole procedure are available in greater detail in the Safe Work Procedure in Appendix F):

1- Stir the beaker containing the emulsion with the glass rod. This is necessary before pouring the emulsion into the settler because after the emulsion preparation, as shown in Figure 3.5, oil droplets gradually start to rise and gather at the top of the emulsion in a phenomenon called creaming. Hence, stirring ensures a uniform concentration of oil droplets in the emulsion.

2- Pour 125 ml of the emulsion into the Plexiglas settling column using a graduated cylinder.
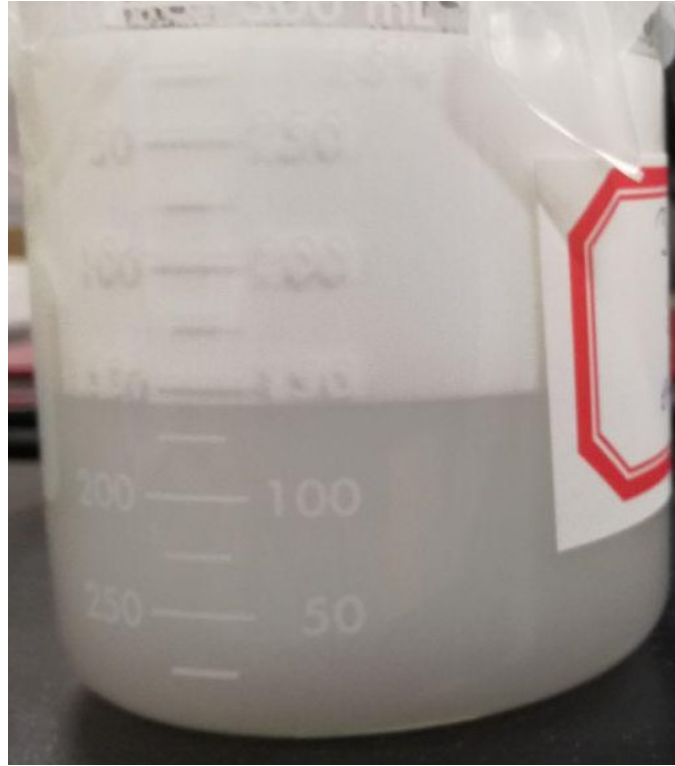
Figure 3.5- Emulsion oil droplets rising and creaming at the top (white area) after a few hours being undisturbed.

3- Calculate the mass of particles needed to obtain the particle volume fraction (φ_p) for each test using the following equation:

$$M_p = \frac{\varphi_p}{1 - \varphi_p} \rho_p \forall_e \qquad\qquad 3.5$$

where M_p and $\forall_e$ are mass of particles and volume of the emulsion respectively.

4- Measure the mass of particles calculated in Step 3 using the mass scale before adding them to the emulsion.

5- Stir the mixture with up/down movements of the T-shape stirrer for around 15-20 seconds so that the particles and emulsion droplets become well mixed.

6- Stop stirring and observe the settling process after Step 5.

7- Use the camera to record a video of the settling process. Also, take multiple photos from different stages of settling (such as fingering phenomenon (if it happens) and settling before and after disengagement).

8- Save the video file and photos for further investigation.

9- Review the video and measure the settling velocity of the particles. Particle settling velocity can be measured by dividing the displacement of the settling particles upper interface by the elapsed time. In other words, the slope of line in the graph shown as Figure 3.6 is the particle settling velocity.
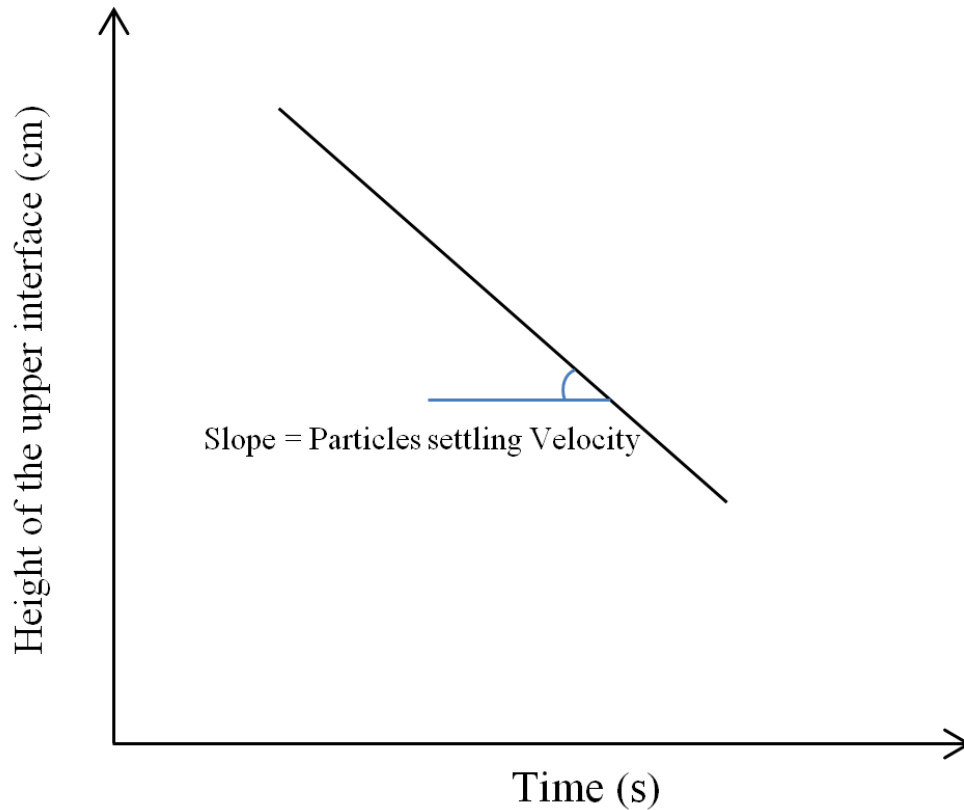
Figure 3.6- Schematic illustration of a typical particle settling curve, showing the change of the upper particle interface height (H) with time (t). The slope of the H=F(t) line is taken as the particle settling velocity

Figure 3.7 illustrates the different stages of an unstable settling process conducted in this project, where 26 μm particles with φ_p= 0.2 are settling through a 20% Isopar M emulsion. For this test, λ = 0.39 and γ = -0.141. Figure 3.7a illustrates the fingers of particles settling through the emulsion. Figure 3.7b shows the disengagement between the settling particles and the rising emulsion. As can be seen, the fingers disappear when the particles disengage from the emulsion. Figure 3.7c shows the settling of particles after disengagement, where they are settling merely in water. Figure 3.7d illustrates the completed settling when all the particles have been settled at the bottom of the settler and formed a packed bed.
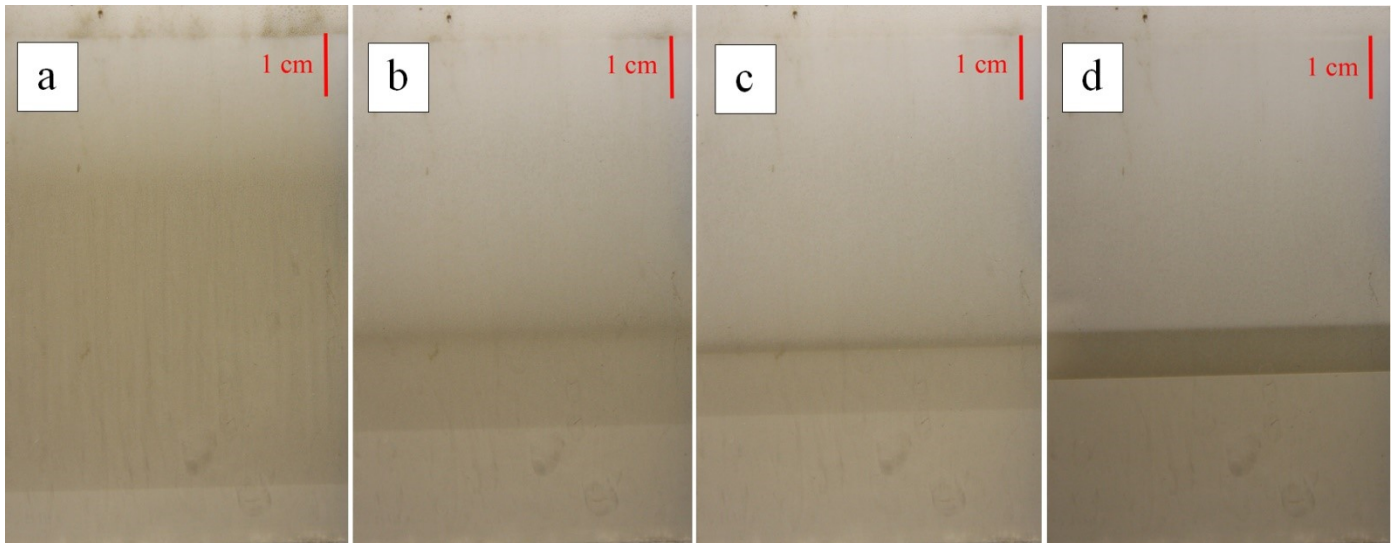
Figure 3.7- Different stages of an unstable settling test; a) engagement of particles and emulsion with the presence of fingering phenomenon, b) the moment of particles disengagement from the emulsion, c) particles settling in water after disengagement, d) settling completed

Figure 3.8 shows the different stages of a stable settling process conducted in this project, where 51 μm particles with φ_p= 0.15 are settling through a 10% Isopar M emulsion. For this test, λ= 0.20 and γ = -0.141. This Figure shows that particle settling finishes before disengagement happens, which occurred for all stable tests. In the stable tests, the rise velocity of the droplets is so slow that part of the emulsion droplets cannot exit the settling particles before the settling ends, so that they become trapped among the settled particles.
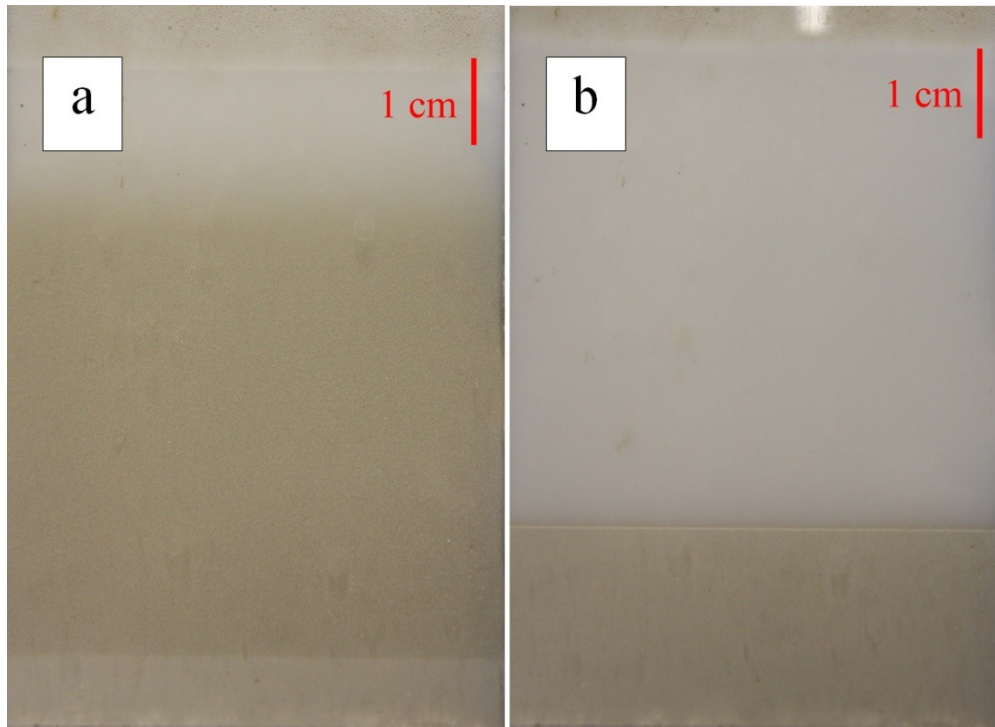
Figure 3.8- Different stages of a stable test; a) particles settling through emulsion without fingers formation, b) settling completed before disengagement happens

As mentioned earlier, the stability status of the system was not the only parameter recorded in the tests. For each test, the settling velocity of the particles was measured by tracking the displacement of the settling particles upper interface through time. In Figure 3.7 and 3.8, this interface is distinguishable in both stable and unstable tests as a horizontal line between the settling particles and the white emulsion above them. These velocity measurements were carried out to be used in further analysis. Settling velocity analysis is presented in Chapter 5 of this thesis.

Figure 3.9 summarizes the experimental steps from emulsion preparation to settling measurements.
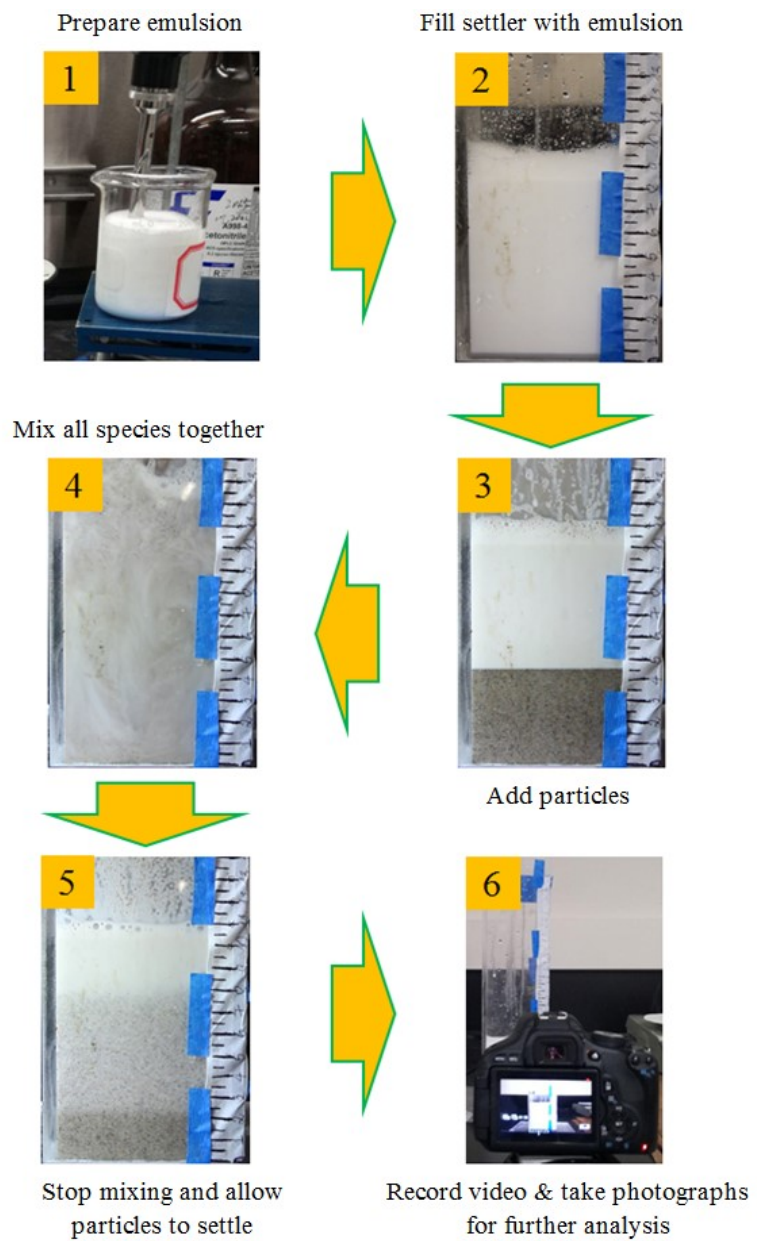
Figure 3.9- Overview of the settling tests experimental steps

3.4. Velocity Calculation Method

The emulsion is considered as the continuous phase for settling velocity calculations. Therefore, the calculation method is dependent on the particle settling medium: emulsion (when the particles are still engaged with the emulsion) or water (after disengagement).

Calculating particle settling velocity when the particles and emulsion are disengaged poses no problem because the particles are settling through water ($\mu_f = \mu_{water}$).

However, when the particles and the emulsion are engaged, assuming the emulsion as a continuous fluid, its viscosity can be calculated using the Pal [42] equation that is exclusively defined for emulsions:

$$\mu_r \left(\frac{2\mu_r + 5K}{2 + 5K} \right)^{1.5} = \left(1 - \frac{\beta_o}{\beta_m} \right)^{-2.5\beta_m}, \qquad K = \frac{\mu_o}{\mu_w} \qquad\qquad 3.6$$

where μ_r is the relative viscosity of the emulsion to that of water ($\frac{\mu_e}{\mu_w}$); β_o and μ_o are volume fraction and viscosity of the oil respectively; and β_m is the maximum attainable concentration of the oil droplets (~0.6). **Note**: The reason for using β instead of φ is that here β is the volume fraction in the emulsion which should not be confused with φ which is the volume fraction in the whole mixture.

The same argument applies to fluid density (ρ_f). When the particles and emulsion are disengaged: $\rho_f = \rho_{water}$. Before disengagement, when the particles are settling through emulsion:

$$\rho_f = \rho_{emulsion} = \beta_o \rho_o + (1 - \beta_o)\rho_{water} \qquad\qquad 3.7$$

Using the equations mentioned above and the ones provided in Section 2.1, the velocity calculation procedure would be as follows:

1- Calculate ρ_f and μ_f:

> For calculating the settling velocity when the settling particles are engaged with emulsion: use Equation 3.6 for fluid viscosity and Equation 3.7 for fluid density.

> For calculating the settling velocity when the settling particles are disengaged from emulsion: $\rho_f = \rho_{water}$ and $\mu_f = \mu_{water}$

2- Calculate Ga using Equation 2.10

3- Calculate $Re_{p\infty}$ (and consequently $v_{p\infty}$) using Equation 2.11

4- Calculate the R-Z index using Eq. 2.15

5- Calculate the particle settling velocity (v_p) using the Richardson-Zaki equation (Equation 2.19)

3.5. Experimental Plan

To do the settling stability tests, four particle concentrations (φ_p =0.15, 0.2, 0.25, and 0.3) and three values of emulsion oil% (($\beta_o \times 100$)% =10%, 20%, and 30%) were chosen. For each set of (φ_p, emulsion oil%), a stability map would be produced. Figure 3.10 shows the test points on the proposed stability maps. Emulsions comprising the same oils have similar droplet sizes. Since there are four particle sizes purchased for the experiments, four λ values would be available for the settling tests using the emulsions made of each oil. λ_1, λ_2, λ_3, and λ_4 in Figure 3.10 illustrate four different λ values that could be obtained for settling of particles with different sizes in the different emulsions.
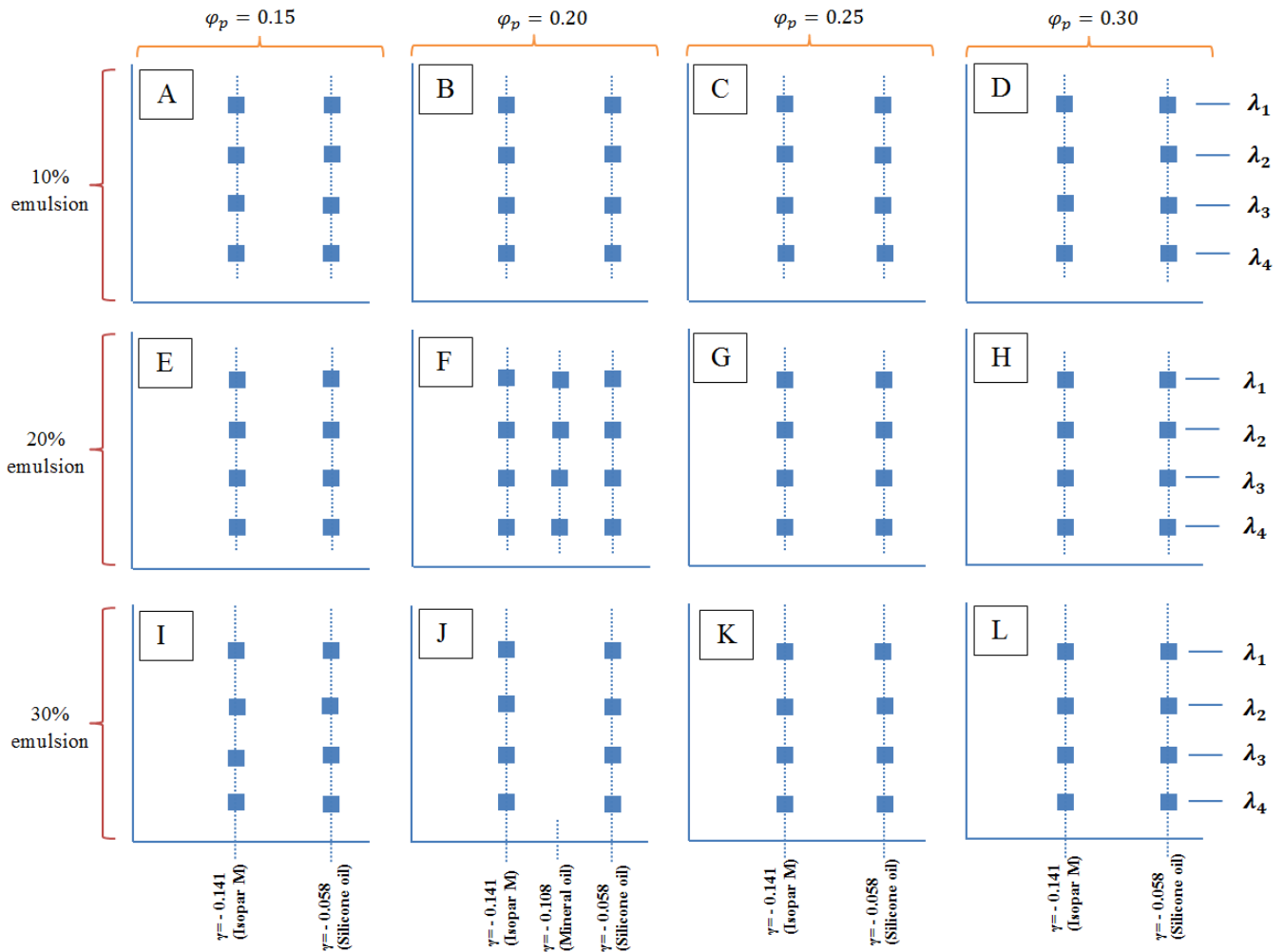
Figure 3.10- The proposed test points on the twelve stability maps assigned to be produced in the project

Maps F and L are the first and second maps whose stability tests would be done, respectively. Map F has an average particle and oil concentrations (i.e., not too high or too low), close to particle/oil concentrations of Batchelor and Van Rensburg stability map. Therefore, doing its tests would have a high chance of producing the stability boundary. The tests in Map F were done in the emulsions made of all three oils. It would help to figure out the general shape of the stability boundary. On the other hand, Map L has the highest particle/oil concentrations of all maps. Comparing the results of Maps F and L could provide useful information about how stability boundary behaves when concentrations are significantly changed. An example of this boundary behavior is schematically shown in Figure 3.11. Then, deciding about how to design

49

the test plan for other maps would be easier. Based on the results of the stability tests in map L, one of the following approaches would be employed:

- If comparison of Map L with Map F shows that the stability boundary only shifts upward or downward, without changing the shape (Figure 3.11a), all the tests in the rest of the maps would only be done with one type of oil (Isopar M).
- If comparison of Maps F and L shows that the shape of stability boundary changes (Figure 3.11b), then all the other tests in the rest of the maps would be done with both Isopar M and Silicone Oil emulsions.
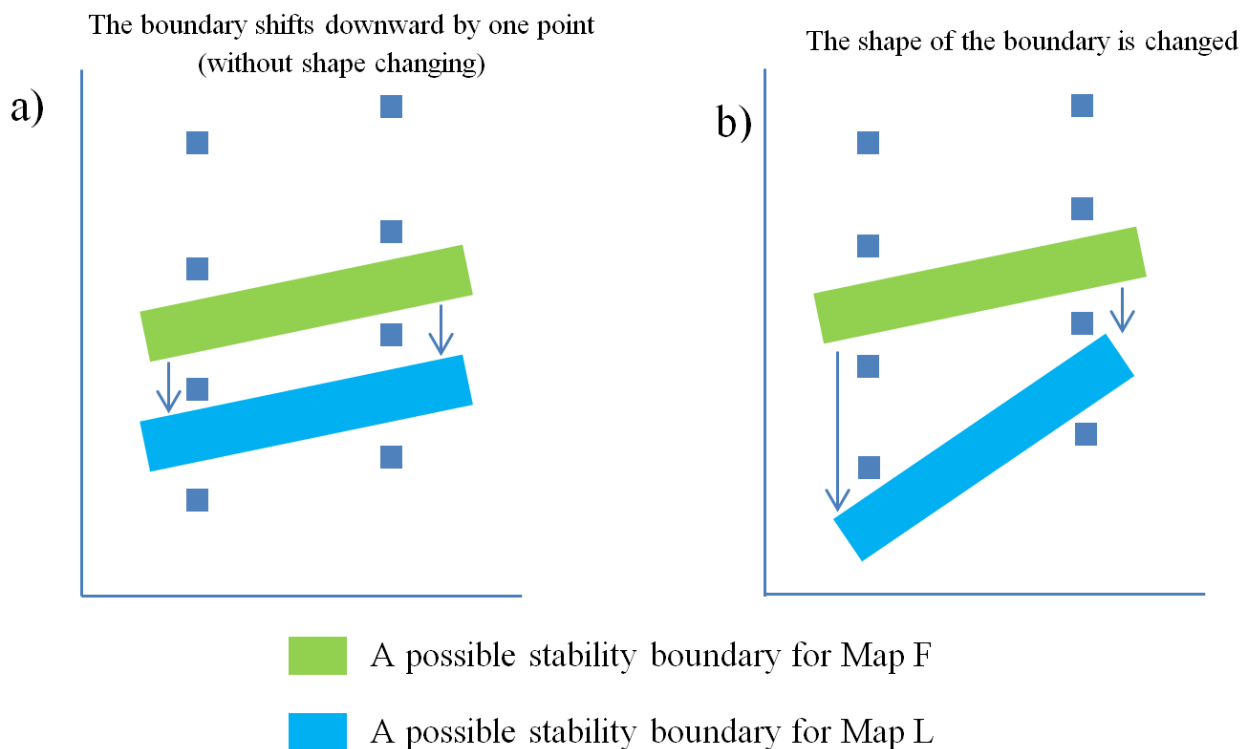
Figure 3.11- Two possible outcomes for stability boundary in different maps: a) The boundary shifts downward without changing shape, b) The shape of the boundary is changed.

In order to avoid doing unnecessary tests, the following procedure was designed and performed:

Figure 3.12 shows all four test points that could be done with Isopar M emulsion in each map. With the four λ values selected for the tests, there are five possible areas for the stability

boundary to cross: between points #1 and #2, between points #2 and #3, between points #3 and #4, below point #4, and above point #1 (the last two options are less likely to happen than the others because the particles sizes for points #1 and #4 are too small and too large respectively).
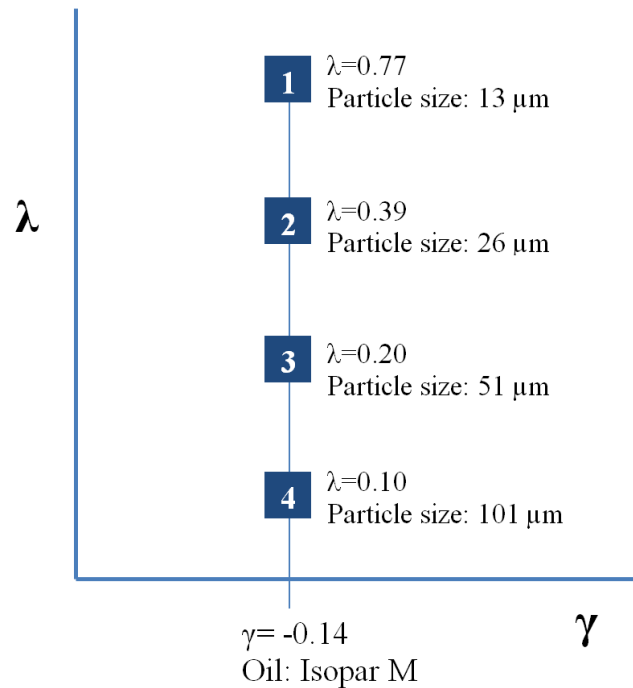
Figure 3.12- The four test points of the particle settlings in Isopar M emulsion on each map

With the following plan, it is not necessary to complete all 4 tests to find the stability boundary. Instead, the following approach was taken:

1- Do the test for points #2 and #3

2- If fingering occurs for one of the test points but not for the other, it means that the stability boundary crosses somewhere between these two points, and the work is done with Isopar M in that map.

3- If the fingering phenomenon occurs for both test points #2 and #3, it means that both are in the unstable region and the stability boundary crosses somewhere below test point #3. In that case, the test point #1 must be inside the unstable region. Therefore, there would be no need to do that test. Accordingly, the last test point to do will be #4, to ensure that the boundary crosses somewhere between points #3 and #4 or not.

(Note: it is very unlikely that the boundary crosses somewhere below test point #4 but to support the hypothesis, this test point has to be done.)

4- If the fingering phenomenon does not happen for both test points of #2 and #3, it means that both of them are in the stable region and the stability boundary crosses somewhere above the test point #2. By the same argument provided above, test #1 should be done next.

5- After doing two or three settling tests (depending on the results of Steps 1 and 2) with the Isopar M emulsion and finding the stability boundary for that value of γ, it is time to do the settling tests with an emulsion made of a different oil (different γ). The whole procedure is summarized in a flowchart shown in Figure 3.13.

6- The same procedure will be followed for the settling tests conducted with the emulsions made of the other two oils.
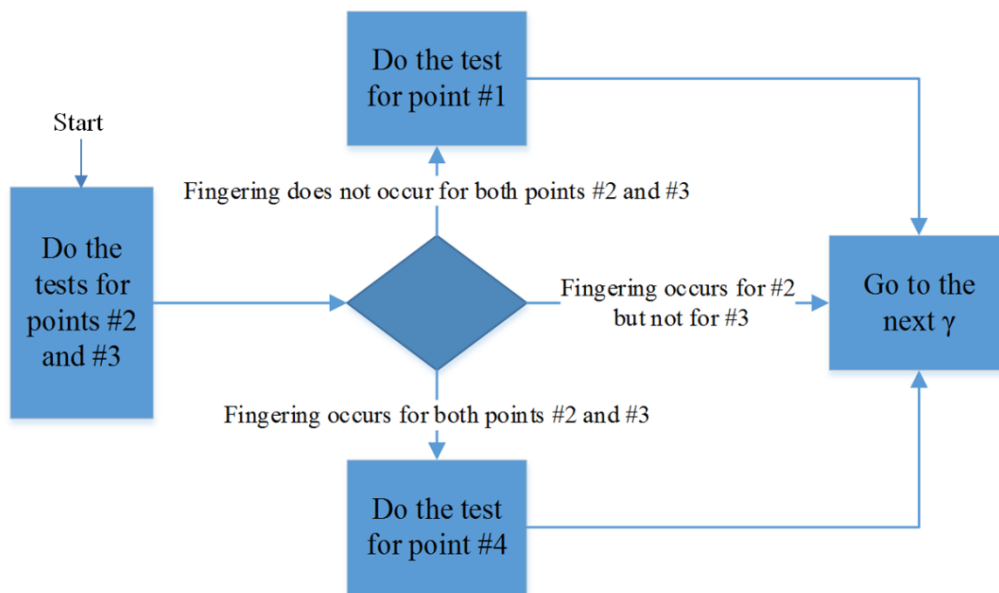
Figure 3.13- The flowchart of choosing the test points to be performed in order to avoid doing unnecessary tests

Chapter 4
Stability Maps

4.1. Introduction

The discussion so far in this thesis illustrates that emulsion-particle settling systems become unstable under certain conditions. The instability appears as fingering streams and causes the particles to settle more rapidly than would be predicted by assuming the particles are settling through a fluid continuum with the density and viscosity of the oil-in-water emulsion. However, there is still a considerable knowledge gap about when fingering phenomenon occurs in these systems.

It is crucial to know when and under which conditions the system becomes unstable. Knowing the stability status of the system helps decide if conventional correlations of settling velocity predictions are applicable. Presently, there is no tool for predicting the stability status of emulsion-particle settling systems.

Therefore, the main goal of this project is to draw stability maps for emulsion-particle settling systems. As concluded in Chapter 2, λ, γ, φ_p, and β_o are the four main control parameters of the stability tests in this project. After obtaining the maps, one can just insert given information (λ, γ, φ_p, and β_o) of their emulsion-particle settling system into the stability maps and predict its stability status.

4.2. Inserting λ and γ values on the Batchelor-Rensburg stability map

As mentioned in Section 3.3.2, emulsion droplet sizes were measured through microscopy. Figure 4.1 illustrates the microscopic image and the volumetric size distribution of the mineral oil emulsion droplets. Microscopic image and the size distribution of the droplets for the rest of the oils are provided in Appendix D.
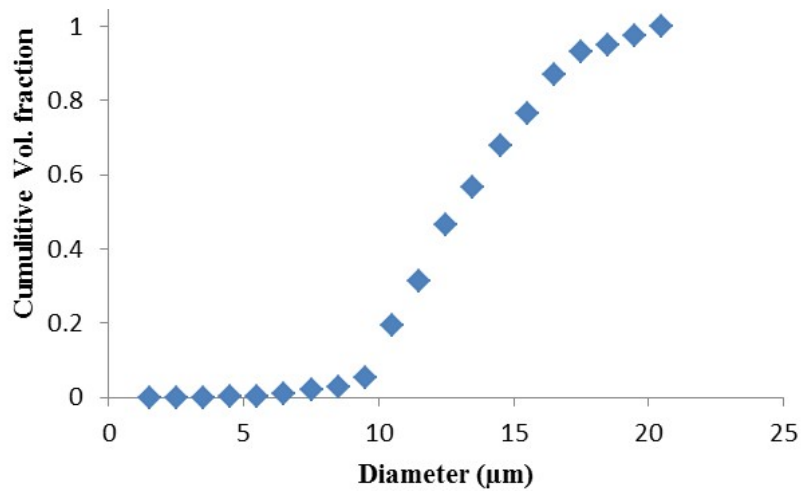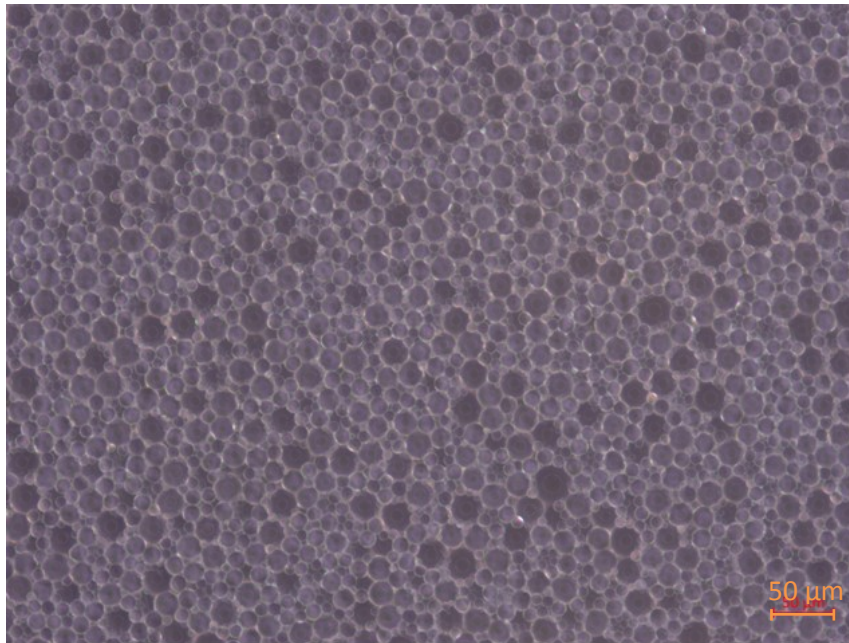
Figure 4.1- Microscopic image of Mineral Oil droplets (top) of a 20% oil emulsion and their size distribution (bottom)

Table 4.1 shows the mean diameter of the oil droplets for emulsions made using different oils used in this project.

Table 4.1- Oil droplet size for the emulsions made of each oil type

Emulsion oil type	Droplets Sauter mean diameter (µm)
Isopar M	10
Light Mineral Oil	15
Silicone Oil	15

Knowing the mean diameter of the particles, the λ ($\frac{droplet\ size}{particle\ size}$) values could be calculated. These values are provided in Table 4.2.

Table 4.2- λ values for each particle size and oil-in-water emulsion type

Emulsion Oil Type	Particle size (µm)	λ
Isopar M	13	**0.77**
	26	**0.39**
	51	**0.20**
	101	**0.10**
Light Mineral Oil	13	**1.15**
	26	**0.58**
	51	**0.29**
	101	**0.15**
Silicone Oil	13	**1.15**
	26	**0.58**
	51	**0.29**
	101	**0.15**

As mentioned earlier, γ is calculated as $\frac{\rho_o - \rho_w}{\rho_p - \rho_w}$. Since the densities of the fluid (water) and the particles are constant, γ changes only with the oil density. Therefore, there would be three possible γ values for each settling test, depending on the emulsion oil type. These values are presented in Table 4.3.

Table 4.3- γ values for the settling tests conducted with oil-in-water emulsions made of different types of oil

Emulsion Oil Type	γ
Isopar M	-0.141
Light Mineral Oil	-0.108
Silicone Oil	-0.058

It was crucial to choose values of λ and γ that more readily facilitate the targeting of the stability boundary. To increase the confidence level of the chosen values of λ and γ of this project, they were inserted into Batchelor and Van Rensburg [37] stability map for heavy-light particle systems. If the assigned test points of this project covered both sides of the Batchelor and Van Rensburg stability boundary, then there would be a good chance that those tests would also indicate the stability boundary of the emulsion-particle settling systems tested here. Figure 4.2 shows how these test points cover both stable and unstable regions of the Batchelor and Van Rensburg stability map, indicating that there is a good chance to locate the stability boundary for emulsion-particle settling systems with these test points.
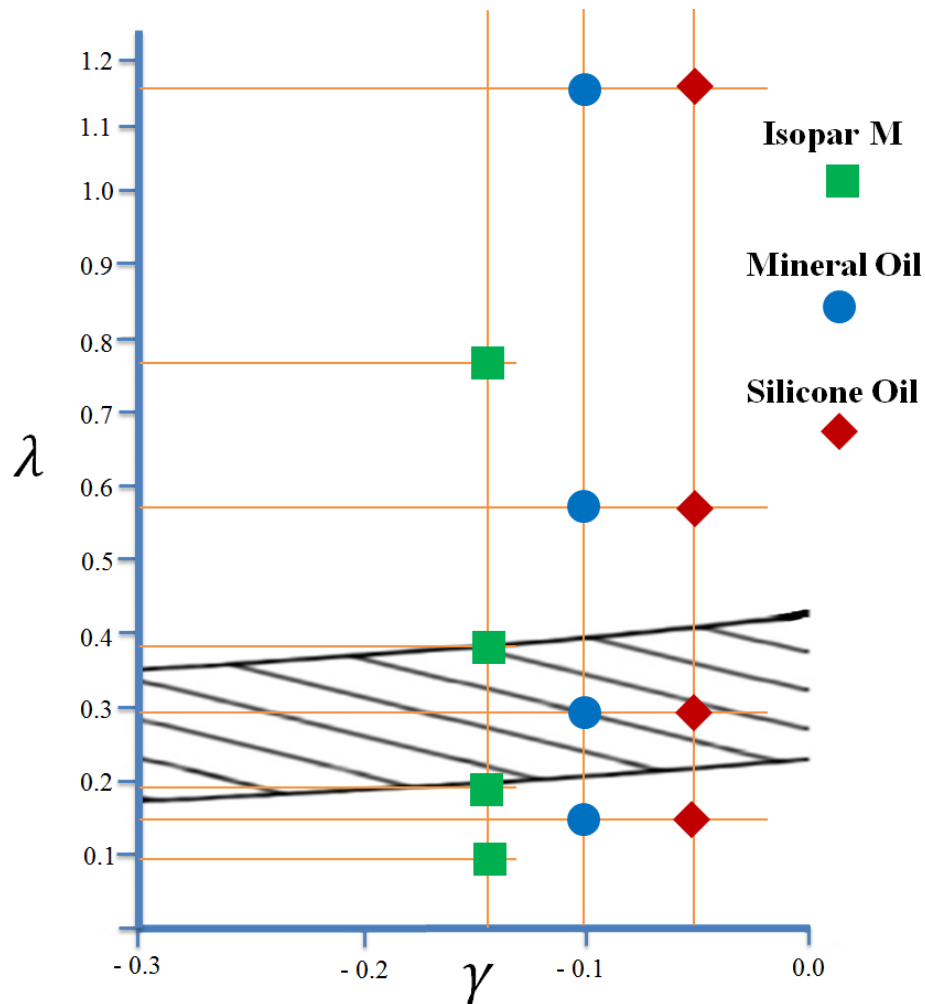
Figure 4.2- λ and γ values of this project on the Batchelor and Van Rensburg [37] **stability map**

4.3. Visual observations

Figure 4.3 shows the difference between stable and unstable settling tests conducting during this project. Figure 4.3a shows an unstable settling test. In this photo, 26 μm particles with $\varphi_p = 0.3$ are settling through a 30% Silicone Oil emulsion. For this test, $\lambda = 0.58$ and $\gamma = -0.058$. As can be seen in Figure 4.3a, when the system is unstable, particles settle down in segregated vertical finger-shaped streams. Figure 4.3b illustrates one of the stable settling tests of the project. In this experiment, 51 μm particles with $\varphi_p = 0.2$ are settling in a 20% Mineral Oil

emulsion. For this test, λ = 0.29 and γ = -0.108. It can be seen that in a stable emulsion-particle settling system a normal settling without formation of fingering streams occurs.
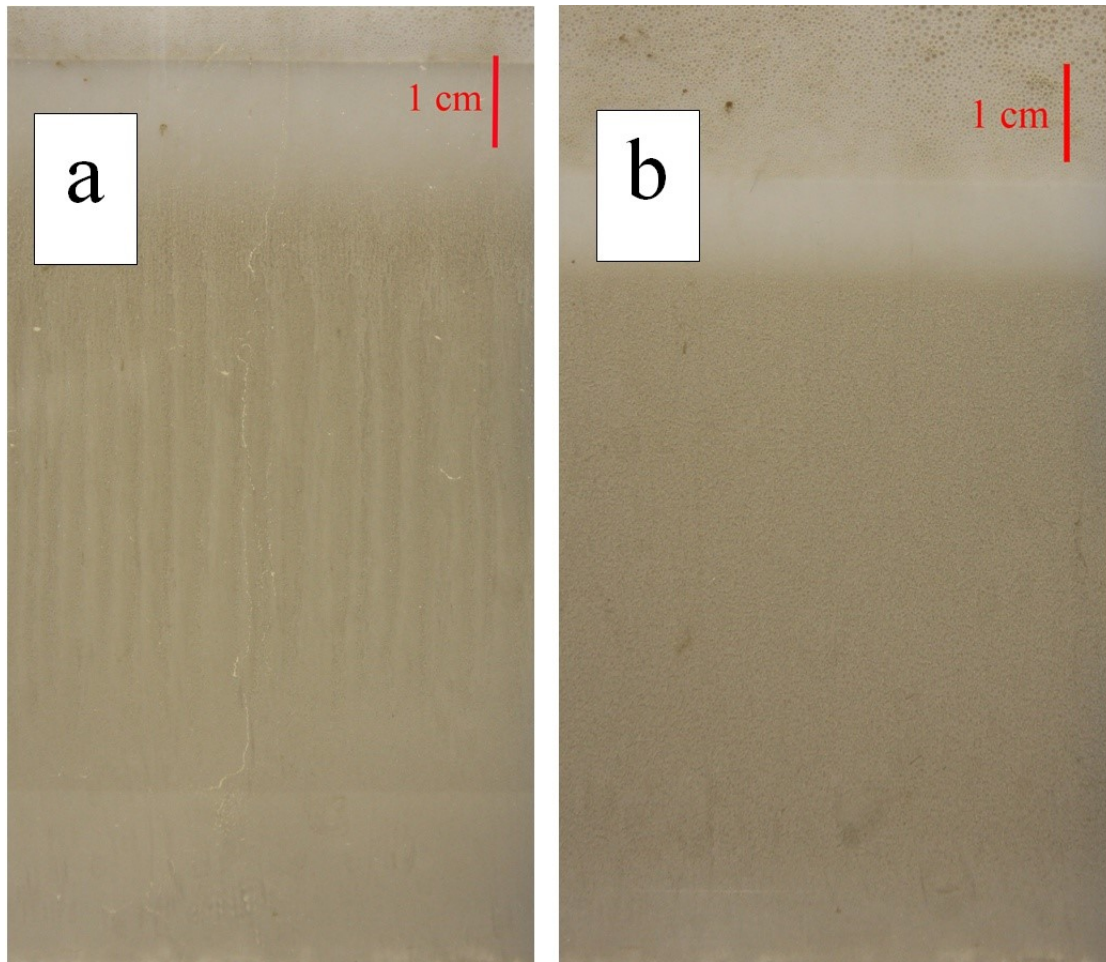
Figure 4.3- Visual comparison of an unstable settling test (a) with φ_p= 0.2, $\beta_o = 0.2$, λ = 0.29, and γ = -0.108 and a stable test (b) with φ_p= 0.3, $\beta_o = 0.3$, λ = 0.58, and γ = -0.058

4.4. Two key maps

As described in Section 3.5, tests were done first to produce stability map F (see Figure 3.10). Again, the goal here was to find the general shape of the stability boundary. Therefore, it is the only map that includes tests done using all three emulsions types. The settling tests in this map have been performed with $\varphi_p = 0.2$ in $\beta_o = 0.2$ emulsions.

Figure 4.4 shows the final result of tests carried out for this map, where the symbol "x" represents the unstable tests (the ones in which the fingering phenomenon occurred) and the symbol "♦" represents the stable tests (the ones in which the fingering phenomenon did not happen). Note that based on the proposed experimental procedure (Section 3.5), there was no need to do all the test points to find the boundary. In Figure 4.4, only the tests marked with a circle around them have been done, and the rest have been interpreted by knowing the results of the ones that were actually performed.

Based on the results of the stability tests, Map F (Figure 4.4) can be divided into three regions:

1- Stable region (below the hatched area):
It shows the conditions under which the fingering phenomenon does not happen, and hence the emulsion-particle settling system is stable.
2- Unstable region (above the hatched area):
It shows the conditions under which the fingering phenomenon happens, and hence the emulsion-particle settling system is unstable.
3- Undetermined region (the hatched area):
The stability status of the system under the conditions of this region is undetermined. However, it could be said that the stability boundary definitely passes through this region.
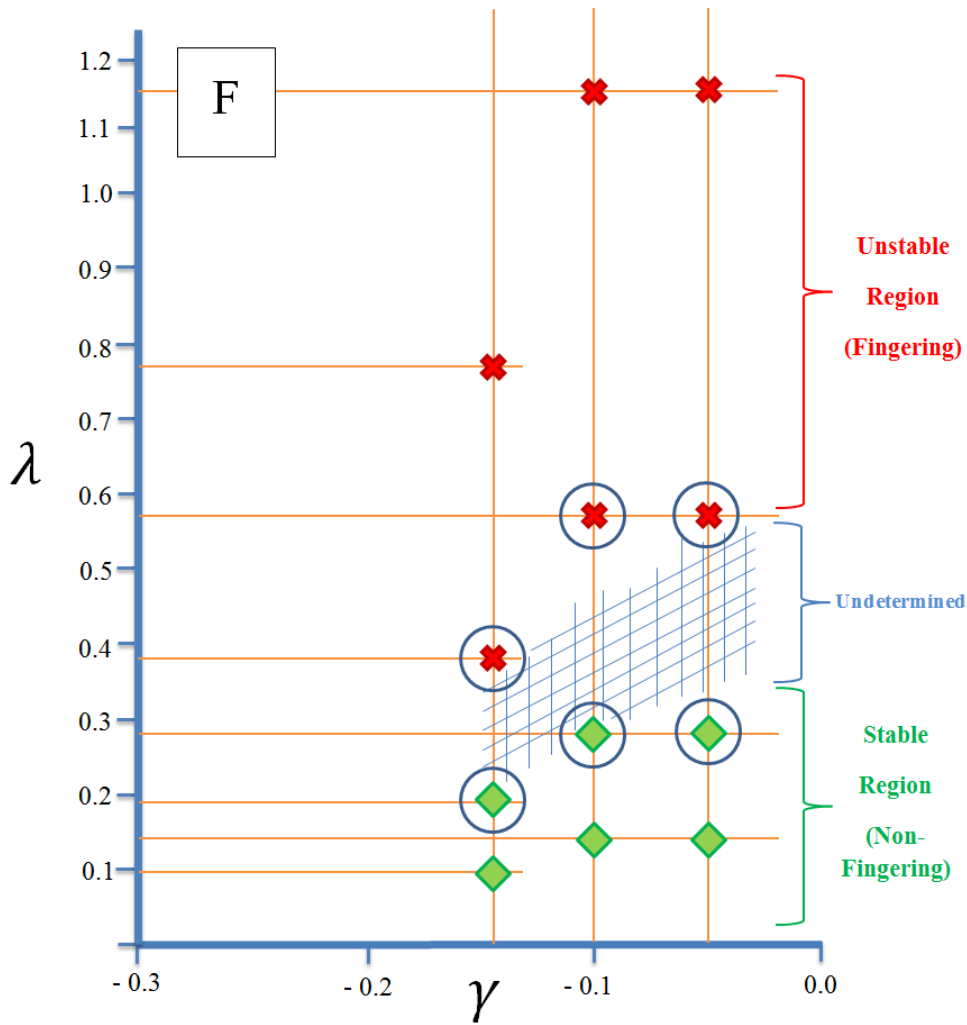
Figure 4.4- Map F and the final result of the stability tests on it

Figure 4.5 illustrates the results of the stability tests conducted for Map L. The tests done to produce Map L had $\varphi_p= 0.3$ in $\beta_o = 0.3$ emulsions made of either Isopar M or Silicone Oil. In Figure 4.5, the circled points were actually conducted, and the stability of the uncircled points interpreted by knowing the results of the completed tests.

61
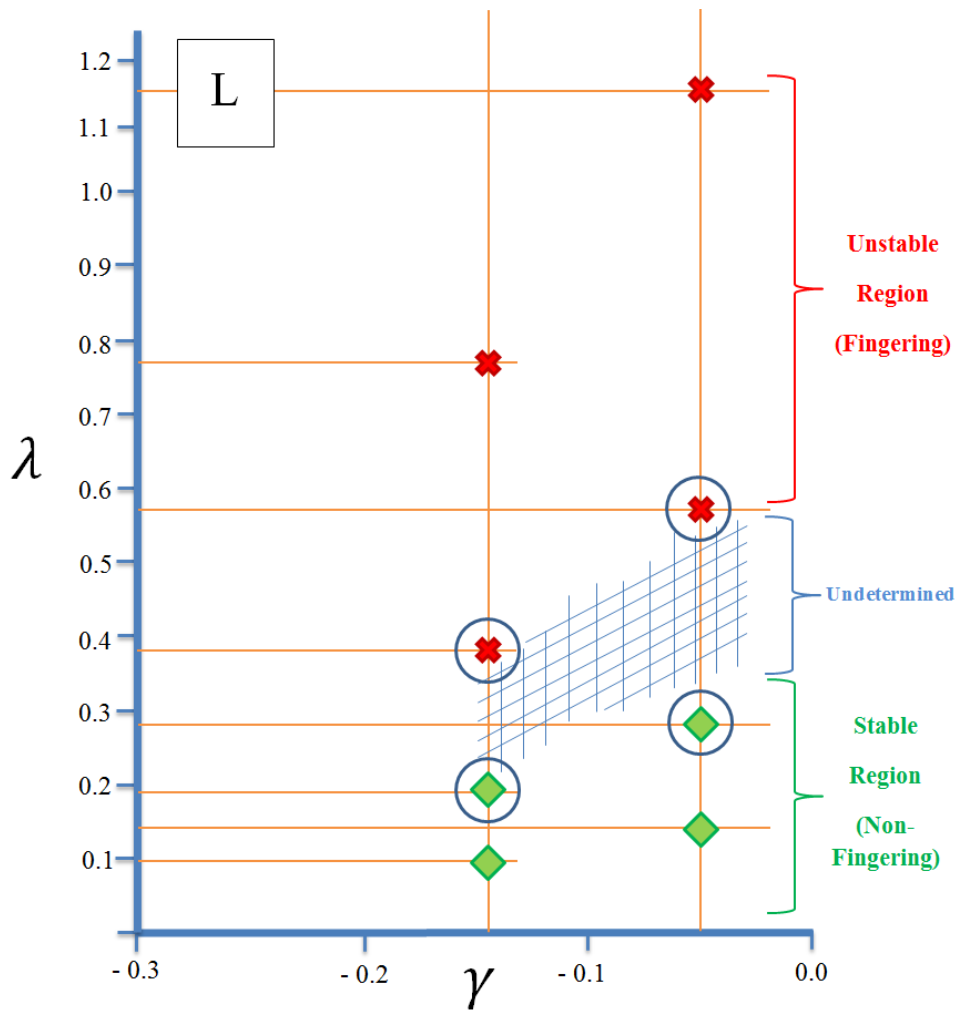
Figure 4.5- Map L and the final results of the stability tests on it

Comparing Figure 4.4 and Figure 4.5 shows that the Maps F and L are identical. This similarity leads to the following interpretations:

- Because of the identical shape of Maps F and L, a concrete decision about shifting/shape-changing of the boundary could not be made. In other words, from the results of these two maps, it cannot be determined if the stability boundary completely changes its shape or just simply shifts upward or downward with changes in particle and oil concentrations.

- Since any combination of oil/solids concentrations in the maps G, H, J, and K are somewhere between oil/solids concentrations of the maps F and L (see

Figure 3.10), their tests are unnecessary because they are expected to give the results similar to those of Maps F and L.

4.5. Remaining maps

All the settling tests for Map A were done with $\varphi_p = 0.15$ in the $\beta_o = 0.1$ emulsions (lowest particle and oil concentrations of the experimental plan (see Figure 3.10).

In Map A, first, the settling tests through Isopar M emulsions ($\gamma = -0.141$) were performed. The results of the stability tests with Isopar M emulsion in Map A shows that the 'undetermined region' (through which the stability boundary crosses) shifts one point upward (compared to the Isopar M tests in the Maps F and L).

The results of the stability tests with Silicone Oil emulsion ($\gamma = -0.058$) in Map A help to decide between shifting or shape-changing of the boundary:

- If the stability boundary for Silicone Oil tests just shifts one point upward (similar to Isopar M tests), the implication would be that the whole boundary just shifts one point upward.
- If not, it indicates that the shape of the map actually changes.

Figure 4.6 illustrates the final result of Map A (by adding the results of the Silicone Oil tests to the Isopar M tests). The circled test points were actually done, and others have been interpreted by knowing the results of the performed tests. As can be seen in Figure 4.6, in the settling tests through Silicone Oil emulsion (points #2, #4, and #6) fingering phenomenon happens for 13 µm particles ($\lambda=1.15$), but for 26 µm ($\lambda=0.58$) and 51 µm ($\lambda=0.29$) particles the settling system is stable.
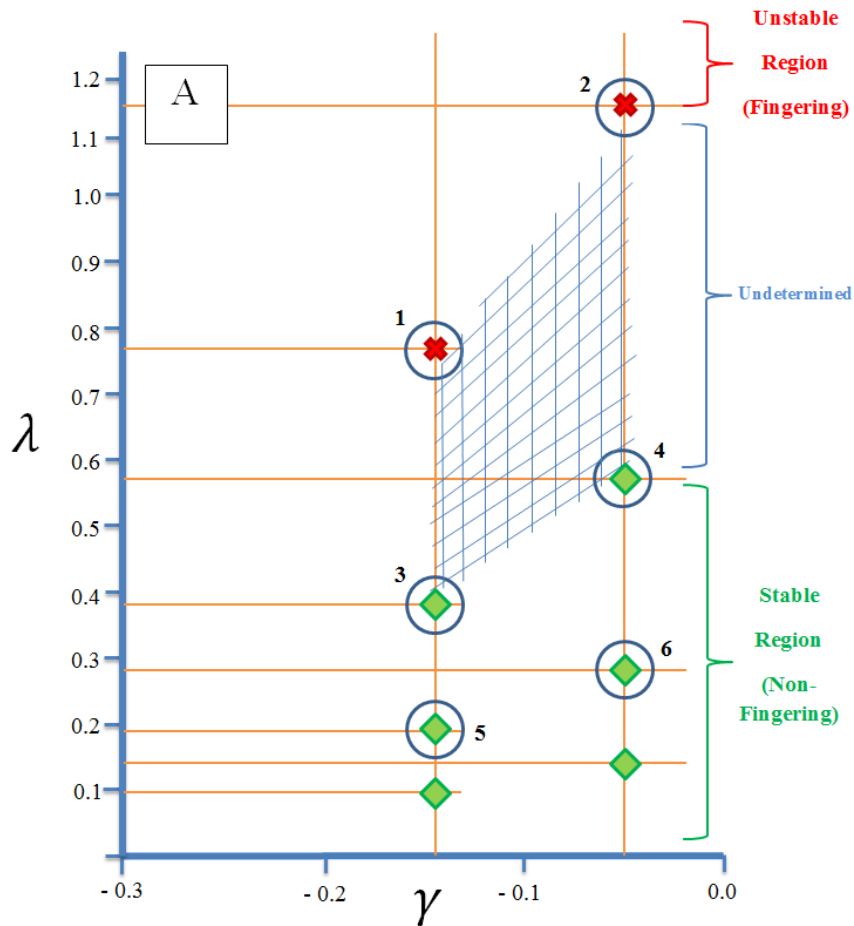
Figure 4.6- Stability Map A

These results show that the stability boundary in Map A has been shifted one point upward compared to Maps F and L, indicating that at lower oil/particle concentrations, system "instability" requires particles to have a smaller size.

After knowing what happens to the boundary on different maps (different oil/particle concentrations), the stability tests were done for the remaining maps using Isopar M emulsions. The stability test results showed that Maps B, C, D, and E are similar to Map A; and Map I is similar to Map L.

As mentioned in the previous section, the stability tests for the maps G, H, J, and K were not done to avoid doing unnecessary tests and save the time and materials because it was obvious that those maps would be identical to Maps F and L.

4.6. Full set of maps

After performing stability tests as described in Sections 4.4 and 4.5, a full set of twelve maps were drawn for the emulsion-particle settling systems. Figure 4.7 shows the full set of maps.
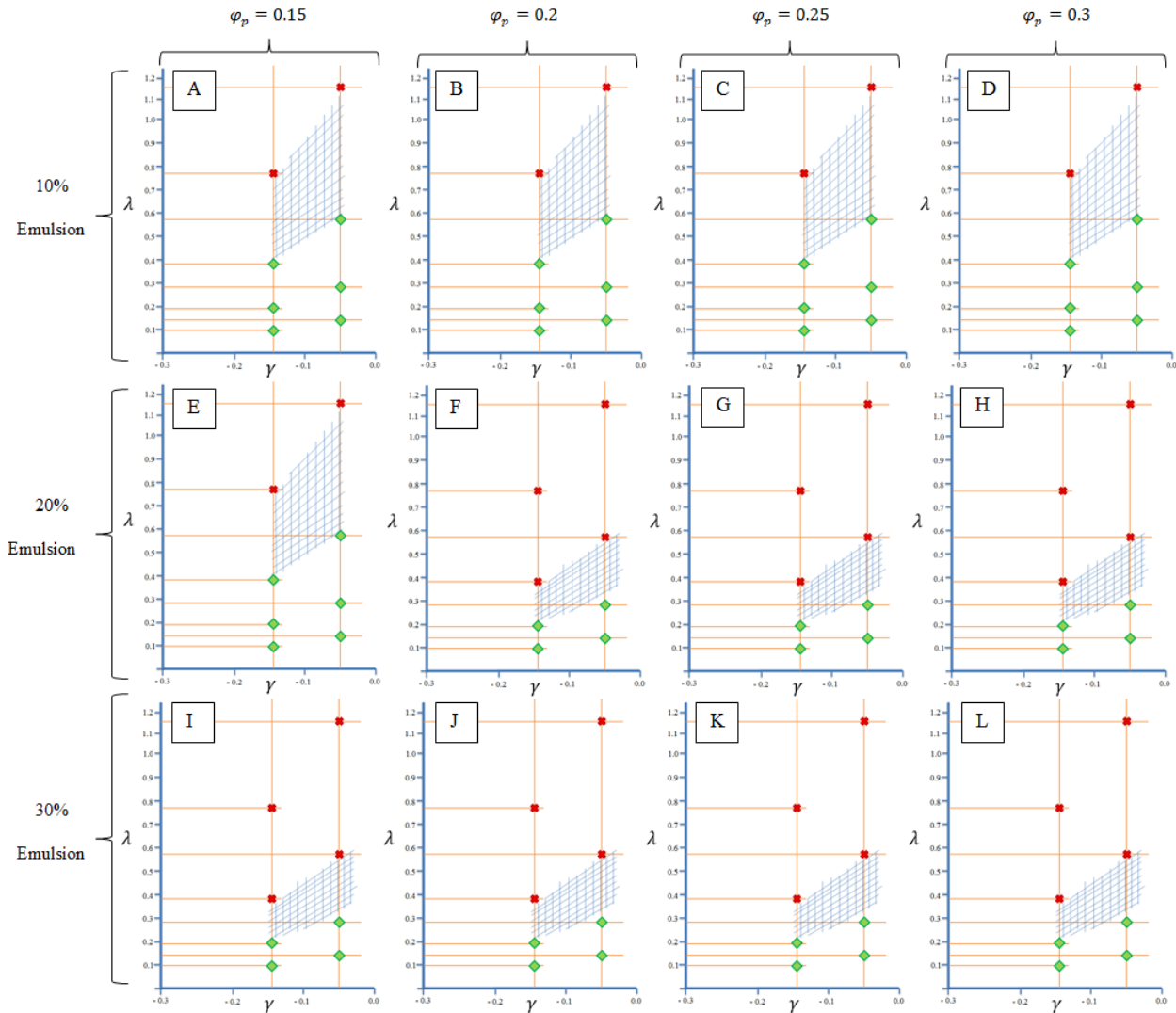
Figure 4.7- Full set of the 12 stability maps produced for emulsion-particle settling systems in this project

The maps produced in this project can be used to predict the stability status of emulsion-particle settling systems in a wide range of given conditions. These maps will allow engineers

and researchers to determine if conventional methods of settling velocity predictions are applicable to a particular emulsion-particle settling system. Alternatively, one can simply adjust the system conditions so that they fall into the "unstable" region of the stability maps to enhance particle settling velocity.

Chapter 5
Settling Velocity Analysis

5.1. Introduction

The production of stability maps for emulsion-particle settling systems is a significant contribution to the body of knowledge in this area of research. However, there are still other aspects of these settling systems yet to be studied and many unanswered questions. The goal of this chapter is to give a better understanding of the behavior of emulsion-particle settling systems, especially when they become unstable.

In this Chapter the fingering phenomenon in unstable tests that enhances settling velocity is investigated. First, particle settling velocities in both stable and unstable tests have been predicted using the calculation method explained in Section 3.4. The predicted values were then compared with the measured settling velocities. Since the velocity calculation method considers the emulsion as a continuous phase, this comparison also indicates conditions under which the emulsion can be considered as a continuous phase.

Currently, the only information known from the literature is that particle settling velocity increases with the formation of the fingers. Therefore, a model is developed for the unstable systems, which describes the behavior of the particles, droplets, and the fluid inside the segregated fingers when the system becomes unstable.

5.2. Stable tests

During the experiments, settling velocities were measured for all of the tests performed, including both stable and unstable tests. Multiple runs for each settling test were performed. Very close values of settling velocities measured in different runs of each test indicate the repeatability of the velocity measurement (see Appendix B). Additionally, a settling velocity prediction was carried out for each test using the Richardson-Zaki equation through the calculation method explained in Section 3.4.

Note that the emulsions were considered as a continuous phase for all velocity calculations. Recall as mentioned in Section 3.3.3, the disengagement between the particles and emulsion

occurred only in unstable tests. Therefore, the particles settled only through the emulsion when the system was stable.

Table 5.1 shows the comparison of the measured settling velocities with the values predicted using the Richardson-Zaki equation. The last column of Table 5.1 shows that the Richardson-Zaki equation successfully predicts the particle settling velocities of the stable tests.

Table 5.1- Comparison of measured particle settling velocities in the 'stable tests' with the values predicted using the Richardson-Zaki equation

Map	φ_p	Emulsion Oil%	Oil type	d_p (μm)	R-Z eq. v_P (cm/s)	Measured v_P (cm/s)	$\dfrac{v_{P,mesured}}{v_{P,R-Z}}$
F	0.2	20%	Isopar M	51	4.42×10^{-2}	4.05×10^{-2}	**0.916**
	0.2	20%	Mineral Oil	51	4.09×10^{-2}	4.17×10^{-2}	**1.02**
	0.2	20%	Silicone Oil	51	4.23×10^{-2}	4.1×10^{-2}	**0.970**
L	0.3	30%	Isopar M	51	1.79×10^{-2}	1.45×10^{-2}	**0.807**
	0.3	30%	Silicone Oil	51	1.62×10^{-2}	1.34×10^{-2}	**0.827**
A	0.15	10%	Isopar M	26	2.06×10^{-2}	1.96×10^{-2}	**0.952**
	0.15	10%	Isopar M	51	7.49×10^{-2}	7.14×10^{-2}	**0.952**
	0.15	10%	Silicone Oil	26	2.0×10^{-2}	1.8×10^{-2}	**0.899**
	0.15	10%	Silicone Oil	51	7.27×10^{-2}	7.83×10^{-2}	**1.08**
B	0.2	10%	Isopar M	26	1.55×10^{-2}	1.53×10^{-2}	**0.988**
	0.2	10%	Isopar M	51	5.66×10^{-2}	5.49×10^{-2}	**0.970**
C	0.25	10%	Isopar M	26	1.14×10^{-2}	1.1×10^{-2}	**0.961**
	0.25	10%	Isopar M	51	4.19×10^{-2}	4.07×10^{-2}	**0.971**
D	0.3	10%	Isopar M	26	8.28×10^{-3}	7.89×10^{-3}	**0.952**
	0.3	10%	Isopar M	51	3.04×10^{-2}	2.8×10^{-2}	**0.921**
E	0.15	20%	Isopar M	26	1.59×10^{-2}	1.53×10^{-2}	**0.956**
	0.15	20%	Isopar M	51	5.86×10^{-2}	5.21×10^{-2}	**0.889**
I	0.15	30%	Isopar M	51	4.45×10^{-2}	3.72×10^{-2}	**0.835**

The overall accuracy of the velocity predictions indicates that the emulsion can be considered as a continuum for the stable emulsion-particle settling system. It also confirms that if an emulsion-particle settling system is located on the stable areas of the stability maps, conventional methods of settling velocity predictions, like the Richardson-Zaki equation, are applicable for such systems. This finding reinforces the importance of the stability maps.

5.3. Unstable tests

The disengagement that occurs between the particles and the emulsion in the unstable tests requires the use of two separate velocity predictions for each test:

1- "Engaged" settling velocity predictions for the velocities when particles are settling through the emulsion.

2- "Disengaged" settling velocity predictions for the velocities after disengagement of the particles from the emulsion, when they are settling through the water.

One significant parameter that is important for further analysis is the 'disengagement point', which is the height of the mixture where the settling particles disengage from the rising emulsion. Visually locating this point through the settling column was challenging. Thus, a more accurate way to determine this point was needed. This was accomplished by drawing a graph of the height variation of the particle upper interface with time. In unstable tests, particle settling velocity, when particles are engaged with the emulsion, is different from their velocity after disengagement. Therefore, at some point, the settling line of "engaged" settling velocity intersects with the line of "disengaged" velocity. That intersection is, in fact, the disengagement point. Figure 5.1 shows the graph of height variation with time for the test of 26 μm particles settling through the emulsion containing of 20% Isopar M oil. The vertical axis in Figure 5.1 represents the height of the settling particles' upper interface. Similar settling graphs for the other tests are presented in Appendix C.
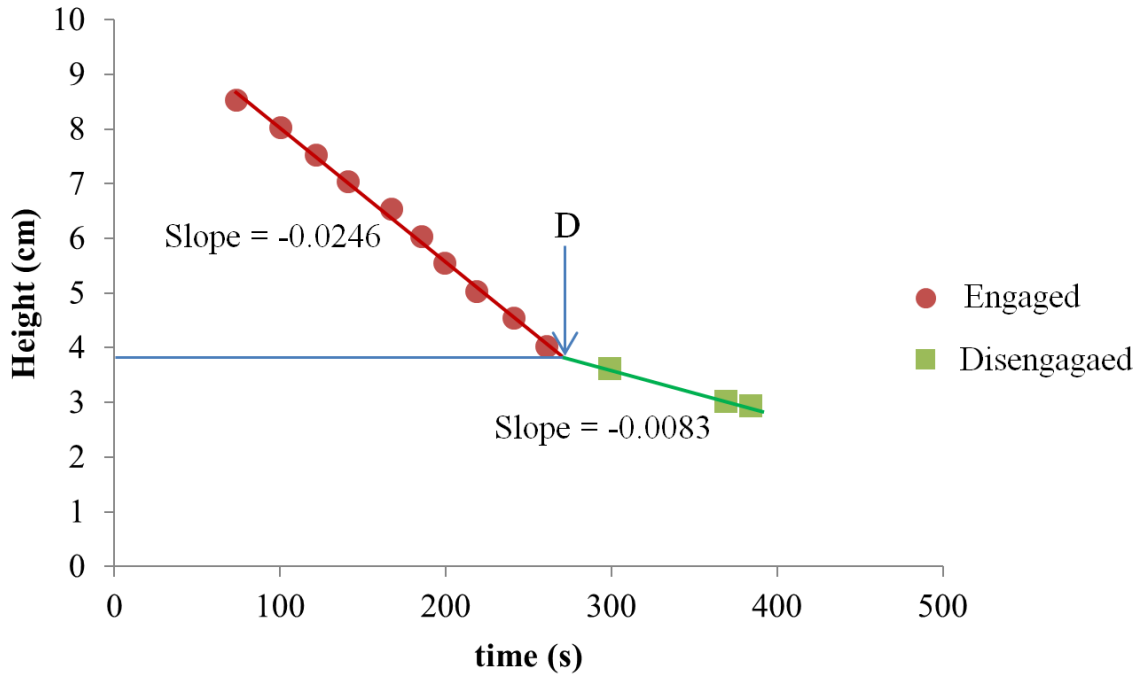
Figure 5.1- Settling graph of an unstable settling test, showing the displacement of the particles' upper interface with time for 26 μm particles with $\varphi_p = 0.2$ settling through $\beta_o = 0.2$ Isopar M emulsion; the disengagement point is indicated as 'D'

The slopes of the straight lines on Figure 5.1 indicate the particle settling velocities. In Figure 5.1, the intersection of the two settling lines, which is labeled as point D, is the disengagement point. As mentioned earlier, in the unstable tests (in which the fingering phenomenon occurs), particle settling velocity through emulsion (where the fingering phenomenon occurs) is higher than their settling rate after disengagement (where the fingers disappear and particles are settling through the water). As can be seen, the slope of the settling line when the particles are engaged with emulsion (the red part of the curve before disengagement) is higher than the slope of the line after disengagement.

5.3.1. Unstable tests: Engaged Settling Velocities

Table 5.2 compares the measured engaged settling velocities of the unstable tests with the values predicted from the Richardson-Zaki equation.

Table 5.2- Comparison of measured 'engaged' velocities in the 'unstable tests' with the values predicted using the Richardson-Zaki equation

Map	φ_p	Oil% of Emulsion	Oil type	d_p (μm)	R-Z eq. v_P (engaged) (cm/s)	Measured v_P (engaged) (cm/s)	$\dfrac{v_{P,mesured}}{v_{P,R-Z}}$
F	0.2	20%	Isopar M	26	1.2×10^{-2}	2.46×10^{-2}	**2.04**
	0.2	20%	Mineral Oil	26	1.11×10^{-2}	3.42×10^{-2}	**3.07**
	0.2	20%	Silicone Oil	26	1.12×10^{-2}	2.18×10^{-2}	**1.89**
L	0.3	30%	Isopar M	26	4.68×10^{-3}	9.2×10^{-3}	**1.89**
	0.3	30%	Silicone Oil	26	4.38×10^{-3}	9.1×10^{-3}	**2.08**
A	0.15	10%	Isopar M	13	5.34×10^{-3}	2.04×10^{-2}	**3.82**
	0.15	10%	Silicone Oil	13	4.65×10^{-3}	1.89×10^{-2}	**4.06**
B	0.2	10%	Isopar M	13	4.02×10^{-3}	1.43×10^{-2}	**3.56**
C	0.25	10%	Isopar M	13	2.97×10^{-3}	9×10^{-3}	**3.03**
D	0.3	10%	Isopar M	13	2.15×10^{-3}	5.2×10^{-3}	**2.42**
E	0.15	20%	Isopar M	13	4.14×10^{-3}	1.96×10^{-2}	**4.74**
I	0.15	30%	Isopar M	26	1.21×10^{-2}	2.16×10^{-2}	**1.79**

The last column of Table 5.2 shows that the measured engaged settling velocities of the particles in the unstable tests are considerably higher than the values predicted by the Richardson-Zaki equation.

The first interpretation of these results is that the conventional methods of predicting settling velocity are inapplicable to an unstable emulsion-particle settling system. It should be noted that in the velocity prediction procedure, the emulsion has been considered as a continuous phase. As a result, the other conclusion is that the emulsion will not act as a continuous phase when the emulsion-particle settling system becomes unstable.

5.3.2. Unstable tests: Disengagement Concentration

The first attempts to calculate the 'after disengagement' settling velocities produced surprising results. The measured velocities were considerably lower than the predicted values, whereas after being disengaged from the emulsion, the particles settle merely in water. Therefore, one should expect accurate velocity predictions from the Richardson-Zaki equation. Through a measurement procedure, particle concentration after disengagement was measured. The results of these measurements showed that the reason for aforementioned discrepancy between the measured settling velocities and the calculated values is that the concentration of the particles after disengagement is higher than their initial concentration. The disengagement concentration was identified through the following procedure:

Figure 5.2 shows the settling particles after being disengaged from the emulsion. As can be seen in Figure 5.2, the particles can only be in one of the following zones:

1- Zone A (packed bed of the settled particles)
2- Zone B (settling particles through water)

Hence, concentrations of the settling particles after disengagement were found through the following steps:

1- The volume of the packed bed of the settled particles ($\forall_A$) (zone A in Figure 5.2) was measured; and
2- The volume of the settled particles (settled particles occupy ~0.6 of the packed bed) was calculated:

$$\forall_{settled} = 0.6\,\forall_A \qquad\qquad 5.1$$

3- The volume of the settling particles was determined:

$$\forall_{settling} = \forall_{total} - \forall_{settled} \qquad\qquad 5.2$$

($\forall_{total}$ is the total volume of the particles used in each test)

4- The volume of zone B ($\forall_B$) was measured.

5- The concentration of the settling particles after disengagement (φ_{p_dis}) was determined:

$$\varphi_{p\_dis} = \frac{\forall_{settling}}{\forall_B} \qquad\qquad 5.3$$

Figure 5.2- The particles after being disengaged from the rising emulsion are divided into two zones: settling particles through water (zone B) and packed bed of settled particles (zone A)

Table 5.3 shows the results of the procedure mentioned above.

Table 5.3- Comparison of the particles' concentrations after disengagement with their initial concentrations: unstable tests

Map	Emulsion Oil%	Oil Type	Particle size (μm)	Initial φ_p	φ_{p_dis}
F	20	Isopar M	26	0.2	0.325
	20	Mineral Oil	26	0.2	0.34
	20	Silicone Oil	26	0.2	0.31
L	30	Isopar M	26	0.3	0.48
	30	Silicone Oil	26	0.3	0.47
A	10	Isopar M	13	0.15	0.21
	10	Silicone Oil	13	0.15	0.22
B	10	Isopar M	13	0.2	0.26
C	10	Isopar M	13	0.25	0.3
D	10	Isopar M	13	0.3	0.335
E	20	Isopar M	13	0.15	0.29

The last column of Table 5.3 shows that the disengagement concentration of the particles (φ_{p-dis}) for each of unstable tests is higher than the initial concentration. Prediction of the disengaged velocities were made using φ_{p-dis} in the Richardson-Zaki equation and these predictions were compared with the measured settling velocities (after disengagement). These are discussed in the following section.

5.3.3. Unstable tests: Disengaged Settling Velocities

Using the post-disengagement concentrations measured as explained in the previous section, particles disengaged settling velocities were calculated using the Richardson-Zaki equation. Table 5.4 shows the comparison between the measured and predicted disengaged velocities.

Table 5.4- Comparison of the measured 'disengaged' velocities with the values predicted using the φ_{p-dis} in the Richardson-Zaki equation: unstable tests

Map	Emulsion%	Oil Type	Particle size (μm)	Initial φ_p	φ_{p_dis}	$v_{p,R-Z,disengaged}$ (using φ_{p_dis}) (cm/s)	$v_{p,measured}$ (disengaged) (cm/s)	$\dfrac{v_{measured}}{v_{R-Z}}$
F	20	Isopar M	26	0.2	0.325	8.53×10^{-3}	8.3×10^{-3}	**0.973**
	20	Mineral Oil	26	0.2	0.34	7.68×10^{-3}	8.3×10^{-3}	**1.08**
	20	Silicone Oil	26	0.2	0.31	9.46×10^{-3}	8.4×10^{-3}	**0.888**
L	30	Isopar M	26	0.3	0.48	2.52×10^{-3}	2.7×10^{-3}	**1.07**
	30	Silicone Oil	26	0.3	0.47	2.75×10^{-3}	2.9×10^{-3}	**1.06**
A	10	Isopar M	13	0.15	0.21	4.64×10^{-3}	5.2×10^{-3}	**1.12**
	10	Silicone Oil	13	0.15	0.22	4.37×10^{-3}	5×10^{-3}	**1.14**
B	10	Isopar M	13	0.2	0.26	3.42×10^{-3}	4.1×10^{-3}	**1.19**
C	10	Isopar M	13	0.25	0.3	2.63×10^{-3}	3×10^{-3}	**1.14**
D	10	Isopar M	13	0.3	0.335	2.07×10^{-3}	2×10^{-3}	**0.968**
E	20	Isopar M	13	0.15	0.29	2.81×10^{-3}	3.1×10^{-3}	**1.10**

As can be seen in the last column of Table 5.4, the Richardson-Zaki equation can predict the disengaged velocities in the unstable tests with good accuracy using φ_{p-dis} (which is greater than the initial φ_p in each test)

5.4. A Model for Unstable Settling

Results from the previous sections of this chapter prove that the emulsion can no longer be considered a continuous phase when the emulsion-particle settling system becomes unstable. In that case, the oil droplets of the emulsion should be treated as separate species moving in the opposite direction of the settling particles. Figure 5.3 schematically illustrates this phenomenon.
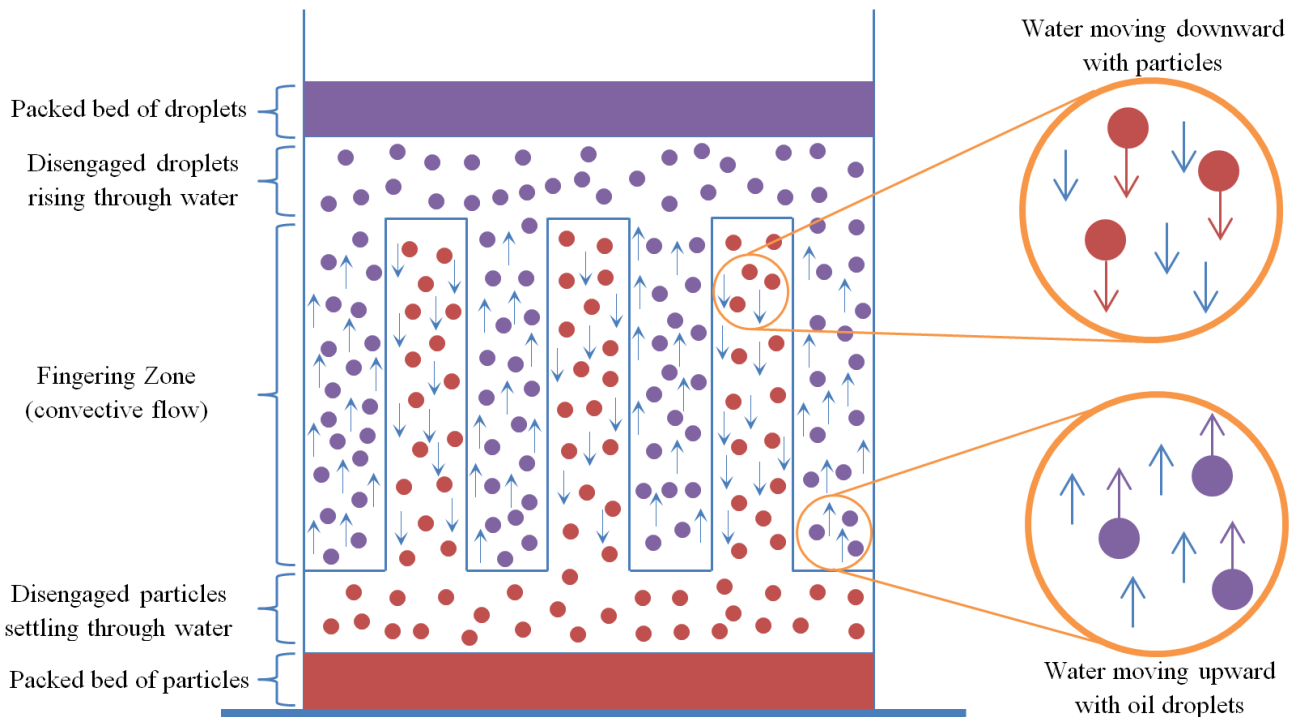
Figure 5.3- Schematic view of the movement of particles, oil droplets and water inside the fingering streams when the emulsion-particle system becomes unstable

Figure 5.3 illustrates the idea that particles settle through segregated parallel fingering streams in an unstable system, as do the rising emulsion droplets but in different fingers. Here, the fingers through which the particles settle and the droplets rise will be referred to as 'suspension fingers' and 'emulsion fingers,' respectively. Based on this idea, it can be said that adjacent fingers have different densities. In other words, the mixture inside a suspension finger is heavier than the mixture inside an emulsion finger. This density difference between the

suspension and emulsion fingers creates a relative movement, producing a convective flow inside each finger. The term 'convective flow' here means that the whole mixture inside a suspension finger (greater mixture density) moves downward while the mixture inside an emulsion finger (less dense) moves upward. It follows that all the species including the water are moving inside each finger. The water motion inside each finger is in the same direction as the dispersed species of that finger (i.e., particles in the suspension fingers and oil droplets in the emulsion fingers). Note, however, that the particles are heavier, and the oil droplets are lighter than water. Therefore, the particles would have a relative downward velocity to that of water in the suspension fingers due to their higher density. By the same reasoning, the oil droplets have a relative upward velocity to that of water in the emulsion fingers due to their lower density.

In conclusion, it could be said that the settling velocity of the particles is a result of water movement plus their motion relative to that of water. Based on the convective flow described above, a settling model is developed for unstable emulsion-particle settling systems. It should be noted that particle-particle, particle-droplet, and droplet-droplet interactions and colloidal forces are neglected in this model.

The model is developed based on the following assumptions:

1- Particle settling velocity in the suspension fingers is equal to the water velocity plus the relative velocity of the particles to that of water; and the same approach is taken for the oil droplets in the emulsion fingers:

$$v_{p\_fing} = v_{p\_rel} + v_{w\downarrow} \qquad\qquad 5.4$$

$$v_{d\_fing} = v_{d\_rel} + v_{w\uparrow} \qquad\qquad 5.5$$

In Equations 5.4 and 5.5:

v_{p_fing}: Particle settling velocity in the fingering zone (this velocity is measured from visual observations through the experiments)

v_{d_fing}: Droplet rising velocity in the fingering zone

$v_{w\downarrow}$: Downward water velocity in the suspension fingers

$v_{w\uparrow}$: Upward water velocity in the emulsion fingers

v_{p_rel}: Relative velocity of the particles to that of water

v_{d_rel}: Relative velocity of the oil droplets to that of water

2- There are no oil droplets in the suspension fingers and no particles in the emulsion fingers.

3- Particle concentration inside the suspension fingers is equal to their disengagement concentration:

$$\varphi_{p\_dis} = \varphi_{p\_fing} \qquad \qquad 5.6$$

where φ_{p_fing} is the concentration of the particles inside the fingers.

4- The net flow rate of the water in the fingering region is zero. In other words, the amount of water descending in the suspension fingers is equal to the amount of water ascending in the emulsion fingers:

$$Q_{w\uparrow} = Q_{w\downarrow} \qquad \qquad 5.7$$

in Equation 5.7, $Q_{w\uparrow}$ and $Q_{w\downarrow}$ indicate upward and downward flow rates of water, respectively.

To calculate $Q_{w\downarrow}$, the following parameters are required:

- Downward velocity of water ($v_{w\downarrow}$)
- The cross-sectional area through which the water is moving down (the sum of the cross-sectional area of the suspension fingers)

Based on assumption #1 it could be said that:

$$v_{w\downarrow} = v_{p\_fing} - v_{p\infty}(1 - \varphi_{p\_fing})^{n-1} \qquad \qquad 5.8$$

where $v_{p\infty}$ and n are terminal settling velocity and Ricardson-Zaki index of the particles in water, respectively. Both parameters can be calculated using the properties of the particles and water. Based on assumption #3, φ_{p_fing} is equal to φ_{p_dis} which was measured as described in Section 5.3.2. Values of v_{p_fing} were measured for each of the unstable tests. Therefore, all the parameters are available to calculate $v_{w\downarrow}$ in Equation 5.8.

If we take a cross-sectional cut of the settler when the fingering phenomenon occurs, a plan view is shown in Figure 5.4. The point here is not to have a precise image of the settling area, but to simply indicate that the settling area would be divided into different suspension and emulsion regions.

Settling suspension
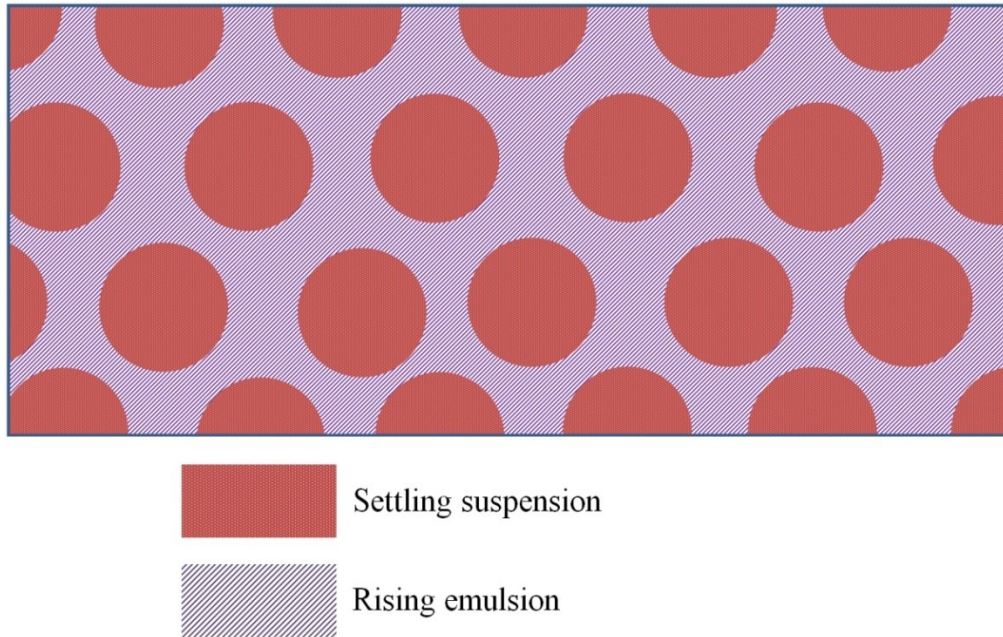
Rising emulsion

Figure 5.4- Schematic view of the cross-sectional area of the settler divided into separate suspension and emulsion regions when fingering phenomenon occurs

As shown in Figure 5.4, each of the settling suspension and rising emulsion fingers occupy a fraction of the settler cross-sectional area so that:

$$A_{total} = Cross-sectional\ area\ of\ the\ settler$$

$A_{p-fing} = Cross-sectional\ area\ occupied\ by\ the\ suspension\ fingers$

$A_{e-fing} = Cross-sectional\ area\ occupied\ by\ the\ emulsion\ fingers$

If the system was stable, the particles would be evenly distributed throughout the whole settling area (A_{total}) and their concentration would be equal to their initial concentration ($\varphi_{p\_initial}$). Here, the same number of particles are confined into a smaller area (A_{p_fing}) due to the occurrence of the fingering phenomenon, which means the concentration of particles inside the fingers should be higher than their initial concentration. Based on assumption #3, the concentration of the particles inside the fingers (φ_{p_fing}) is equal to their disengagement concentration (φ_{p_dis}), which has been measured through the experiments. Therefore, φ_{p-fing} is a known value. In conclusion, A_{p-fing} can be calculated via:

$$A_{p\_fing} = A_{total}\frac{\varphi_{p\_initial}}{\varphi_{p\_fing}} \qquad 5.9$$

Finally, $Q_{w\downarrow}$ can be calculated from:

$$Q_{w\downarrow} = v_{w\downarrow} \times A_{p\_fing} \times (1 - \varphi_{p\_fing}) \qquad 5.10$$

Using assumption #4, the upward flow rate of water inside the emulsion fingers ($Q_{w\uparrow}$) is: $Q_{w\uparrow} = Q_{w\downarrow}$.

The cross-sectional area occupied by the emulsion fingers (A_{e-fing}) can be calculated from:

$$A_{e\_fing} = A_{total} - A_{p\_fing}$$

5.11

By the same reasoning described above, for the particles, the concentration of oil droplets inside emulsion fingers (φ_{d-fing}) can be calculated using the following equation:

$$\varphi_{d\_fing} = \varphi_{d\_initial} \frac{A_{total}}{A_{e\_fing}}$$

5.12

Note that $\varphi_{d\_initial}$ is the initial concentration of the oil droplets, which can be calculated using the following equation:

$$\varphi_{d\_initial} = \frac{Emulsion\ Oil\% \times (1 - \varphi_{p\_initial})}{100}$$

5.13

From the calculated values of $Q_{w\uparrow}$, A_{e_fing}, and φ_{d_fing}, the upward velocity of water inside the emulsion fingers is:

$$v_{w\uparrow} = \frac{Q_{w\uparrow}}{A_{e\_fing}(1 - \varphi_{d\_fing})}$$

5.14

Finally, the upward velocity of the oil droplets inside the fingering zone (v_{d-fing}) is:

$$v_{d-fing} = v_{w\uparrow} + v_{d\infty}(1 - \varphi_{d\_fing})^{n-1}$$

5.15

In Equation 5.15, $v_{d\infty}$ and n are the terminal rising velocity and the Richardson-Zaki index of the oil droplets in water. Equation 5.15 shows that the output of the model is the rising velocity

of the droplets. To validate the accuracy of the model, its results should be compared to the measured v_{d-fing} values of the experimental tests. The problem with this measurement was that the interface of the rising emulsion could not be easily seen and tracked in the tests. Therefore, the rising velocity of the droplets in the fingering region was measured using the following method:

- Although the interface of the rising emulsion was not visible through the settling particles, it was easy to locate the height where the settling particles and the rising emulsion disengage from each other. In Section 5.3, this height is introduced as the disengagement point (D) and has been measured for the unstable tests.

- It is schematically shown in Figure 5.5 that disengagement occurs at the height H. It is also known, for each unstable settling test, the time it takes for the emulsion to disengage from the particles. Therefore, the rising velocity of the oil droplets can be taken as:

$$v_{d-fing} = \frac{H}{t_D} \qquad\qquad 5.16$$

where t_D is the time between the beginning of the settling and the moment when the disengagement occurs.
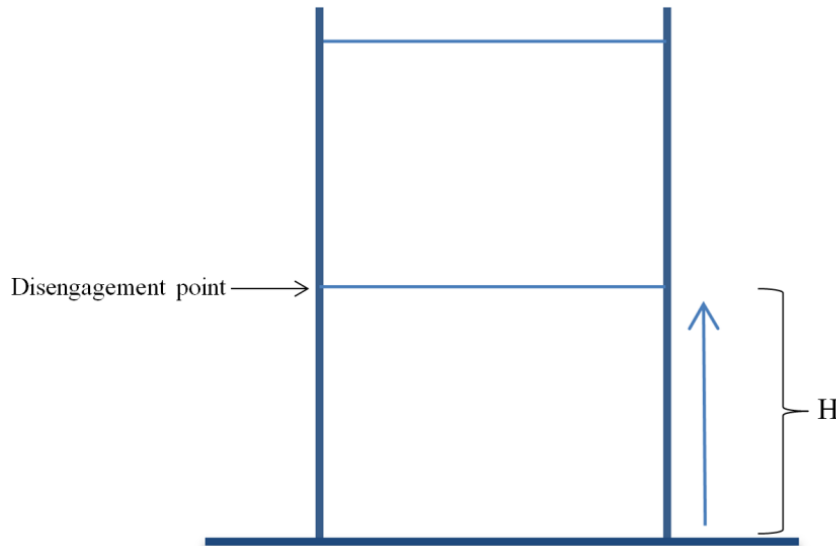
Figure 5.5- A simple schematic view of the settling column showing that the droplets should travel the distance of H to be disengaged from the settling suspension of particles

Table 5.5 shows the results of the comparison between the measured values of v_{d-fing} and the values predicted by the model for each test.

Table 5.5- Comparison of the measured rising velocity of droplets in the unstable tests with the model predictions

Map	Oil Type	Emulsion Oil%	d_p (μm)	φ_p	d_p(μm)	$\dfrac{Predicted\ V_{d-fing}}{Measured\ V_{d-fing}}$
F	Isopar M	20	10	0.2	26	**1.09**
	Silicone Oil	20	15	0.2	26	**1.06**
	Mineral Oil	20	15	0.2	26	**1.10**
L	Isopar M	30	10	0.3	26	**0.87**
	Silicone Oil	30	15	0.3	26	**0.92**
A	Isopar M	10	10	0.15	13	**1.04**
	Silicone Oil	10	15	0.15	13	**1.08**
B	Isopar M	10	10	0.2	13	**1.14**
C	Isopar M	10	10	0.25	13	**1.05**
D	Isopar M	10	10	0.3	13	**1.12**
E	Isopar M	20	10	0.15	13	**1.07**

The last column of Table 5.5 shows that the model predicted the rising velocity of the oil droplets with good accuracy. This successful prediction indicates that the model is working well and can be used to obtain deeper insights into unstable emulsion-particle settling systems.

The accuracy of the model suggests that the model assumptions described previously are reasonable. This leads to the following inferences:

- The main reason for the velocity enhancements in the unstable emulsion-particle settling system is the fluid movement due to convective flow inside the fingers. In fact, particle settling velocity inside the fingers is a combination of fluid velocity plus the particles' relative velocity to that of fluid.

- Suspension fingers contain only particles and water, while emulsion fingers contain only oil droplets and water.
- Particle concentration inside the fingers is equal to their disengagement concentration, which is greater than the initial concentration.

Chapter 6
Conclusions and Recommendations

6.1. Summary and Conclusions

The goal of this project was to investigate the instabilities in emulsion-particle settling systems. In an unstable emulsion-particle settling system, the particles are unevenly distributed and form segregated settling streams. This phenomenon is known as fingering. Yan and Masliyah [16] discovered these instabilities in emulsion-particle settling systems and reported a resulting enhancement in particle settling velocity.

The literature also shows the existence of another type of bi-dispersed settling system containing two species of heavy and light solid particles, in which the unstable settling occurs. A study by Batchelor and Van Rensburg [37] showed that the stability status of heavy-light particle systems is a function of size, density, and the concentration of both particle species. Their work was used as a helpful guide during the present study of emulsion-particle settling systems.

Although the Yan and Masliyah [16] study was a valuable source of primary information about unstable emulsion-particle settling systems, important questions were left unanswered, including:

- What variables contribute to the instability of the system?
- How can the instability of an emulsion-particle settling system be predicted?
- What happens to the particles, emulsion droplets, and the fluid when an emulsion-particle settling system becomes unstable?

To address these questions, series of settling experiments were designed and performed. The key results included the following:

- A set of 12 stability maps were produced for emulsion-particle settling systems. Each map has unique values of particle concentration (φ_p) and emulsion oil concentration (β_o). On each map, the stability status of an emulsion-particle settling system can be found by locating the $\lambda = \frac{d_d}{d_p}$ and $\gamma = \frac{\rho_o - \rho_w}{\rho_p - \rho_w}$ values of the system on the map.
- Particle settling velocities were measured in each test. Also, settling velocities were predicted using the Richardson-Zaki equation for both stable and unstable

tests. A comparison between the measured and the predicted velocities was made for each test.

- A model for the enhanced particle settling during the unstable tests was developed. The model is based on the assumption of convective flow within the fingering streams.

The following are the main conclusions of the project:

- The resulting stability maps could be used to predict the stability status of the emulsion-particle settling systems. These maps will allow engineers and researchers to determine if conventional settling velocity correlations are applicable to the particular emulsion-particle settling system they are working on.
- Comparing the measured and predicted settling velocities confirmed Yan and Masliyah [16] statements about settling velocity enhancements in the unstable tests. The results of the unstable tests showed that measured settling velocities were higher than the predicted values (before particle disengagement from the emulsion).
- In unstable tests, the measured 'disengagement concentration' of the particles is higher than their initial concentrations.
- Considering the emulsion as a continuous phase would not be a valid assumption when the system is unstable, and the particles are engaged with emulsion.
- Successful prediction of the droplet rising velocity by the model suggest that the model assumptions are valid and that the model accurately predicts system behavior. As a result, the following conclusions could be made from the model:
  - Enhanced settling velocities in the unstable tests are caused by the convective motion of the all species (particles, droplets, and water) in the fingering streams. Particle settling velocity in the fingers is a result of two components: velocity of water plus the relative velocity of the particles to that of water. The same thing happens to the oil droplets in their own streams, except that they rise.

- Particle concentration inside the fingers is equal to their disengagement concentration. Inside the fingers, the particles have a concentration higher than their initial concentration (the same thing happens to droplets). It accentuates the impact of the fingering phenomenon on the velocity enhancement even more. At higher concentrations, particles are usually expected to settle with lower velocity while the exact opposite happens in the unstable tests.

6.2. Recommendations for Future Work

The experimental plan of this project was mainly designed to find the stability boundary of the emulsion-particle settling systems under a variety of conditions. Additionally, velocity measurements and corresponding predictions were conducted for each test. A model was designed for the unstable tests and validated using the experimental measurements.

To develop a comprehensive equation that can predict settling velocities in unstable settling systems under a variety of conditions, a new set of experiments could be designed with the primary goal of developing an equation to predict the settling velocities in the unstable tests. The stability maps can be used as a source to design the test matrix so that all the test points lie in the unstable regions of the maps. Additionally, more advanced velocity measurement methods like PIV (Particle Image Velocimetry) [43] can be used to obtain more accurate velocity measurements and better describe the flow inside the fingering streams. Refractive index matching should be used for water, oil droplets, and a large portion of particles so that only a small portion of the particles would be visible. This is necessary because the laser light scattering by the particles and oil droplets would be so high that nothing would be detectable by the PIV method at high concentrations of particles and oil droplets.

The other recommendation for future work would be to repeat the stability experiments using water-in-oil emulsions. Note that all the emulsions prepared and used in this project are oil-in-water emulsions, which causes all the γ values to be negative. Nevertheless, the Batchelor and Van Rensburg stability map for heavy-light particle systems [37] (Figure 2.8) suggests that instability also occurs for positive values of γ, even though the shape and formation of the

unstable structures at those γ values might be different from the fingering streams observed in this project. To have a positive γ value in an emulsion-particle settling system, the type of emulsion should be water-in-oil (with the oil lighter than water). In that case, contrary to the experiments of the present study, the particles and the water droplets would move in the same direction. It would be also interesting to know if the velocity enhancement occurs in the water-in-oil emulsion-particle systems.

6.3. Potential Applications

Settling processes are encountered in many industries, including oil sands extraction and processing. In almost all of the bitumen recovery processes, it is desirable to have rapid settling of particles.

Making intentionally unstable settling could be a potential application of this research in industry. This should reduce vessel residence time and save operating costs in any industrial settling process where an enhanced particle sedimentation rate is desirable. To achieve this, a certain amount of emulsion with specific droplet size and concentration could be added to the settling system to make it unstable. The exact condition of the unstable process could be defined using the stability maps produced in this project. For example, in the oil sands industry, inclined settlers are being used to enhance the settling rate of the particles. Adding an emulsion with specified conditions so that the settling system becomes unstable can boost the performance of inclined settlers. Then, the added emulsion could be separated using emulsion breaking techniques.

References

[1]   B. J. Bluck, "Sedimentation in the meandering River Endrick," *Scottish J. Geol.*, vol. 7, no. 2, pp. 93–138, 1971.

[2]   S. C. Turbak, G. J. Olson, and G. A. McFeters, "Impact of western coal mining-I. Chemical investigations of a surface coal mine sedimentation pond," *Water Res.*, vol. 13, no. 11, pp. 1023–1031, 1979.

[3]   T. Matko, N. Fawcett, A. Sharp, and T. Stephenson, "Recent progress in the numerical modelling of wastewater sedimentation tanks," *Process Saf. Environ. Prot.*, vol. 74, no. 4, pp. 245–258, 1996.

[4]   G. Jin, T. W. Patzek, and D. B. Silin, "Physics-based Reconstruction of Sedimentary Rocks," in *SPE Western Regional/AAPG Pacific Section Joint Meeting*, 2003.

[5]   L. Svarovsky, *Solid-Liquid Separation*, 4th ed. Butterworth-Heinemann, 2000.

[6]   V. Wolff and Hatch Ltd., "Bitumen Separation," in *Handbook on Theory and Practice of Bitumen Recovery from Athabasca Oil Sands, Volume 2: Industrial Practice*, Kingsley Knowledge Publishing, 2013, pp. 165–198.

[7]   A. Falconer, "Gravity separation: Old technique/new methods," *Phys. Sep. Sci. Eng.*, vol. 12, no. 1, pp. 31–48, 2003.

[8]   A. Acrivos and E. Herbolzheimer, "Enhanced sedimentation in settling tanks with inclined walls," *J. Fluid Mech.*, vol. 92, no. 3, pp. 435–457, 1979.

[9]   J. Matthews and S. C. Ltd., "Tailings Management," in *Handbook on Theory and Practice of Bitumen Recovery from Athabasca Oil Sands, Volume 2: Industrial Practice*, Kingsley Knowledge Publishing, 2013, pp. 291–319.

[10]   R. S. Sanders and R. G. Gillies, "Hydrotransport," in *Handbook on Theory and Practice of*

Bitumen Recovery from Athabasca Oil Sands, Volume 2: Industrial Practice, Kingsley Knowledge Publishing, 2013, pp. 119–164.

[11] Oil Sands Magazine, "Froth Settling Units," 2019. [Online]. Available: https://www.oilsandsmagazine.com/technical/mining/froth-treatment/paraffinic/fsu-froth-settling-unit.

[12] F. Goodarzi and S. Zendehboudi, "A Comprehensive Review on Emulsions and Emulsion Stability in Chemical and Energy Industries," *Can. J. Chem. Eng.*, vol. 97, no. 1, pp. 281–309, 2019.

[13] D. Beydoun, D. Guang, R. P. Chhabra, and J. A. Raper, "Particle settling in oil-in-water emulsions," *Powder Technol.*, vol. 97, no. 1, pp. 72–76, 1998.

[14] N. O. Skeie and M. Halstensen, "Level estimation in oil/water separators based on multiple pressure sensors and multivariate calibration," *J. Chemom.*, vol. 24, no. 7–8, pp. 387–398, 2010.

[15] E. Tipman and G. Hodgson, "Sedimantataion in Emulsions of Water in Petroleum," *J. Pet. Technol.*, vol. 8, no. 9, pp. 91–93, 1956.

[16] Y. Yan and J. H. Masliyah, "Sedimentation of Solid Particles in Oil-in-Water Emulsions," *Int. J. Multiph. Flow*, vol. 19, no. 5, pp. 875–886, 1993.

[17] J. H. Masliyah, J. Czarnecki, and Z. Xu, "Fluid Particle Dynamics as Applied to Oil Sands Operation," in *Handbook on Theory and Practice of Bitumen Recovery from Athabasca Oil Sands, Volume 1: Theoreical Basis*, Kingsley Knowledge Publishing, 2011, pp. 129–172.

[18] L. Schiller and A. Naumann, "Über die grundlegenden Berechnungen bei der Schwerkraftaufbereitung," *Zeitschrift des Vereins Dtsch. Ingenieure*, vol. 77, pp. 318–320, 1933.

[19] G. G. Stokes, "On the Effect of the Internal Friction of Fluids on the Motion of Pendulums," in *Mathematical and Physical Papers (Cambridge Library Collection - Mathematics), vol.3*, Cambridge University Press, 1851, pp. 1–10.

[20] T. Acher, "A Moments Model for the Numerical Simulation of Bubble Column Flows," Technical University of Munich, 2015.

[21] M. Hartman, V. Havlin, O. Trnka, and M. Carsky, "Predicting the free-fall velocities of spheres," *Chem. Eng. Sci.*, vol. 44, no. 8, pp. 1743–1745, 1989.

[22] R. Turton and N. N. Clark, "An explicit relationship to predict spherical particle terminal velocity," *Powder Technol.*, vol. 53, no. 2, pp. 127–129, 1987.

[23] G. B. Wallis, *One-dimensional two-phase Flow*, 1st ed. McGraw-Hill, 1969.

[24] J. F. Richardson and W. N. Zaki, "Sedimentation and Fluidisation: Part 1," *Trans. Inst. Chem. Eng.*, vol. 32, pp. 35–53, 1954.

[25] R. H. Davis and H. Gecol, "Hindered settling function with no empirical parameters for polydisperse suspensions," *AIChE J.*, vol. 40, no. 3, pp. 570–575, 1994.

[26] P. N. Rowe, "A Convenient Empirical Equation for Estimation of the Richardson-Zaki Exponent," *Chem. Eng. Sci.*, vol. 42, no. 11, pp. 2795–2796, 1987.

[27] A. R. Khan and J. R. Richardson, "Fluid-Particle Interactions and Flow Characteristics of Fluidized Beds and Settling Suspensions of Spherical Particles," *Chem. Eng. Commun.*, vol. 78, no. 1, pp. 111–130, 1989.

[28] J. D. Henry, M. Prudich, and C. Lau, "Liquid, Liquid, Solid Systems: Role of Water in Particle Removal from Hydrocarbon Suspensions," *Colloids and Surfaces*, vol. 1, no. 3–4, pp. 335–348, 1980.

[29] R. L. Whitmore, "The sedimentation of suspensions of spheres," *Br. J. Appl. Phys.*, vol. 6, no. 7, pp. 239–245, 1955.

[30] R. H. Weiland and R. R. Mcpherson, "Accelerated Settling by Addition of Buoyant Particles," *Ind. Eng. Chem. Fundam.*, vol. 18, no. 1, pp. 45–49, 1979.

[31] R. H. Fessas, Yiannis P; Weiland, "Convective Solids Settling Induced by a Buoyant Phase theoretical attempts to calculate the bulk sedimentation velocity," *AIChE J.*, vol. 27, no. 4, pp. 588–592, 1981.

[32] Y. P. Fessas and R. H. Weiland, "Concevtive Solids Settling Induced by a Buoyant Phase - A New Method for the Acceleration of Thickening," *Resour. Conserv.*, vol. 9, pp. 87–93, 1982.

[33] Y. P. Fessas and R. H. Weiland, "The Settling of Suspensions Promoted by Rigid Buoyant Particles," *Int. J. Multiph. Flow*, vol. 10, no. 4, 1984.

[34] R. H. Weiland, Y. P. Fessas, and B. V. Ramarao, "On instabilities arising during sedimentation of two-component mixtures of solids," *J. Fluid Mech.*, vol. 142, pp. 383–389, 1984.

[35] G. K. Batchelor, "Sedimentation in a Dilute Polydisperse System of Interacting Spheres. part 1. General Theory," *J. Fluid Mech.*, vol. 119, pp. 379–408, 1982.

[36] G. K. Batchelor and C. S. Wen, "Sedimentation in a dilute polydisperse system of interacting spheres. Part 2. Numerical Results," *J. Fluid Mech.*, vol. 124, pp. 495–528, 1982.

[37] G. K. Batchelor and R. W. Janse Van Rensburg, "Structure formation in bidisperse sedimentation," *J. Fluid Mech.*, vol. 166, pp. 379–407, 1986.

[38] Y. Yamashita, R. Miyahara, and K. Sakamoto, "Emulsion and Emulsification Technology," in *Cosmetic Science and Technology: Theoretical Principles and Applications*, Elsevier Ltd, 2017, pp. 489–506.

[39] J. H. Masliyah, J. Czarnecki, and Z. Xu, "Basic Scientific Background," in *Handbook on Theory and Practice of Bitumen Recovery from Athabasca Oil Sands, Volume 1: Theoretical Basis*, Kingsley Knowledge Publishing, 2011, pp. 51–127.

[40] Sigma Alderich, "Triton X-100," 2019. [Online]. Available: https://www.sigmaaldrich.com/catalog/product/sial/x100?lang=en&region=CA.

[41] F. Menaa, "Emulsions Systems for Skin Care: From Macro to Nano-Formulations," *Pharm. Care Heal. Syst.*, vol. 1, no. 2, 2014.

[42] R. Pal, "Novel viscosity equations for emulsions of two immiscible liquids," *J. Rheol. (N.*

Y. N. Y)., vol. 45, no. 2, pp. 509–520, 2001.

[43]   M. Raffel, C. E. Willert, F. Scarano, C. J. Kähler, S. T. Wereley, and J. Kompenhans, *Particle Image Velocimetry, A Practical Guide*, 3rd ed., no. 1. Springer, 2018.

Appendices

Appendix A: Preliminary tests to examine silver-coated glass beads credibility

Some preliminary tests were done with small volumes of silver-coated particles and emulsion to confirm the visibility of the particles. Figure A.1 shows that the fingering streams and upper interface of the settling silver-coated glass beads are traceable through the emulsion. Figure A.1a shows the formation of visible fingering streams of the silver-coated particles through the emulsion. Stirring causes a foam layer to form above the settling zone, which does not affect the settling process. Figure A.1b shows that the upper interface of the settling particles (that is the key factor in particle settling velocity measurements) is visible. Figure A.1c shows the disengagement of the settling particles from the rising emulsion. Figure A.1d illustrates the settling of particles after disengagement when a growing layer of water has been formed between the emulsion and particle suspension. The particles lower interface in Figure A.1 is the height of settled particles packed bed. Overall, the results from Figure A.1 confirm the suitability of silver-coated glass beads for the settling stability tests of this project.

The preliminary tests showed that the particles are not recoverable and, therefore, could not be reused for subsequent settling tests.
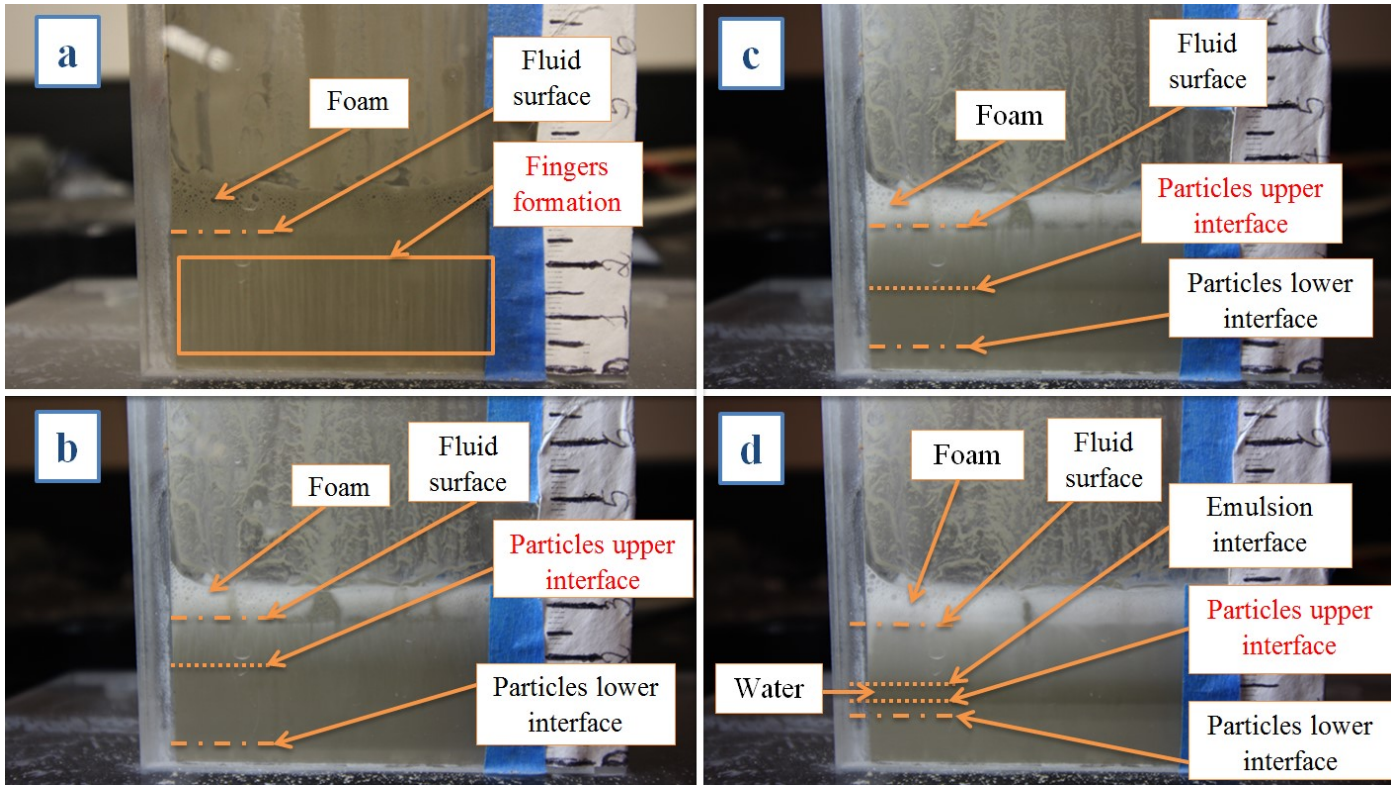
Figure A.1- A preliminary test to check the visibility of the fingers and particles upper interface through the emulsion; a) Fingers formation, b) visibility of particles interface, c) particles disengagement from the emulsion, d) particles settling in water after disengagement

Appendix B: Repeatability of velocity measurements

Table A.1 shows the measured velocities of different runs for two of the settling tests (one stable and one unstable) performed in this project.

<div align="center">

Table A.1- Comparison of measured particle settling velocities in different runs for two of the settling tests

</div>

Test	Stability Status	φ_p	Emulsion Oil%	Oil Type	d_p (μm)	Engaged / Disengaged	Measured Settling Velocity (cm/s)	
							Run #1	Run #2
I	Stable	0.3	30%	Silicone Oil	51	Engaged	1.34×10^{-2}	1.38×10^{-2}
II	Unstable	0.2	20%	Isopar M	26	Engaged	2.46×10^{-2}	2.51×10^{-2}
						Disengaged	8.3×10^{-3}	8.5×10^{-3}

Appendix C: Rest of the settling graphs of unstable tests
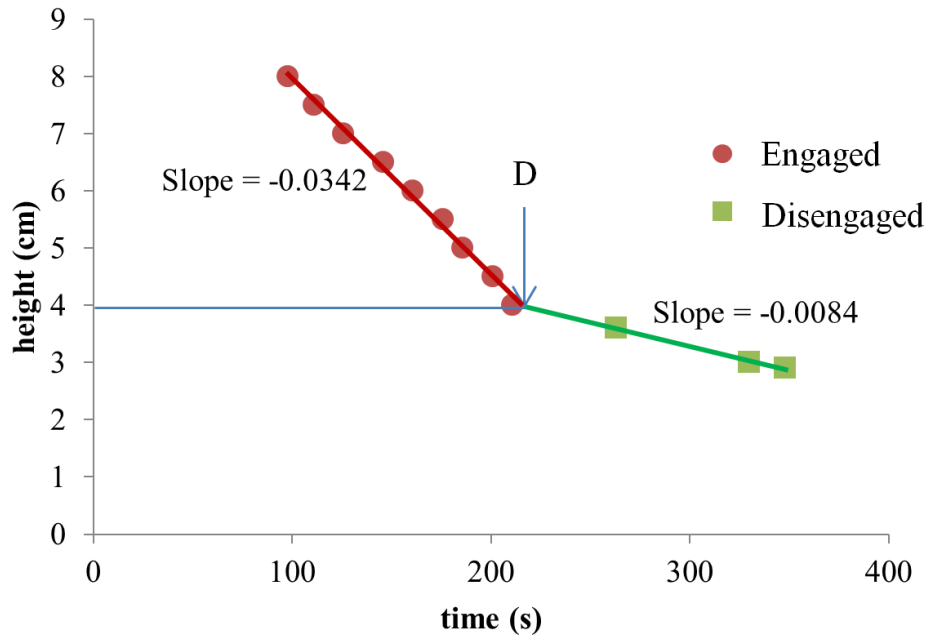
Figure A.2- Settling graph of particles upper interface displacement with time for 26 μm particles with $\varphi_p = 0.2$ settling through 20% Mineral Oil emulsion; 'D' illustrates the disengagement point
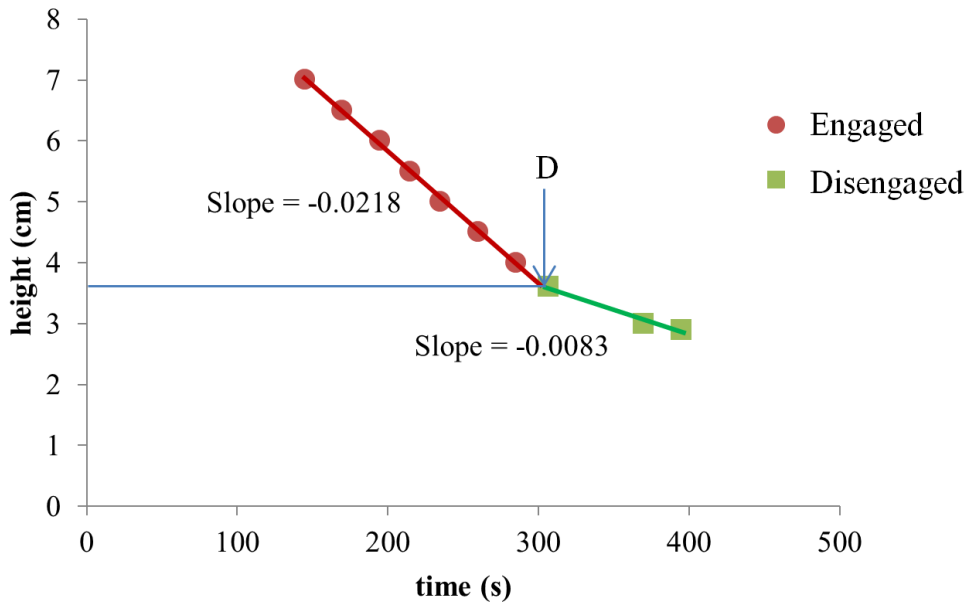
Figure A.3- Settling graph of particles upper interface displacement with time for 26 μm particles with $\varphi_p = 0.2$ settling through 20% Silicone Oil emulsion; 'D' illustrates the disengagement point
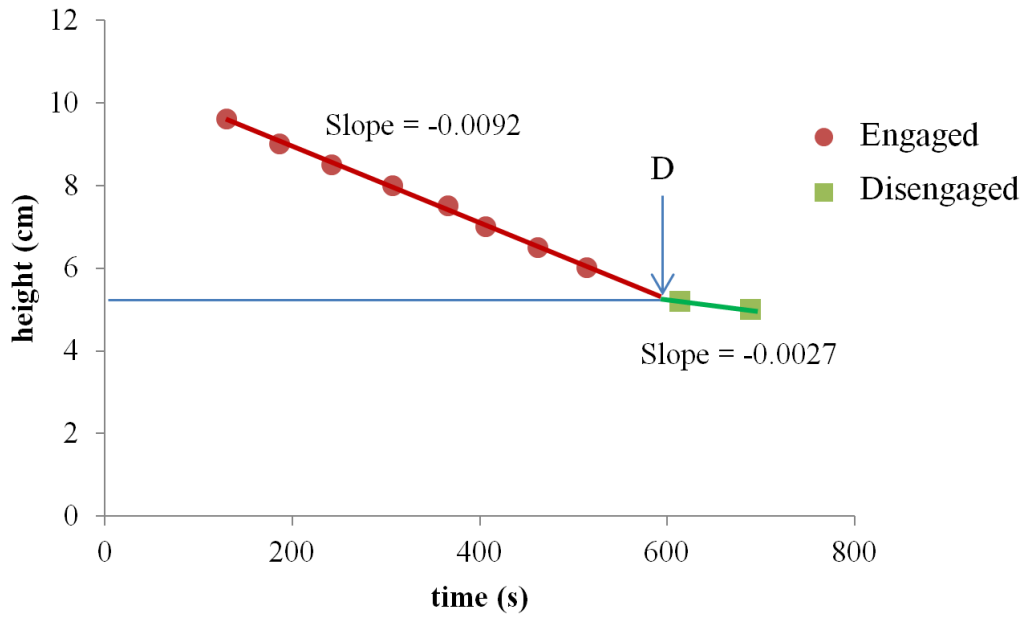
Figure A.4- Settling graph of particles upper interface displacement with time for 26 μm particles with $\varphi_p = 0.3$ settling through 30% Isopar M emulsion; 'D' illustrates the disengagement point
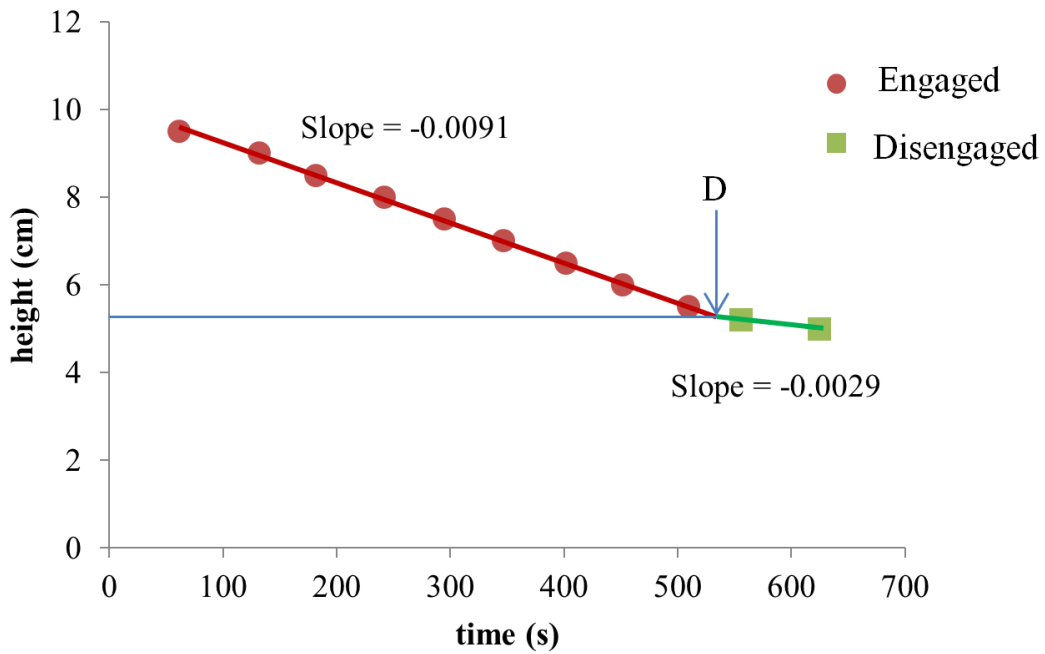
Figure A.5- Settling graph of particles upper interface displacement with time for 26 μm particles with $\varphi_p = 0.3$ settling through 30% Silicone Oil emulsion; 'D' illustrates the disengagement point
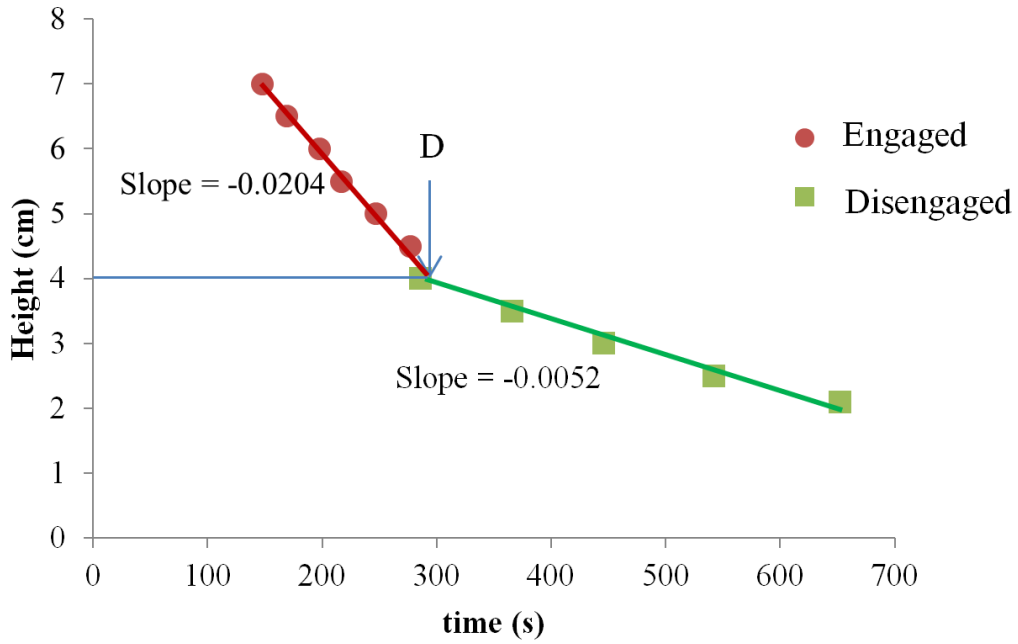
Figure A.6- Settling graph of particles upper interface displacement with time for 13 μm particles with $\varphi_p = 0.15$ settling through 10% Isopar M emulsion; 'D' illustrates the disengagement point
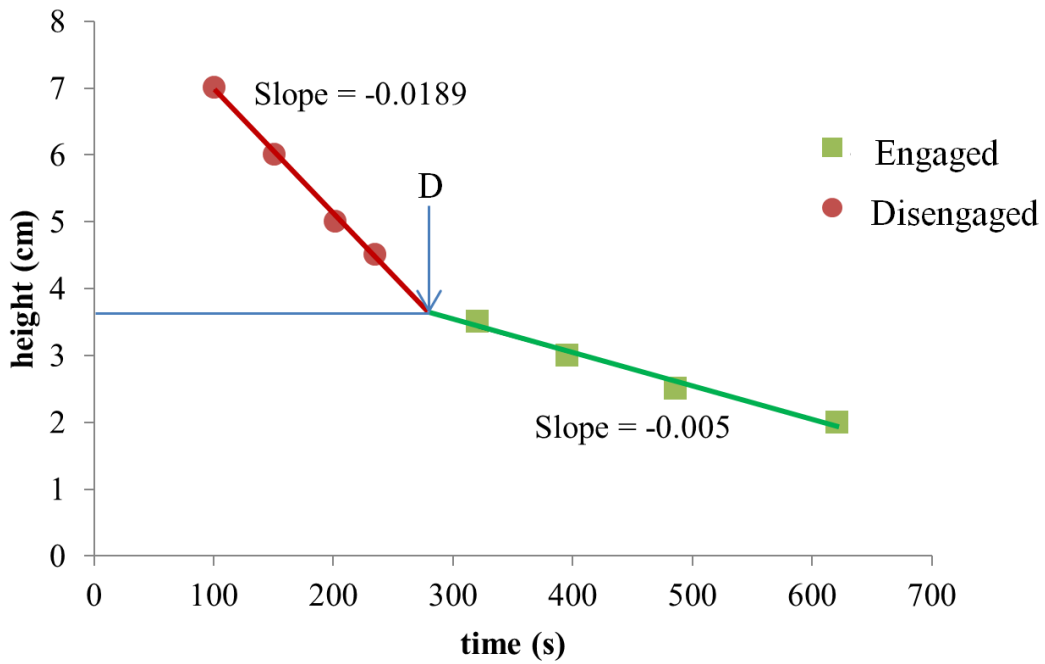
Figure A.7- Settling graph of particles upper interface displacement with time for 13 μm particles with $\varphi_p = 0.15$ settling through 10% Silicone Oil emulsion; 'D' illustrates the disengagement point
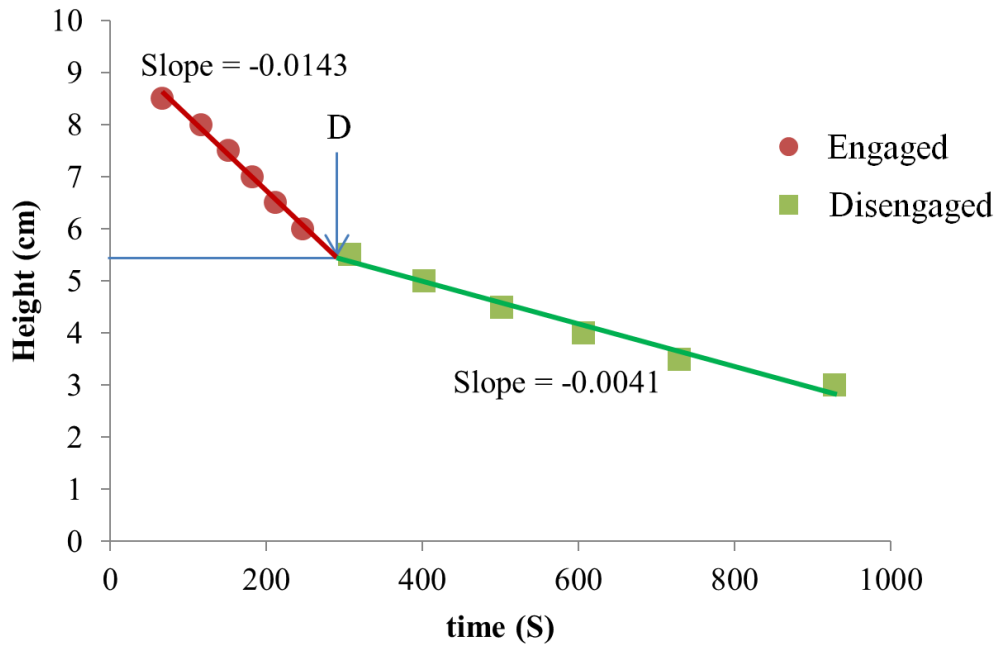
FigureA.8- Settling graph of particles upper interface displacement with time for 13 μm particles with $\varphi_p = 0.2$ settling through 10% Isopar M emulsion; 'D' illustrates the disengagement point
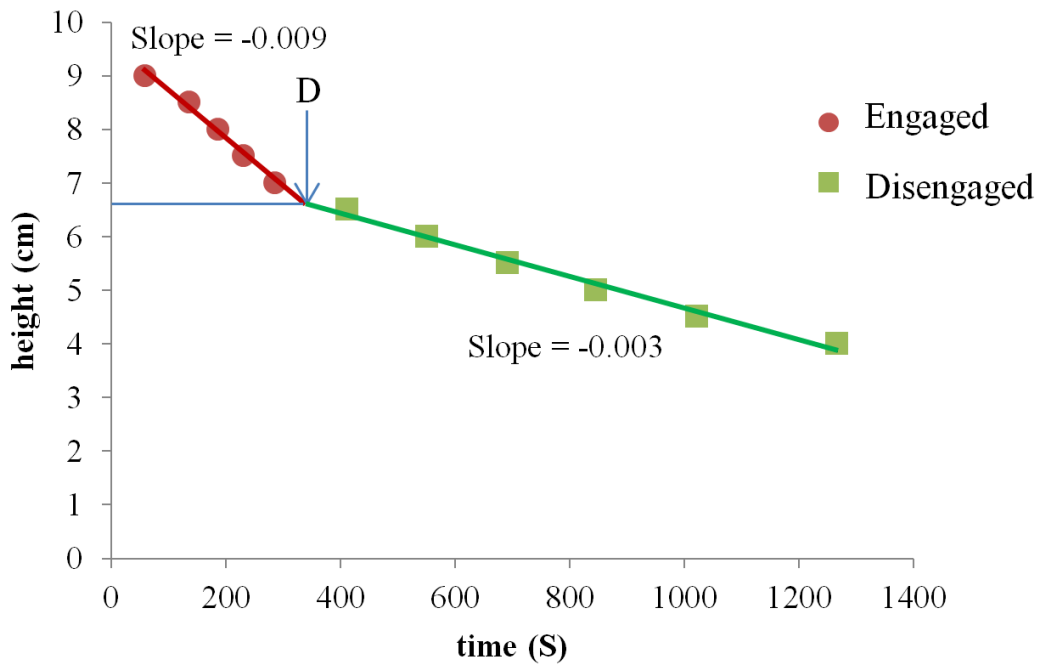
Figure A.9- Settling graph of particles upper interface displacement with time for 13 μm particles with $\varphi_p = 0.25$ settling through 10% Isopar M emulsion; 'D' illustrates the disengagement point
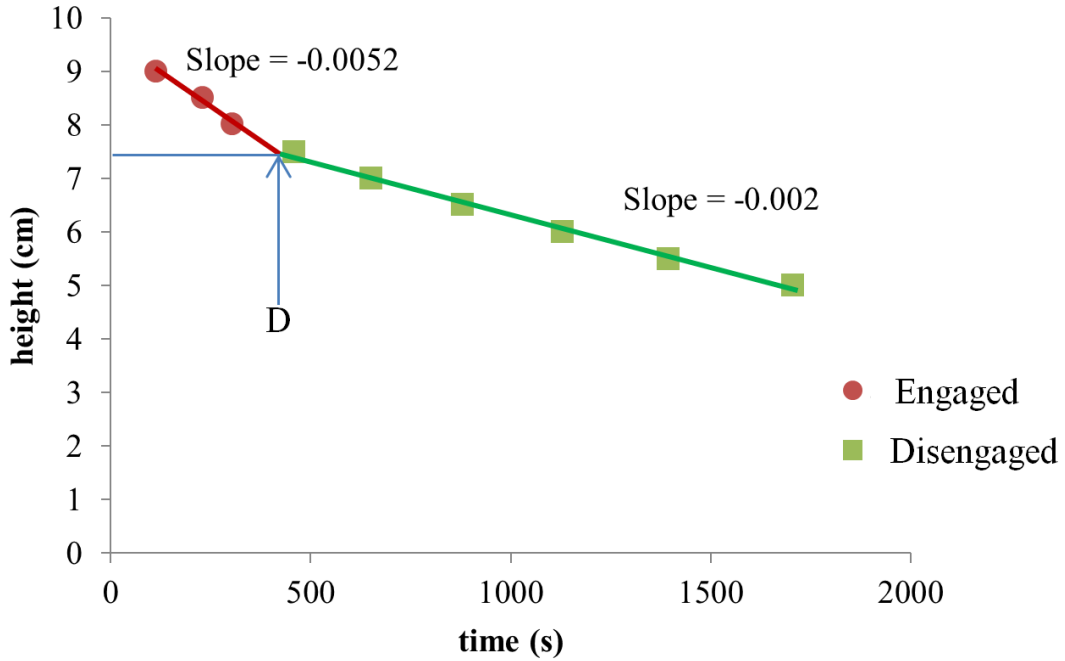
Figure A.10- Settling graph of particles upper interface displacement with time for 13 µm particles with $\varphi_p = 0.3$ settling through 10% Isopar M emulsion; 'D' illustrates the disengagement point
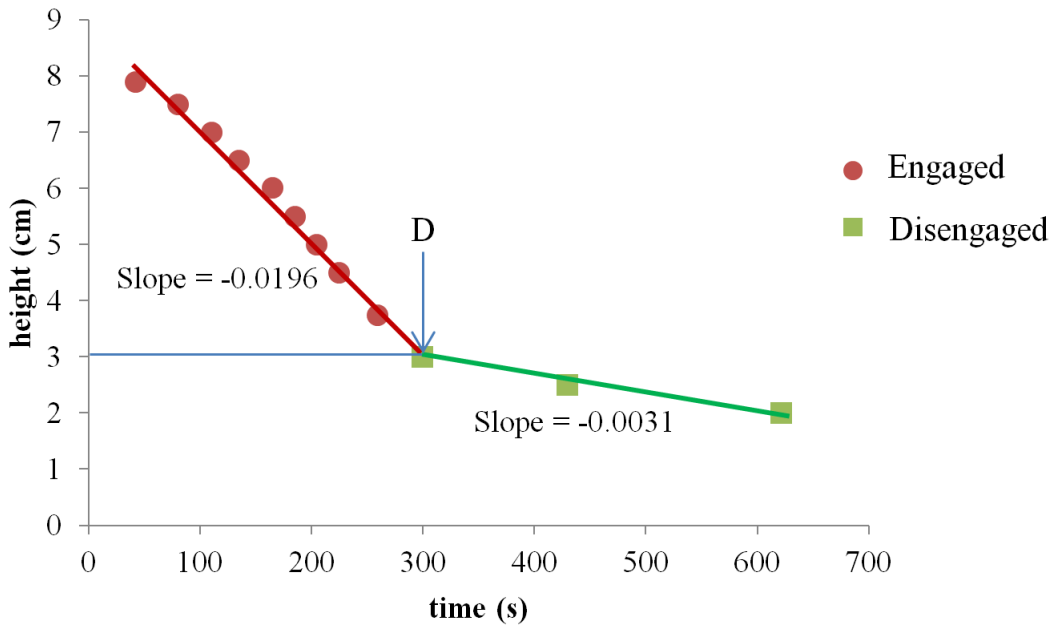
Figure A.11- Settling graph of particles upper interface displacement with time for 13 µm particles with $\varphi_p = 0.15$ settling through 20% Isopar M emulsion; 'D' illustrates the disengagement point

Appendix D: Rest of the microscope image and size distribution of emulsions
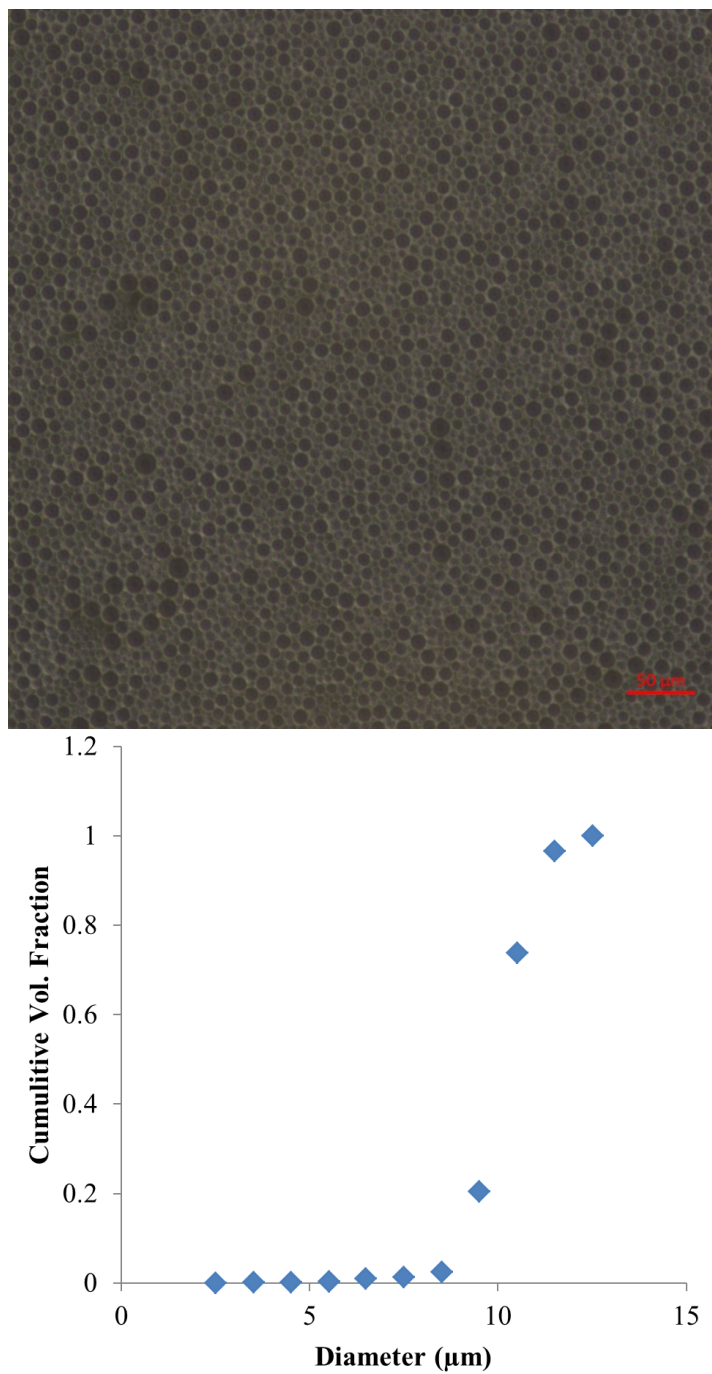
Figure A.12- Microscopic image of Isopar M droplets (top) and their size distribution (bottom)
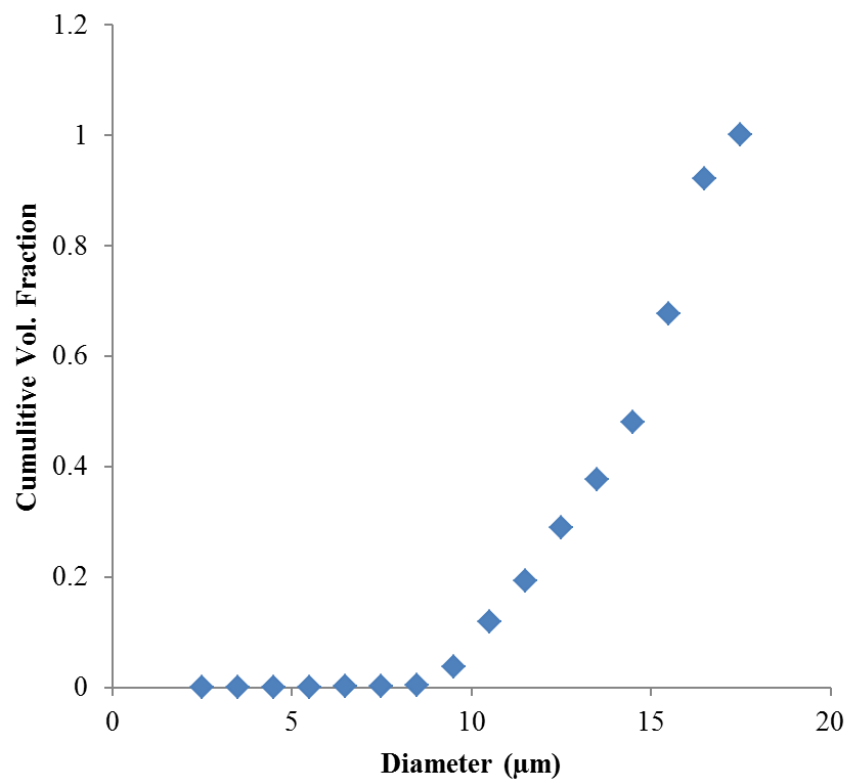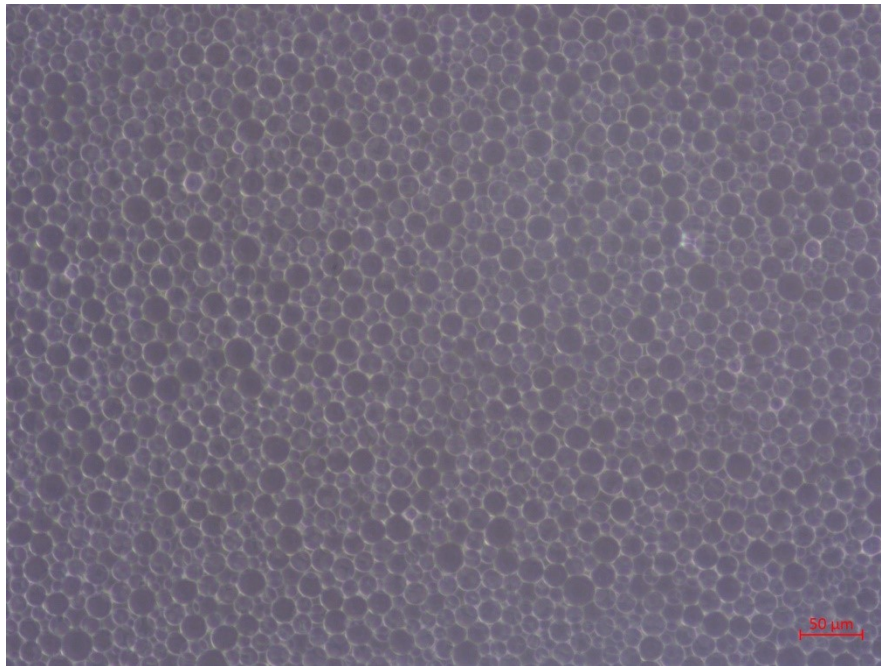
Figure A.13- Microscopic image of Silicone Oil droplets (top) and their size distribution (bottom)

Appendix E: MATLAB script for finding droplets size distributions from microscope images

```matlab
% Load original image
x = imread('Untitled29.jpg');
figure
imshow(x)
title(' O/W Emulsion Microscope Image Captured with Droplets Detected and
Measured')

% Decrease sensivitiy for less droplets and vice versa
% Decrease Edge Threshold for more droplets

% Break up the droplets into 2 radius range to avoid overlap and imrpove
% detection quality

 [centersDarksmall, radiiDarksmall, metricDarksmall] = imfindcircles(x,[3
16], ...
    'ObjectPolarity','dark','Sensitivity',0.7,'EdgeThreshold',0.05);
hDarksmall = viscircles(centersDarksmall, radiiDarksmall,'Color','b');

[centersDarkbig, radiiDarkbig, metricDarkbig] = imfindcircles(x,[16 35], ...
    'ObjectPolarity','dark','Sensitivity',0.9,'EdgeThreshold',0.05);
hDarkbig = viscircles(centersDarkbig, radiiDarkbig,'Color','r');

n = numel(radiiDarksmall)+ numel(radiiDarkbig); % Number of droplet detected
combinedradius_pixels = [radiiDarkbig;radiiDarksmall];
combinedradius_microns = combinedradius_pixels ./ 2.95;
% Pixel/microns ratio determined by ImageJ with scalebar on image

diameter = combinedradius_microns .*2;

% calculate and print quartile values
d50 = prctile(diameter,50);
d75 = prctile(diameter,75);
d90 = prctile(diameter,90);
d100 = prctile(diameter,100);

fprintf('There are %i droplets detected from the picture\n', n)
fprintf('D50: %i , D75: %i , D90: %i , D100: %i , \n',d50,d75,d90,d100)

% Distribution
figure
histogram(diameter);
title('Droplet Size Distribution of O/W Emulsion from Microscope Image')
```

Appendix F: Safe Work Procedures

1- Emulsion preparations

Job title: **Preparation of oil-in-water emulsions**	Year: 2019
Written by: Aref Fozooni Kangarshahi, Carlos Sanchez, Bach Vo	Conducted by: Aref Fozooni Kangarshahi
Required protective equipment: Safety glasses, Plastic gloves, Lab coat, Full length pants, Closed toe shoes	
First aid measures: First aid kit, large spill kit and fire extinguisher (All the chemicals including the surfactant and the oils are flammable.)	

Objective: The procedure for preparation of emulsion is presented in this SWP. These emulsions will be used later in the stability experiments.

I. Preparation of 1% surfactant aqueous solution

#	Tasks	Potential hazards
1	Thoroughly wash three beakers (the beaker in which the emulsion would be prepared should be 400 ml), a 10 ml graduated pipette (or a syringe) and three graduated cylinders: one of 50 ml and two of 100 ml (material Pyrex 1060). Rinse carefully by using tap water, a soap-water solution and distillated water. Use moderate tap pressure. Handle glassware gently with caution.	Possibility of slipping and glassware breakage while washing. Potential splashes of soap-water solution into the eye. **Potential injury:** Cuts by broken glassware and eye irritation by soap-water solution. Do not use cracked glass equipment or with sharp edges. In case of breakage, do not take the broken glasses by hands. Use a brush to sweep and collect the pieces into a dust pan. Then, dispose them into the container for broken glassware. Spill kit, paper towel, clean-up bucket, and mops should be placed nearby, and first aid kit should be available and quickly reachable.
2	Calculate the volume of the surfactant (Triton X-100) to prepare an aqueous solution of surfactant by 1% of volume. Knowing the volume of the emulsion (V_e) and the oil volume percentage: $$V_{aq.sol} = V_e \left(1 - \frac{Oil\ vol.percentage}{100} \right)$$ $$V_{surfactant} = 0.01 \times V_{aq.sol}$$ $$V_{water} = V_{aq.sol} - V_{surfactant}$$	

	(Note: Maximum amount of emulsion that could be prepared each time is 300 ml)	
3	Pour the defined amount of distillated water (calculated in step 2) into the 400 ml beaker. Hold the beaker firmly while pouring the water into it.	Possibility of slipping and glassware breakage **Potential injury:** Cuts by broken glassware (See step 1).
4	Introduce the defined amount of Triton X-100 (calculated in step 2) into the pipette (or a graduated syringe). Avoid using your mouth to draw the liquid into the pipette. Use a pro-pipette or pipette pump instead. Then insert the pipette into the liquid and press gently the valve or wheel of the pro-pipette to introduce the liquid into the pipette. Carefully adjust the liquid level in the pipette to ensure that the bottom of the meniscus coincide to the pipette calibration.	Possibility of slipping and glassware breakage. Potential spills of Triton X-100. **Potential injuries:** Cuts by broken glassware (See step 1)**.** Although, Triton X-100 is not highly toxic it may cause irritation on skin and/or eyes. It must not be ingested. Its flammability is restricted to high temperatures. However, avoid using it at high temperatures. Be careful, when the pro-pipette or pipette pump is connected to the pipette. Avoid putting stress on the pipette, so it might shatter. Wear proper PPE (lab coat, gloves, safety glasses, close toe shoes and long pants) In case of Triton X-100 eye contact: • Remove glasses (including contact lenses). • Flush abundant water for at least 15 minutes. • Get medical attention immediately. In case of skin contact: • Wash with water and soap. • Cover irritated skin with an emollient. • Get medical attention if the irritation remains. If triton X-100 is ingested: • Do not provoke to vomit • Get medical attention immediately

#	Tasks	Potential hazards
5	Introduce the collected Triton X-100 into the 400 ml beaker which contains water. Ensure that the beaker is placed on a flat and safe surface (lab table). After pouring the Triton X100 into the water, gently agitate with a glass rod to form the solution.	Possibility of slipping and glassware breakage. Potential spills of Triton X-100. **Potential injuries:** Cuts by broken glassware**.** Although, Triton X-100 is not highly toxic it may cause irritation on skin and/or eyes. Follow the safety guidance of steps 1 & 4. Keep wearing the proper PPE.

II. Adding the oil and preparing the oil-in-water emulsions

#	Tasks	Potential hazards
6	Calculate the volume of the oil (V_o): $$V_o = V_e \left(\frac{Desired\ oil\ vol.percentage}{100} \right)$$	
7	Pour the required oil quantity into a 100 ml graduated cylinder or into a 50 ml graduated cylinder (Depending on the quantity required)	Possibility of slipping and glassware breakage. Potential spills of the oil. Potential fire caused by the oil ignition. **Potential injuries:** Cuts by broken glassware (See step 1)**.** Wear proper PPE (lab coat, gloves, safety glasses, close toe shoes and long pants). Fire extinguisher should be reachable. In case of oil eye exposure: • Remove glasses (including contact lenses). • Flush abundant water. • If the irritation persists, get medical attention immediately. In case of skin contact: • Wash with water and soap. • Remove contaminated water.
8	Check the homogenizer and ensure that it could work safely and	Potential electrical charges/shock

#	Tasks	Potential hazards
	correctly. Check the cables to make sure that the equipment is in the safe working condition. Ensure to switch off the devise during the inspection and plugging in.	if cables are open and plugged to an electric source. Potential damage to equipment if there is a bridge of open cable. Potential electric fire from electrical sparks of open cables. Fire extinguisher should be reachable.
9	Introduce the homogenizer's rod inside the beaker containing the Triton X-100 aqueous solution. Choose the appropriate speed (10000 rpm) and turn the homogenizer on.	Potential electrical charges/shock, liquid spills, and breakage of glassware. Use safety guidance of steps 1, 4 & 7. Wear proper PPE. Fire extinguisher should be reachable. Spill and first aids kits should be available.
10	Add the oil slowly into the Triton X-100 aqueous solution under the action of the homogenizer. The oil water mixture should be sheared for at least 10 minutes. Then remove the beaker containing the prepared emulsion and cover it with paraffin film.	Potential electrical charges/shock, liquid spills, and breakage of glassware. Use safety guidance of steps 1, 4 & 7. Wear proper PPE.

III.   Cleaning up and waste disposal

#	Tasks	Potential hazards
11	Put an empty beaker under the homogenizer and rinse the homogenizer probe with water	Potential liquid spills. Use safety guidance of steps 1, 4 & 7. Wear proper PPE. Equipment manual should be available.
12	Keep the emulsions for microscopy and particle sedimentation tests. Clean carefully all the equipment including beakers, pipette, and graduated cylinders using soap-water solution. Tidy the working area. Hang the washed equipment on a dry rack.	Potential liquid spills, and breakage of glassware. Use safety guidance of steps 1, 4 & 7. Wear proper PPE.

2- Homogenizer cleaning

Job title: **Homogenizer cleaning by toluene and water**	Year: 2019
Written by: Aref Fozooni Kangarshahi	Conducted by: Aref Fozooni Kangarshahi
Required protective equipment: Safety glasses, Plastic gloves, Lab coat, Full length pants, Closed toe shoes	
First aid measures: First aid kit, spill kit and fire extinguisher	

#	Task	Potential hazards
1	Bring a wash bottle containing DI water and a small jar of toluene along with an empty wash bottle for toluene. (When filling the small jar with toluene, make sure you wear proper PPE (plastic gloves, lab coat, safety glasses, full length pants, and closed toe shoes) and it is done under the fume hood. After filling the jar, make sure that its cap is tightened.). Gloves must be inspected prior to use. When transferring toluene between labs, use a cart to provide secondary containment of spill. Put absorbent pads in the cart in case of spill.	Possibility of slipping and glassware breakage. **Potential injuries:** Cuts by broken glassware. Do not use cracked glass equipment or with sharp edges. In case of breakage, do not take the broken glasses by hands. Use a brush to sweep and collect the pieces into a dust pan. Then, dispose them into the container for broken glassware. Spill kit, paper towel, clean-up bucket, and mops should be placed nearby, and first aid kit should be available and quickly reachable. In case of toluene eye contact: - Flush eyes with plenty of water for at least 15 minutes, lifting lower and upper eyelids occasionally. Get medical attention immediately. In case of ingestion: - Do NOT induce vomiting. Never give anything by mouth to an unconscious person. Rinse mouth with water. Get medical attention immediately. In case of skin contact: - Wash off with soap and plenty of water. Consult a physician. In case of inhalation:

		- Move into fresh air. If not breathing, give artificial respiration to the victim. Consult a physician. Fire extinguisher should be reachable.
2	After finishing the job of emulsion preparation turn off the homogenizer and unplug it.	Potential electrical charges/shock if cables are open and plugged to an electric source. Potential damage to equipment if there is a bridge of open cable. Potential electric fire from electrical sparks of open cables. Fire extinguisher should be reachable.
3	Put an empty beaker under the homogenizer.	Possibility of slipping and glassware breakage. **Potential injuries:** Cuts by broken glassware. Do not use cracked glass equipment or with sharp edges. In case of breakage, do not take the broken glasses by hands. Use a brush to sweep and collect the pieces into a dust pan. Then, dispose them into the container for broken glassware.
4	Bring the toluene jar and the empty wash bottle under the fume hood. Open the jar lid and pour the toluene into the empty wash bottle. Make sure you wear proper PPE.	Use safety guidance of step 1.
5	Carefully rinse the outer wall of the homogenizer probe with toluene and water using the DI water wash bottle and toluene wash bottle. This task should be done under the fume hood.	Use safety guidance of step 1.
6	Carefully rinse the inner rod of the probe with toluene and water using the the DI water wash bottle and toluene wash bottle through the holes on the probe's body. This task should be done under the fume hood.	Use safety guidance of step 1.
7	Take the beaker (which is now containing water, toluene and dissolved materials) and empty it to the big bottle (labeled organic waste) under the fume hood.	Use safety guidance of step 1.
8	Leave the unplugged homogenizer to be dried under the fume hood.	

| 9 | Wash the beaker by using tap water and soap. Use moderate tap pressure. Wear proper PPE. | Possibility of slipping and glassware breakage while washing. Potential splashes of soap-water solution into the eye. **Potential injury:** Cuts by broken glassware and eye irritation by soap-water solution. Do not use cracked glass equipment or with sharp edges. In case of breakage, do not take the broken glasses by hands. Use a brush to sweep and collect the pieces into a dust pan. Then, dispose them into the container for broken glassware. Spill kit, paper towel, clean-up bucket, and mops should be placed nearby, and first aid kit should be available and quickly reachable. |

3- Using microscope for droplet size measurement

Job title: **Droplets' size distribution measurements using Axiolab microscope**	Year: 2019
Written by: Aref Fozooni Kangarshahi	Conducted by: Aref Fozooni Kangarshahi
Required protective equipment: Safety glasses, Plastic gloves, Lab coat, Full length pants, Closed toe shoes	
First aid measures: First aid kit, large spill kit and fire extinguisher (All the chemicals including the surfactant and the oils are flammable.)	

Objective: This SWP offers the step by step procedure of measuring the emulsion droplets size by the Axiolab microscope in a safe manner. Using this procedure, emulsion droplets' size will be obtained.

#	Task	Potential hazards
1	Using a pipette put a small droplet of the emulsion on the microscope slide. Then carefully put another slide on it and wait for the droplet to be expanded between the slides.	Cuts by the microscope slides' sharp edges. First aid kit should be available and quickly reachable.
2	Turn on the microscope light and place the prepared slide under the microscope lenses.	
3	Choose the appropriate lens (20x lens is suitable for this task)	
4	By the rotary stage locking screw choose the DF stage (Dark Field)	
5	Choose a suitable location to take pictures (any part of the slide with high numbers of droplets). This task could be done by adjusting the microscope plate under the slide.	
6	Manipulate the lens focus to have a picture with high contrast.	
7	Software: Choose the same features in the software (20x lens and DF) Adjust the exposure time to have a vivid picture. Take the final snapshot and save it.	
8	Turn off the microscope light.	
9	Find the size distribution and the mean diameter of the droplets using the Matlab script which is already prepared for this purpose.	

4- Settling experiments

Job title: **Sedimentation of particles in oil-in-water emulsions and checking the stability of the settling system**	Year: 2019
Written by: Aref Fozooni Kangarshahi	Conducted by: Aref Fozooni Kangarshahi
Required protective equipment: Safety glasses, Plastic gloves, Lab coat, Full length pants, Closed toe shoes	
First aid measures: First aid kit, large spill kit and fire extinguisher (All the chemicals including the surfactant and the oils are flammable.)	

Objective: This SWP provides the experimental steps to investigate the settling of particles in the emulsions in a safe manner. These steps help to achieve two goals: 1- finding the conditions under which the fingering phenomenon occurs; 2- measuring the average settling velocity of particles in the emulsions.

A step by step procedure:

#	Tasks	Potential hazards
1	Clean and dry the Plexiglas settler. Use tap water, water-soap solution and distilled water to wash the settler. After washing, dry the settler using absorbent paper.	Potential splashes of soap-water solution into the eye. **Potential injury:** Cuts by broken glassware and eye irritation by soap-water solution. Spill kit, paper towel, clean-up bucket, and mops should be placed nearby, and first aid kit should be available and quickly reachable.
2	Follow the steps 1 to 10 of the emulsion preparation SWP. Prepare 300 ml of oil-in-water emulsion with defined amount of oil volume percentage (follow the protocol mentioned before).	Potential chemical spills, electrical charges/ shocks and chemicals spills. Wear proper PPE (lab coat, plastic gloves, closed toe shoes and long pants). Have spills and first aid kits available. The manuals of the equipment to be used should be available as well. Fire extinguisher should be reachable.
3	Select the particles to use. There are four sizes of silver coated glass beads (12, 25, 50, and 100 μm).	

4	Calculate the required mass of particles (M_p). Using the desired volume fraction of glass beads (φ_p), the volume of emulsion used in each batch (V_e) and the particles density (ρ_p): $$V_p = \frac{\varphi_p}{1 - \varphi_p} V_e$$ $$M_p = V_p \rho_p$$	
5	Use a beaker to collect and weigh the particles.	**Potential injury:** Cuts by broken glassware. Do not use cracked glass equipment or with sharp edges. In case of breakage, do not take the broken glasses hands. Use a brush to sweep and collect the pieces into a dust pan. Then, dispose them into the container for broken glassware. The first aid kit should be available and quickly reachable.
6	Ensure that the weighing balance (Manufacturer: A&D, Model: FX-3000) is stable on a flat surface.	
7	Check if the balance cables are safe to use. The equipment has to be turned off and unplugged while the inspection is carried out. After the inspection, plug the weighting balance and turn it on.	Potential electrical charges/shock if cables are open and plugged to an electric source. Potential damage to equipment if there is a bridge of open cable. Potential electric fire from electrical sparks of open cables. Fire extinguisher should be reachable.
8	Place the beaker (Future glass beads container) on the weighting balance and tare weight by pressing the "Zero" button of the balance. Add the glass beads very carefully into the container until achieved the desire quantity	Possibility of slipping and glassware breakage **Potential injury:** Cuts by broken glassware (See step 5)
9	Carefully load the Plexiglas settler with the specified oil-in-water emulsion which was previously prepared.	Potential slip and breakage of glassware. Possible spills of liquids. Follow safety guidance of step 7 of Emulsion Preparation SWP. Wear proper PPE. Allocate the first aid kit and the spills kit nearby.

10	Carefully add the particles to the settler by the action of the T-shape wooden stirrer which is manually operated. Make sure that all bubbles originated during the mixing escape before making any measurement. Make sure that the mixture is well mixed by the stirrer.	Potential slip and breakage of glassware. Possible spills of liquids Wear proper PPE. Allocate the first aid kit and the spills kit nearby.
11	Take the T-shape stirrer out of the settler. Carefully watch the settler to see if the fingering streams are formed. Record a video of the settling process by camera and track and register the movement of the solid-liquid upper interface with time.	
12	After finishing the experiments drain out the emulsion-particle mixture from the Plexiglas settler. Carefully dispose the waste emulsion and particles into a labelled bucket. The label will have the following characteristics: **PIPELINE TRANSPORT PROCESSES RESEARCH GROUP** | **For disposal**	**Date:**	
Contents	Name	Amount (%)
	"The oil name"	
	Triton X-100	
	Water	
	Silver coated glass beads	| Call Terry Runyon in case of doubts about the disposal: Phone: 780-248-1554. Email: trunyon@ualberta.ca	Potential liquid spills, and breakage of glassware. Use safety guidance of steps 1, 4 & 7 of emulsion preparation SWP. Wear proper PPE. First aid and spills kits should be available.
13	Carefully clean the sample containers and other glassware equipment with soap-water solution and water	Potential slip and breakage of glassware. Possible spills of liquids. steps 1, 4 & 7 of emulsion preparation SWP.

5- Toxicology, first aid procedures and main characteristics of chemicals

Table A.2- Health hazards of the chemicals used in the project

	Triton X-100	Light Mineral Oil	Isopar M	Silicone Oil
HMIS	Health 2 Flammability 1 Reactivity 0	Health 0 Flammability 1 Reactivity 0	Health 1 Flammability 1 Reactivity 0	Health 1 Flammability 1 Reactivity 0
Vapor pressure (kPa)	<0.1 at 20C	<0.013 at 20C	0.012 at 20C	>0.7 at 20C
Eyes	Irritating	May cause eye irritation	May cause mild, short-lasting discomfort to eyes	Mild eye irritation
Skin	Slightly irritating	May be harmful if absorbed through skin. May cause skin irritation	Minimally Toxic. May dry the skin leading to discomfort and dermatitis.	Mild skin irritation
Ingestion	May cause gastrointestinal, tract irritation with nausea, vomiting and diarrhea. May be harmful if it is swallowed.	May be harmful if swallowed	Minimally Toxic.	No data available
Inhalation	May cause respiratory track Irritation	May be harmful if inhaled. May cause respiratory tract irritation	Minimally Toxic	No data available
Carcinogenic effects	No evidence	No evidence	No evidence	No evidence

Table A.3- First aids in case of eye contact, skin contact, ingestion or inhalation

Affected area	Triton X-100	Light Mineral Oil	Isopar M	Silicone Oil
Eyes	Remove glasses (including contact lenses). Flush abundant water for at least 15 minutes. Get medical attention Immediately.	Flush eyes with water as a precaution	Flush thoroughly with water. If irritation occurs, get medical assistance.	Rinse thoroughly with plenty of water for at least 15 minutes and consult a physician
Skin	Wash with water and soap. Cover irritated skin with an emollient. Get medical attention if the irritation remains.	Wash off with soap and plenty of water	Wash contact areas with soap and water. Remove contaminated clothing. Launder contaminated clothing before reuse.	Wash off with soap and plenty of water. Consult a physician
Ingestion	Do not provoke vomit and get medical attention immediately	Never give anything by mouth to an unconscious person. Rinse mouth with water	Seek immediate medical attention. Do not induce vomiting.	Never give anything by mouth to an unconscious person. Rinse mouth with water. Consult a physician
Inhalation	Remove with fresh air. Get medical attention.	If breathed in, move person into fresh air. If not breathing, give artificial respiration.	Remove from further exposure. For those providing assistance, avoid exposure to yourself or others. Use adequate respiratory protection. If respiratory irritation, dizziness, nausea, or unconsciousness occurs, seek immediate medical assistance. If breathing has stopped, assist ventilation with a mechanical device or use mouth-to-mouth resuscitation.	If breathed in, move person into fresh air. If not breathing, give artificial respiration. Consult a physician. assist ventilation with a mechanical device or use mouth to mouth resuscitation.

6- Fire and Explosion hazards

Table A.4- Flammability data and fire safety measurements for the chemicals used in the project

Flammability properties				
	Triton X-100	**Light Mineral Oil**	**Isopar M**	**Silicone Oil**
Flash point	247 C	> 160 C	>=94 C	316 C
Flammable limits (Approximate volume % in air)	Not determined	Not determined	LEL: 0.6 UEL: 4.9	Not determined
Auto ignition temperature	Not determined	Not determined	>200 C	> 400 C
Fire safety measures				
Fire extinguishers	"You are not required to put the fire out – but if you attempt to extinguish a fire then you need to know your fire extinguishers" ("University of Alberta", 2014). They are found in all labs and many offices. There are also extinguishers near the exits to the buildings. There are three types of fire extinguishers at the University of Alberta. In the case of flammable liquids, use fire extinguishers **TYPE B**. Only try to put the fire out, if there is clear exit from the room. You only have 30 seconds to put the fire out. Otherwise, leave the area immediately.			
Fire evacuation procedures	1. Activate fire alarm pull-station (can be found along exit route) 2. Close door(s) in fire area… 3. Evacuate fire area and building… 4. Call 911 and give your name, location and nature of the fire… 5. Meet fire department at main entrance.			

Safety Resource References:

- **"www.sigmaaldrich.com". Material Safety Data Sheet: Triton X-100:**
  https://www.sigmaaldrich.com/MSDS/MSDS/DisplayMSDSPage.do?country=CA&language=en&product Number=X100&brand=SIAL&PageToGoToURL=https%3A%2F%2Fwww.sigmaaldrich.com%2Fcatalog %2Fproduct%2Fsial%2Fx100%3Flang%3Den

- **"www.pure-chemical.com". Material Safety Data Sheet: Isopar M:**
  https://www.pure-chemical.com/msds/ISOPAR%20M.pdf

- **"www.sigmaaldrich.com". Material Safety Data Sheet: Silicone Oil.**
  https://www.sigmaaldrich.com/MSDS/MSDS/DisplayMSDSPage.do?country=CA&language=en&product Number=317667&brand=ALDRICH&PageToGoToURL=https%3A%2F%2Fwww.sigmaaldrich.com%2F catalog%2Fproduct%2Faldrich%2F317667%3Flang%3Den

- **"www.fishersci.ca". Material Safety Data Sheet: Light Mineral Oil:**
  https://beta-static.fishersci.ca/content/dam/fishersci/en_US/documents/programs/education/regulatory-documents/sds/chemicals/chemicals-m/S25439.pdf

- **"University of Alberta". Safety Information Site: Fire Safety.**
  https://ssl.eas.ualberta.ca/safety/?page_id=195